

## Two new genera of killifish (Cyprinodontiformes) from the Middle Miocene of the Bugojno Basin, Bosnia and Herzegovina: insights into the lost diversity of Valenciidae

Andrea Herbert Mainero, Davit Vasilyan & Bettina Reichenbacher

**To cite this article:** Andrea Herbert Mainero, Davit Vasilyan & Bettina Reichenbacher (2024) Two new genera of killifish (Cyprinodontiformes) from the Middle Miocene of the Bugojno Basin, Bosnia and Herzegovina: insights into the lost diversity of Valenciidae, *Journal of Systematic Palaeontology*, 22:1, 2412539, DOI: [10.1080/14772019.2024.2412539](https://doi.org/10.1080/14772019.2024.2412539)

**To link to this article:** <https://doi.org/10.1080/14772019.2024.2412539>



© 2024 The Author(s). Published by Informa UK Limited, trading as Taylor & Francis Group.



[View supplementary material](#)



Published online: 23 Dec 2024.



[Submit your article to this journal](#)



Article views: 554



[View related articles](#)



[View Crossmark data](#)



# Two new genera of killifish (Cyprinodontiformes) from the Middle Miocene of the Bugojno Basin, Bosnia and Herzegovina: insights into the lost diversity of Valenciidae

Andrea Herbert Mainero<sup>a</sup>, Davit Vasilyan<sup>b,c</sup> and Bettina Reichenbacher<sup>a,d\*</sup>

<sup>a</sup>Department of Earth and Environmental Sciences, Ludwig-Maximilians-Universität München, Richard-Wagner Straße 10, 80333 Munich, Germany; <sup>b</sup>Jurassica Museum, Route de Fontenais 21, 2900 Porrentruy, Switzerland; <sup>c</sup>Université de Fribourg, Chemin de Musée 1700 Fribourg, Switzerland; <sup>d</sup>GeoBio-Center, Ludwig-Maximilians-Universität München, Munich, Germany

(Received 28 May 2024; accepted 23 August 2024)

Present-day killifishes (Cyprinodontiformes, toothcarps), known for their diversity and ecological adaptability, are represented in Eurasia by two families that each have their own taxonomic diversity, namely the diverse Apaniidae (eight genera, > 40 species) and the less diverse Valenciidae (one genus, three species). The fossil record of both families is quite extensive in the area of Western and Central Europe, but is poor elsewhere. Here we present new fossil killifish material (consisting of 179 individuals, in many cases with otoliths *in situ*) from the Middle Miocene of south-eastern Europe (that is, site Gračanica in the Bugojno Basin, Bosnia and Herzegovina) using both comparative morphology (including meristics, osteology and otoliths) and phylogenetic analysis. For the latter, we used a substantially expanded morphological matrix of a previous work and conducted implied-weight maximum parsimony analyses both without constraints and with a molecular scaffold as a backbone for the extant taxa (with fossils left as floaters). Our results show that the Bugojno killifish assemblage consists exclusively of members of two new genera of the Valenciidae, †*Miovalencia* gen. nov. and †*Wilsonilebias* gen. nov., each of which is represented by two species (three new and one genus reassignment). We also found that not only the saccular otolith (sagitta), which is well known for its taxonomic information, but also the utricular otolith (lapillus) provide important taxonomic information for generic diagnosis. The discovery of the new species from the Bugojno Basin expands the known geographical distribution of the fossil Valenciidae to the Dinaride Lake System of south-eastern Europe. Furthermore, by surveying previous works, we uncovered that the fossil Valenciidae were taxonomically diverse and widely distributed geographically, which is in stark contrast with their diversity and biogeography today. Our results highlight the importance of detailed taxonomic and phylogenetic investigations of fossil killifishes in gaining insight into the evolutionary history of this remarkable group among today's freshwater fish faunas.

<http://zoobank.org/urn:urn:lsid:zoobank.org:pub:890009C0-2758-49AA-931F-0F63A4E46C8E>

**Keywords:** Fossil toothcarps; skeletal material; otoliths *in situ*; phylogeny; biogeography; Cenozoic

## Introduction

The order Cyprinodontiformes Berg, 1940, commonly known as toothcarps, represents a diverse group of typically small freshwater fish that, at time of this publication, encompasses 1483 species (Fricke et al., 2024). They are informally subdivided into livebearing toothcarps and egg-laying toothcarps, with the latter commonly referred to as killifish. Both extant and fossil Cyprinodontiformes have been extensively studied across multiple areas of research such as phylogeny, speciation, intra- and inter-species morphological variability, reproduction and development, ecology and biogeography (Costa, 2013; Gaudant, 2002; Hernandez et al., 2018; Morcillo et al., 2016; Shumka et al., 2020; Teimori, Iranmanesh, et al.,

2021). Generally, Cyprinodontiformes are categorized into the suborders Aplocheiloidei Parenti, 1981 and Cyprinodontoidei Gill, 1865. Aplocheiloidei includes three extant and one extinct family, while Cyprinodontoidei comprises 11 families (Bragança et al., 2018; Pohl et al., 2015); 13 families (Piller et al., 2022). Found in tropical and temperate waters worldwide, the members of both suborders inhabit diverse environments, such as freshwater lakes and brackish, alkaline and hypersaline water bodies, and demonstrate remarkable adaptability to challenging ecological conditions (Aguilera et al., 2019; Riesch et al., 2009; Wildekamp, 1993).

Previous attempts to establish relationships between killifish families and genera were based on morphological characters (Costa, 1997, 1998, 2012a; Parenti,

\*Corresponding author. Email: [b.reichenbacher@lrz.uni-muenchen.de](mailto:b.reichenbacher@lrz.uni-muenchen.de)

1981). However, recent molecular-based research has shown that many families were incorrectly grouped due to phenotypic convergence (Bragança & Costa, 2019; Esmaili *et al.*, 2020; Rodgers *et al.*, 2018). Although significant progress has now been made in elucidating phylogenetic relationships among Cyprinodontiformes, debate continues regarding specific families, such as Orestiidae Bleeker, 1859 and Cubanichthyidae Parenti, 1981 (López-Solano *et al.*, 2023; Piller *et al.*, 2022). According to the most recent molecular-based research (Bragança & Costa, 2019; Piller *et al.*, 2022), the Old World (Eurasia and Africa) Aplocheiloidei suborder encompasses two families, namely Aplocheilidae Bleeker, 1860 and Nothobranchiidae Garman, 1895, while the Old World Cyprinodontoidei suborder consists of four families: the European and Western Asian Aphaniiidae Hoedemann, 1949 (Anatolian and Mediterranean killifish), the European Valenciidae Parenti, 1981 (Valencia killifish, Corfu or Peloponnese killifish), and the African families Procatopodidae Fowler, 1916 (Lampeyes) and Pantanodontidae Myers, 1955. The latter is the sister group to all other cyprinodontoid families (from the Old World and the New World).

However, the fossil record is scarce compared to the extant species diversity of killifish. Finds of fossil killifish are based on skeletons, sometimes with otoliths preserved *in situ*, and on isolated otoliths (found without any articulated skeletal material). The oldest fossils that definitely belong to Cyprinodontiformes come from the Paleocene in the New World (Arratia & Cione, 1996) and from the Oligocene in the Old World (Gaudant, 1982). Of the suborder Aplocheiloidei, only a single fossil species is known from the Upper Miocene of central Kenya (Altner & Reichenbacher, 2015). All other fossil killifish species, from both the New and the Old World, belong to the suborder Cyprinodontoidei, with a particularly large number of fossil finds from Europe (Bogan *et al.*, 2018; Costa, 2011; Gaudant, 2002, 2012, 2013; Reichenbacher & Prieto, 2006; Sferco *et al.*, 2018; Smith, 1981; Vasilyan *et al.*, 2009).

Until the early 2000s, Old World killifish fossils were attributed to the extant genus *Aphanius* Nardo, 1827 (within Aphaniiidae) and to three extinct genera with uncertain familial relationships: †*Prolebias* Sauvage, 1874 (?Cyprinodontidae), †*Aphanolebias* Reichenbacher and Gaudant, 2003 (?Valenciidae) and †*Palaeolebias* Reichenbacher in Reichenbacher and Weidmann, 1992 (family unknown; – see Parenti, 1981; Reichenbacher & Gaudant, 2003; Reichenbacher & Weidmann, 1992). In a subsequent revision, Costa (2012a) reclassified the former †*Prolebias* into four genera belonging to three families: *Pantanodon* Myers, 1955 (Pantanodontidae), †*Eurolebias* Costa, 2012a (Cyprinodontidae), †*Prolebias* (Valenciidae) and †*Francolebias* Costa, 2012a (Valenciidae). Soon after, Gaudant (2013) established the genus †*Paralebias*

Gaudant, 2013 to accommodate the fossils Costa (2012a) had assigned to *Pantanodon* (note that Bragança *et al.*, 2018 reverted †*Paralebias* back to *Pantanodon*).

Apart from †*Prolebias* and †*Francolebias*, the family Valenciidae includes the extant genus *Valencia* Myers, 1928, of which two extinct species were described, namely †*V. reichenbacherae* Rückert-Ülkümen, 2006 and †*V. arcasensis* Gaudant & Reichenbacher in Gaudant *et al.* (2015); it probably also includes †*Aphanolebias*. Consequently, ancient Valenciidae comprised four genera (*Valencia*, †*Prolebias*, †*Aphanolebias*, †*Francolebias*; see Fig. 1), each represented by two or several species. This diversity is notably higher than observed in present-day Valenciidae, which only includes *Valencia*, represented by three species: *V. hispanica* (Valenciennes in Cuvier & Valenciennes, 1846), *V. letourneuxi* (Sauvage, 1880) and *V. robertae* Freyhof, Kärst & Geiger, 2014. Yet, the factors that contributed to Valenciidae's past success and its subsequent decline remain unclear.

The aim of this study is to present a new, rich collection of killifish fossils from a Middle Miocene palaeolake (Bugojno Basin, site Gračanica) located in the Dinarides of Bosnia and Herzegovina (Fig. 2). The material includes articulated fossil skeletons, many with otoliths *in situ*, and in some cases with anatomical details in exceptionally good preservation. Based on comparative morphology and phylogenetic analysis, we show that new members of the family Valenciidae can be identified, and we use our results in conjunction with literature data to substantially enhance our understanding of the present-day family Valenciidae in terms of its past diversity, geographical distribution and ecology.

## Geology and stratigraphy of the Bugojno Basin palaeolake

The Bugojno Basin is located in the central Dinarides of Bosnia and Herzegovina (Fig. 2A). It represents a Middle Miocene palaeolake that developed in an intramontane basin on the Balkan Peninsula of the Dinarides-Anatolian Island (Fig. 2B) during the post-orogenic evolution of the Dinarides mountain belt (de Leeuw *et al.*, 2012; Krstić *et al.*, 2012). The Bugojno Basin is part of the Miocene perennial lake system ('Dinaride Lake System'), which, due to its isolated and long-lived character, has yielded highly diverse and endemic faunas (Jiménez-Moreno *et al.*, 2009; Mandić *et al.*, 2011; Marković *et al.*, 2018; Neubauer *et al.*, 2013).

The site Gračanica in the Bugojno Basin, from which our studied material comes, has revealed remarkable discoveries of fossils including invertebrates (Hajek-Tadesse, 2020; Mandić *et al.*, 2020), ectothermic vertebrates

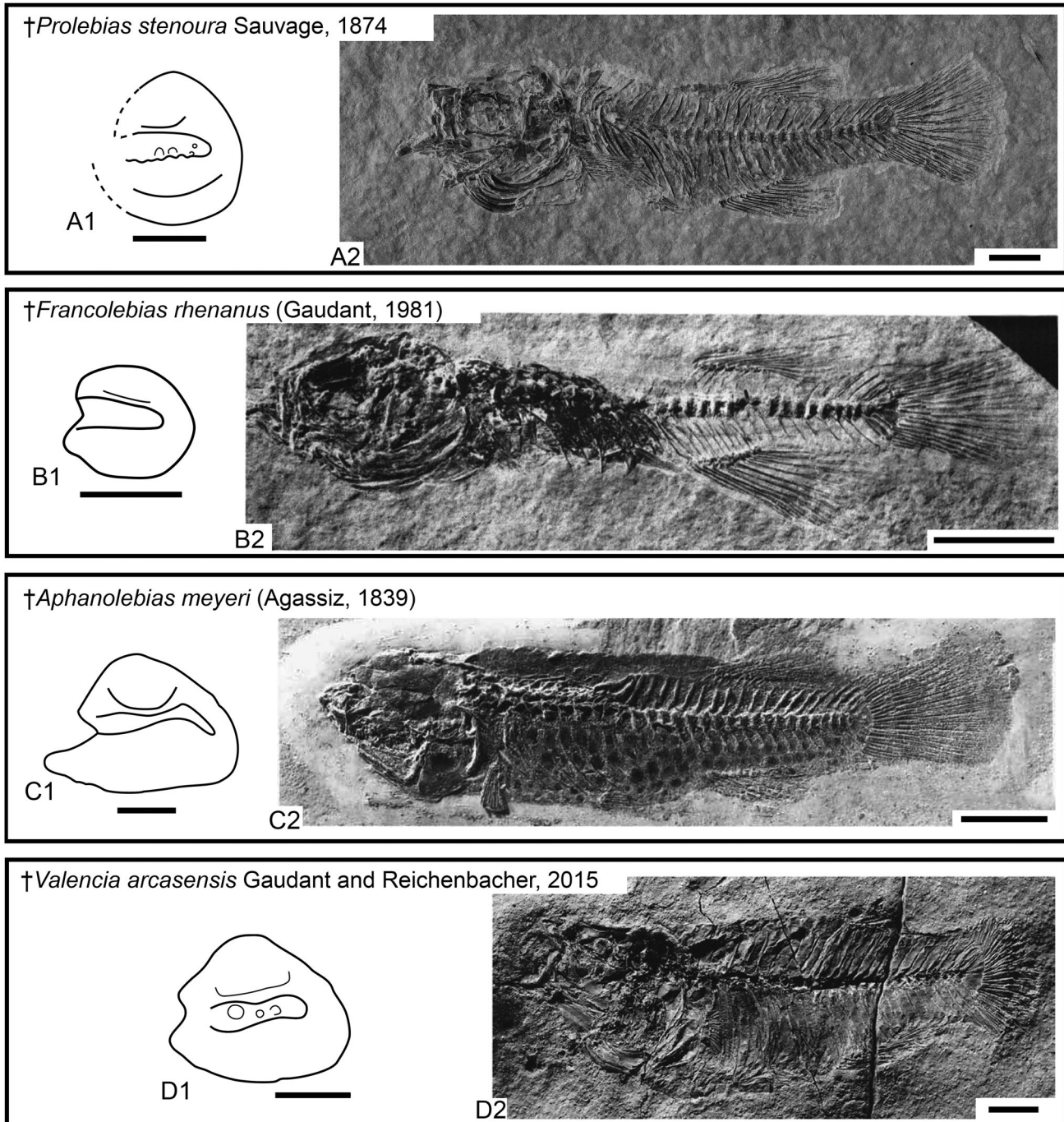


**Figure 1.** Otoliths and skeletons of previously described fossil species of the Valenciidae. **A1**, otolith preserved *in situ* in specimen NHMUK PV P 76303 (this study); **A2**, NHMUK PV OR 28491n (NHMUK digital collection archive). **B1**, SMF P 3328, isolated otolith, reinterpreted as †*Francolebias rhenanus* in this study (redrawn from Weiler, 1963, fig. 18, as †*Prolebias* sp.); **B2**, NHMB Ru 99, holotype (from Gaudant, 1981b, pl. 1: 1). **C1**, SMF PO. 64369, isolated otolith (redrawn from Reichenbacher & Gaudant, 2003, fig. 3: 3a, mirrored); **C2**, SMF P. 9612 (from Reichenbacher & Gaudant, 2003, fig. 2: 3). **D1**, otolith preserved *in situ* in specimen MGUV 23390 (redrawn from Gaudant et al., 2015, fig. 9a); **D2**, MGUV 23388 (from Gaudant et al., 2015: fig. 8b). Scale bars for skeletons = 5 mm, for otoliths = 0.5 mm.

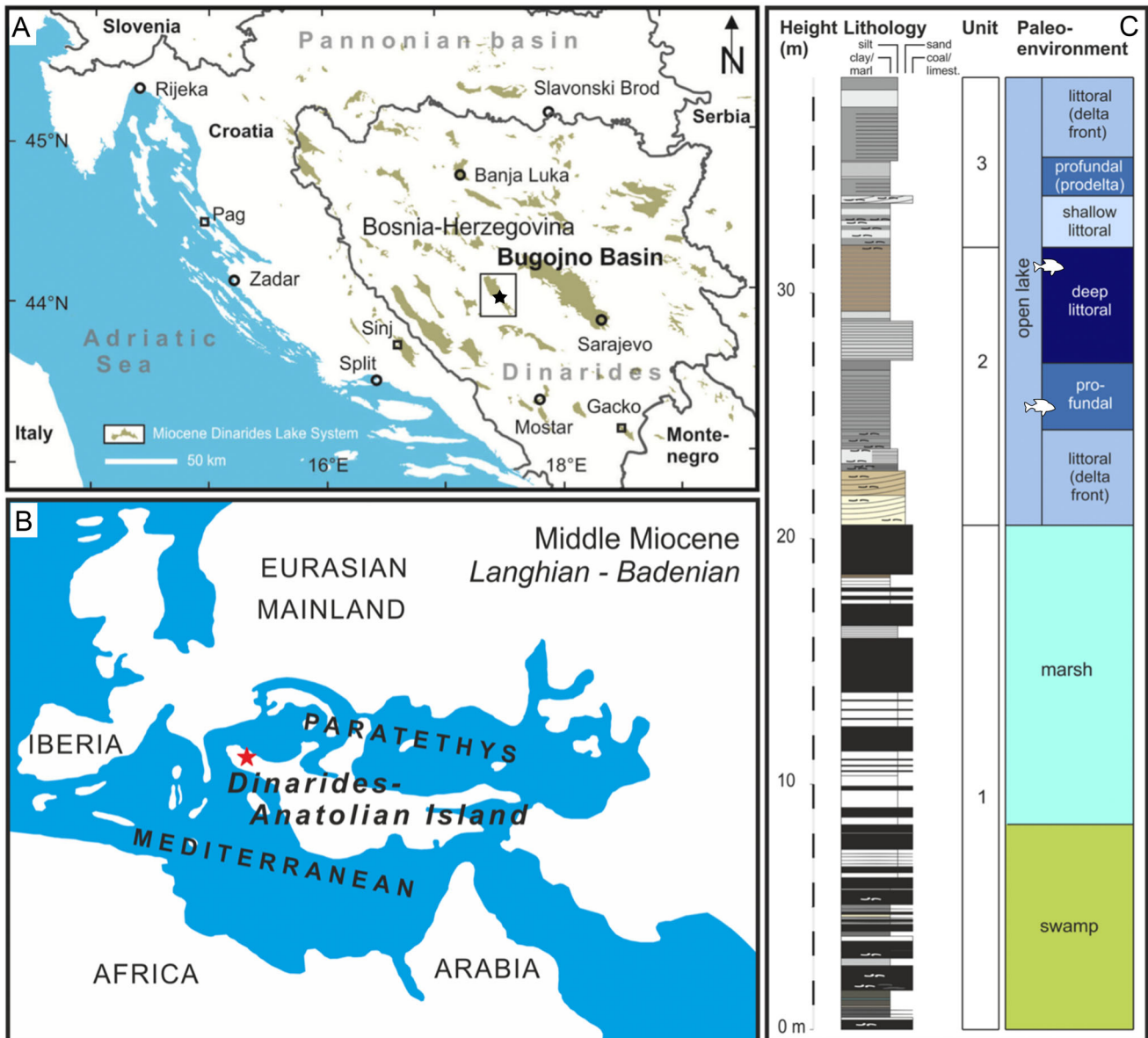


**Figure 2.** A, geographical position of the Bugojno Basin (black rectangle) and the locality Gračanica (black star) within the Dinaride Lake System (DLS, light brown) in Bosnia and Herzegovina. B, palaeogeographical map showing the Dinarides-Anatolian Island and the location of the DLS. C, stratigraphical section of the Gračanica site, palaeoenvironmental interpretation and position of fish-bearing sediments. Modified from Göhlich and Mandić (2020) and Jiménez-Moreno and Mandić (2020).

(Vasilyan, 2020), mammals (van der Made, 2020) and other groups (Göhlich & Mandić, 2020). The outcrop is approximately 40 m thick and was deposited over 250 kyr (14.8 to 14.55 Ma) during the early Middle Miocene (early Langhian) (Jiménez-Moreno & Mandić, 2020). From bottom to top, the profile exposes two sequences, each about 20 m in thickness (Fig. 2C). The lower sequence comprises dark, organic-rich sediments and lignite, indicating gradual flooding of a mainland area. The upper sequence consists of light-coloured, organic-rich marls signifying the

transition from a marsh or swamp environment to a long-lived, progressively deepening lake, with oxygen-depleted deeper areas and possibly slightly alkaline conditions (Hajek-Tadesse, 2020; Jiménez-Moreno & Mandić, 2020; Mandić et al., 2020; Pisera et al., 2019). Combined with rapid sedimentation, these conditions appear to have promoted the good preservation observed in all ectothermic vertebrates (Vasilyan, 2020). The studied fish fossils were found within the upper sequence, from 24 to 26 m and 30.5 to 31.5 m (see Fig. 2C and Vasilyan, 2020).

## Materials and methods

### Remark

In the following, we use quotation marks to indicate genus names of killifish species that are clearly in need of revision. All extinct taxa are marked with a dagger ‘†’.

### New fossil material

The studied material comprises skeletal remains from a total of 179 individuals. Among them, 39 exhibit remarkably well-preserved complete skeletons with otoliths in their original position (that is, *in situ*). A further 55 specimens display otoliths *in situ*, but have skeletons of varying degrees of preservation. Most of the material (173 specimens) is housed at the Jurassica Museum in Porrentruy, Switzerland (the former Musée Jurassien des Sciences Naturelles, MJSN), under the collection number MJSN GRC and serial numbers 001–068, 167–264, 334–335 (we skip MJSN in the text for better readability) and at the Natural History Museum of Vienna (six specimens, NHMW 001–006). For several specimens, both part and counterpart (which may have different serial numbers) are present; others are preserved either as part or counterpart (we consider the slab containing the specimen with the head to the right as the part and the specimen with the head to the left as the counterpart). A list of specimens is provided in the [Supplemental material Table S1](#), sheet 1. A further specimen was donated by Dr T. Přikryl, Prague (listed as BSPG 2024 I 80 in the [Supplemental material](#)).

### Comparative material for the study of skeletal traits

For the comparative study of morphometric, meristic and osteological traits, published data for extant and fossil Valenciidae were compiled from the literature. For the three extant species of *Valencia*, data were used from Costa (1998, 2012a, b), Freyhof et al. (2014), Ghedotti (2000), Ghedotti and Davies (2013) and Parenti (1981); for †*V. arcasensis*, data were used from Gaudant et al. (2015); and for †*Prolebias stenoura* (Sauvage, 1874), data were used from Costa (2012a, b) and Gaudant (2012). For the four species of †*Francolebias* data were used from: Costa (2012a, b), Gaudant (1988) and Gaudant (1989) for both †*F. aymardi* and †*F. delphinensis*; Gaudant (1981a, b) for †*F. rhenanus*; Gaudant (2016) for †*F. arvernensis*. Finally, data for †*Aphanolebias meyeri* were taken from Reichenbacher and Gaudant (2003). Additionally, morphometric, meristic and osteological data were taken for *V. hispanica* based on X-ray images of three specimens

from the SNSB-Zoological State Collection (ZSM-PIS 15451, -15453 and -15454); X-ray images were prepared using a Faxitron Ultrafocus facility housed in the SNSB-ZSM. For *V. letourneuxi*, *V. robertae* and †*V. arcasensis*, morphometric data were not included in the literature sources and we took the measurements used here on previously figured specimens. Finally, for the comparative study of jaw bones, cleared and stained specimens of *V. hispanica* (SNSB-ZSM 2070) and *Aphaniops stoliczkanus* (Aphaniidae, five specimens from Herbert Mainero et al., 2023, BSPG 2024 VII 4 (4, 6, 16, 22, 35) were available. The literature sources and respective data are provided in detail in the [Supplemental material Table S1](#), sheets 2 and 4.

### Comparative material for the study of otolith traits

Data on the otoliths (sagittae and lapilli) of the three extant species of *Valencia* were newly assembled ([Supplemental material Table S1](#), sheet 3). Otoliths (sagittae) of previously described fossil species of Valenciidae were compiled from Bradić-Milinović et al. (2021, †*Aphanolebias bettinae*), Gaudant et al. (2015, †*V. arcasensis*), Reichenbacher (1993, †*A. gubleri*, †*A. konradi*), Reichenbacher (2000, †*Palaeolebias symmetricus*), Reichenbacher, Böhme, et al. (2004, †*A. konradi*), Reichenbacher et al. (2019, †*A. sarmaticus*), Reichenbacher and Gaudant (2003, †*A. meyeri*), Reichenbacher and Kowalke (2009, †*Aphanolebias angulosus*, †*Aphanius chios*), Rückert-Ülkümen (2006, †*V. reichenbacherae*), Weiler (1963, †*Cyprinodontidarum symmetricus*, †*Prolebias* sp.) and Steurbaut (1978, †*Cyprinodontidarum angulosus*). In addition, SEM images were available for unpublished otolith material of †*A. meyeri* (collection SMF and BSPG). All otolith images provided in the mentioned literature sources and collections were used for otolith measurements (for details of data see [Supplemental material Table S1](#), sheet 3).

## Methods

**Morphometry based on skeletal material.** Thirty-seven individuals exhibited complete bodies without significant taphonomic distortion. These specimens were photographed using a Leica M165 C stereomicroscope equipped with a digital camera (type Gryphax Naos) for subsequent morphometric analysis. Utilizing a combination of measurements from previous studies (Freyhof et al., 2017; Gaudant et al., 2015; Gut et al., 2020; Teimori et al., 2012), 20 measurements, each with a precision of 0.01 mm, were taken (see [Supplemental material Fig. S1](#)). Measurements were conducted on, if available, both the part and counterpart, or were conducted twice on the same specimen, with the average

recorded to minimize errors. All measurements were done using ImageJ (Schneider *et al.*, 2012) and standardized based on the standard length or the head length (Measurement/SL  $\times$  100; Measurement/HL  $\times$  100). Standard length (SL) was measured from the upper jaw to the end of the hypural complex, with the most anterior point taken if the jaw was distorted. In cases where fins were complete, fin length was determined based on the longest ray (from the base of the ray to its distal-most point). Head depth (HD) and length (HL) were measured at the most posterior point of the opercle. If the SL was distorted, it was calculated based on the otolith-to-SL ratio from a complete specimen within the same group.

In addition, ratios were computed based on the most well-preserved specimens of each genus for:

- i. Pelvic bone width/length ratio, with pelvic bone length defined as the maximum length from the anterior to the posterior rim, and width as the maximum width, usually situated where the medial process is located (Supplemental material Fig. S2a).
- ii. Thickness of the second and third dorsal-fin rays *vs* the second and third anal-fin rays; the maximum width of rays was measured just before bifurcation.
- iii. Width of neural and haemal spines of preural vertebra 2 relative to the width of preural vertebrae 3 and 4; each measurement was taken at the maximum width in the distal part of the respective spine, following Altner and Reichenbacher (2015) (Supplemental material Fig. S2b).

**Meristic counts.** Vertebrae counts were categorized into abdominal and caudal vertebrae, with the latter including the terminal centrum. The number of rays in the dorsal and anal fins was counted based on the total number observed. In instances of poor ray preservation, the count was based on the number of dorsal and anal fin pterygiophores instead. In the dorsal fin, this count is equal as the first ray articulates with two pterygiophores, subsequent rays with a single pterygiophore, and the last ray is typically deeply branched, and is thus counted as two (see Parenti, 1981). Conversely, in the anal fin, the number of pterygiophores is usually one less than that of the rays, as each ray corresponds to a single pterygiophore, and the last ray, typically deeply branched, is counted as two (Fig. 3A). Principal caudal-fin rays were determined following the methodology outlined by Arratia (2008), encompassing all branched and segmented rays, along with the first segmented and non-branched ray both ventrally and dorsally (Fig. 3A). In addition, the number of caudal-fin rays supported by the hypural plate is provided to facilitate comparison with previous studies.

**Osteology.** The osteological terminology for the descriptions of skull, jaw bones, abdominal and caudal skeleton (Fig. 3A, Supplemental material Fig. S2b) adhere to the guidelines provided by Parenti (1981), Arratia (2008), Costa (2012a, b), Arratia *et al.* (2017) and Charmpila *et al.* (2020).

**Otoliths and teeth.** Out of the total 94 specimens with otoliths *in situ*, 57 specimens displayed well-preserved sagittae, while 54 specimens contained lapilli of similarly good preservation, all of which were carefully extracted. Among these, 43 specimens presented both sagitta and lapilli *in situ*, and two presented both sagitta and asteriscus (lagenar otolith). Furthermore, 33 teeth were meticulously extracted from 20 specimens, with eight specimens contributing jaw teeth and 14 specimens providing pharyngeal teeth. All extracted sagittae, lapilli and teeth were photographed using both light microscopy (Leica M165 C) and scanning electron microscopy (HITACHI SU 5000 Schottky FE-SEM). The morphological description of the sagittae follows Reichenbacher *et al.* (2007), that of the lapilli is based on the criteria established by Assis (2005) and Schulz-Mirbach & Plath (2012) (Fig. 3B, D), and the terminology of the asteriscus is according to Assis (2003).

**Otolith (sagitta) morphometry.** For the new fossil sagitta material and also for the comparative sagitta material of the three extant *Valencia* species, morphometric measurements were conducted based on SEM images using Image J (Supplemental material Table S1, sheets 1 and 3). For the comparative sagitta material of previously described fossil otoliths, the same measurements were performed using published figures (Supplemental material Table S1, sheet 3). Additional comparative sagitta material was available for †*Aphanolebias meyeri* in the SNSB-BSPG collection—this was also measured (Supplemental material Table S1, sheet 3). All measurements followed the methodology outlined by Reichenbacher *et al.* (2007) (Fig. 3C), with values reported as a percentage of the otolith length (OL) or otolith height (OH).

**Statistical analysis and biogeographical map.** Descriptive statistics were conducted for both body morphometry and sagitta morphometry using basic statistical functions integrated in the Statistical Software R version 4.2.3 (R Core Team, 2023).

Furthermore, we investigated differences in sagitta morphometry (linear variables and excisura angle, see Fig. 3C) among the valenciid genera and between the species of the newly defined genera. To assess these differences, we utilized the Welch-ANOVA test with the Games-Howell Post-Hoc Test, as these tests allow handling unequal sample sizes and non-homogeneity of

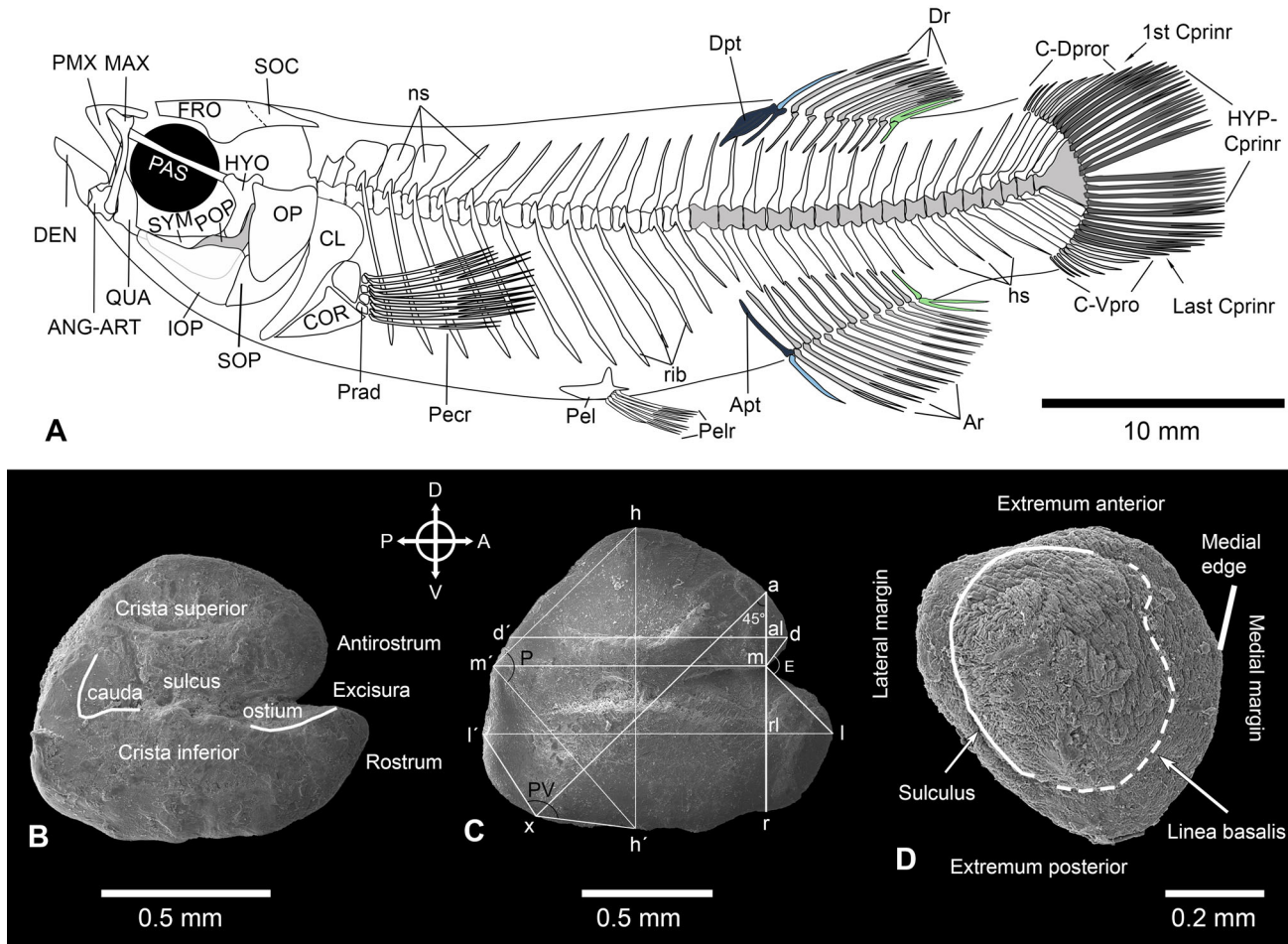


**Figure 3.** Characters of **A**, the fish skeleton and **B–D**, otoliths. **A**, based on X-ray of *Valencia hispanica*, ZSM-PIS-15451; **B**, **C**, based on medial view of sagittae of **B**, †*Wilsonilebias langhianus* gen. et sp. nov., GRC 233 and **C**, †*Miovalencia chios*, GRC 003; **D**, based on ventral view of lapillus of †*W. langhianus* gen. et sp. nov., GRC 236.1. **Abbreviations for the skeleton:** ANG-ART, angulo-articular; Apt, anal-fin pterygiophores (1st Apt in dark blue, last one in light green); Ar, anal-fin rays (1st ray in light blue, last one in light green); C-Dpro, caudal-fin dorsal procurent rays; CL, cleithrum; COR, coracoid; Cprinr, caudal-fin principal rays (shaded in dark grey); C-Vpro, caudal-fin ventral procurent rays (light grey); DEN, dentary; Dpt, dorsal-fin pterygiophores (1st and 2nd Dpt dark blue, last one in light green); Dr, dorsal-fin rays (1st ray in light blue, last one in light green); FRO, frontal; hs, haemal spine; HYO, hyomandibular; HYP-Cprinr, caudal-fin principal rays supported by hypural; IOP, interopercle; MAX, maxilla; ns, neural spine; OP, opercle; PAS, parasphenoid; Pecr, pectoral-fin rays; Pel, pelvic bone; Pelr, pelvic-fin rays; PMX, premaxilla; POP, preopercle; Prad, pectoral radials; QUA, quadrate; SOC, supraoccipital; SYM, symplectic. **Otolith measurements:** a–m, antirostrum height; al–d, antirostrum length; d’–d, dorsal length; E, excisura angle; h’–h, maximum height; l’–l, maximum length; m’–m, medial length; P, posterior angle (h–m’–h’); PV, posteroventral angle (l’–x–h’, where ‘x’ is marked by forming a 45° angle x–a–r); r–m, rostrum height; rl–l, rostrum length.

variances, as observed in our data (see Zar, 2010). Statistical tests were performed using the R package ‘rstatix’ (v. 0.7.2, Kassambara, 2023). †*Francolebias* was excluded from all tests as we have only one otolith record of this genus.

For illustrating the geographical locations of previously described fossil valenciid species, the ‘giscoR’ package version 0.3.3 (Hernangómez, 2023) was employed to retrieve country map data from the Eurostat – GISCO (Geographic Information System of

the Commission) database. The package ‘elevatr’ (v. 0.4.2; Hollister et al., 2023) was utilized to obtain raster elevation data for the topography.

### Phylogenetic reconstructions

**Preparation of matrix.** The character-taxon matrix of Costa (2012a), consisting of 89 characters and 33 in-group taxa, was used as basis. Costa (2012a) had used two *Oryzias* species (Beloniformes) and *Melanotaenia*

*affinis* (Weber, 1907) (Atheriniformes) as outgroup. Here we used one of his *Oryzias* species (*O. matanensis* Aurich, 1935) and *M. affinis* as outgroup because both Beloniformes and Atheriniformes are closely related to Cyprinodontiformes (Betancur-R *et al.*, 2013, 2017; Hughes *et al.*, 2018). To this matrix, we added 10 species and 27 characters. The complete dataset now consists of 43 in-group species (13 of which are fossil species) and 116 characters (Supplemental material Table S1, sheet 6).

The 10 newly added species comprise seven fossil valenciids (†*Aphanolebias meyeri* (Agassiz, 1839), †*Francolebias rhenanus* (Gaudant, 1981a), †*F. arvernensis* Gaudant, 2016 and the four new species of our study), the extant species *V. letourneuxi* (note that the one identified as *V. letourneuxi* in Costa 2012a, b originated from the Pinios River, Greece and is now *V. robertae*), and a second representative each of the Procatopodidae (*‘Lacustricola’ johnstoni* (Günther, 1984)) and the Pantanodontidae (*Malagadon madagascariensis* (Arnoult, 1963)). Character information for the newly added fossil valenciids were taken from Reichenbacher and Gaudant (2003), Gaudant (1981a), Gaudant (2016) and this study; from Ghedotti (2000), Ghedotti and Davies (2013) and Freyhof *et al.* (2014) for *V. letourneuxi*; and from Bragança *et al.* (2018), Bragança *et al.* (2020), Ghedotti (2000), Parenti (1981) and Rosen (1965) for *‘Lacustricola’* and *Malagadon* (for details see Supplemental material Table S1, sheet 4).

Among the 27 characters that were added, four were not used in the matrix of Costa (2012a) and also not in the other literature sources used here (see below). These are (i) number of abdominal vertebrae, (ii) position of anterior epural relative to terminal centrum, (iii) size of posterior anal-fin pterygiophores relative to preceding ones and (iv) extension of posterior anal-fin pterygiophores relative to adjacent haemal spines. The further 23 added characters (char.) were compiled from the previously published matrices of Costa (1997, 1998, 2012b, in total 4 char.), Ghedotti (2000, 13 char.), Ghedotti and Davies (2013, 2 char.), and Sferco *et al.* (2022, 1 char.), and from descriptions provided in Bragança *et al.* (2018, 1 char.) and Parenti (1981, 2 char.) (Supplemental material Table S1, sheet 5). The authors from which the new characters were added, that is Ghedotti (2000) or Sferco *et al.* (2022), had already coded many taxa of the original matrix of Costa (2012a); we adopted these codings for the respective taxa in our matrix. If a taxon was not coded in the matrices from which we have taken the new characters, then other matrices (i.e. Costa, 2011), anatomical descriptions (i.e. Rosen, 1965) or, if available, X-ray images from online databases (for example, the Smithsonian Institution 2024,

or CAS Ichthyology Primary Types Imagebase 2024) were used (see Supplemental material Table S1, sheet 4 for complete information on taxon data sources). All characters were left unordered following Costa (2012a) and Ghedotti (2000).

**Phylogenetic analysis.** To elucidate the relationships of the new genera, maximum parsimony analyses were performed both without constraints and using a molecular scaffold as constraint (see Lee & Palci, 2015; Springer *et al.*, 2001). For the constrained analysis, we used the topology of the most recent molecular phylogenies of Cyprinodontiformes as a scaffold (Bragança *et al.*, 2018; Bragança & Costa, 2019; Piller *et al.*, 2022), while the fossils were left unconstrained (‘floaters’, see Halliday *et al.*, 2017; Meyer *et al.*, 2023). The analyses were conducted with TNT v. 1.6 (Goloboff *et al.*, 2008) employing New Technology Searches (sectorial, ratchet, drift and tree fusing enabled; init. addseqs = 100; find min. length = 10). Analyses were run using either equal weights or implied weights; for the latter different concavity constants were applied (K = 3, K = 12, K = 24). Taking into account the different phylogenetic trees of the individual analyses, the trees presented here are based on implied weights and K = 12, which is consistent with the recommendation of Goloboff (1993) and Goloboff *et al.* (2018) on the use of concavity constants when dealing with morphological data. A strict consensus tree of the trees obtained was calculated for each analysis. To assess node/branch support, a standard bootstrap analysis was performed in TNT based on 500 replicates (New Technology Search; init. addseq = 10; find min. length = 5) and expressed as absolute frequencies.

### Institutional abbreviations

**BSPG**, Bavarian State Collection for Palaeontology and Geology; **MGUV**, Museu de Geologia, University of Valencia, Burjassot, Spain; **MJSN**, Jurassica Museum in Porrentruy, Switzerland (former Musée jurassien des sciences naturelles); **NHMB**, Natural History Museum of Basel, Switzerland; **NHMUK**, Natural History Museum, London, UK; **NHMW**, Natural History Museum Vienna, Austria; **SAIAB**, South African Institute for Aquatic Biodiversity, South Africa; **SMF**, Senckenberg Research Institute and Natural History Museum, Frankfurt, Germany; **SNSB-BSPG**, Bavarian State Collection for Palaeontology and Geology, Munich, Germany; **SNSB-ZSM**, Bavarian State Collection of Zoology, Munich, Germany.

### Anatomical abbreviations

**A**, relative antirostrum height; **AL**, relative antirostrum length; **BD**, body depth; **ED**, eye-diameter; **CPL**, caudal

peduncle length; **CPD**, caudal peduncle depth; **HD**, head depth; **HL**, head length; **hs**, haemal spine; **ns**, neural spine; **OH**, otolith height; **OL**, otolith length; **PU**, preural vertebra; **R**, relative rostrum height; **RL**, relative rostrum length; **SL**, standard length; **V**, vertebra.

## Results

Of the 179 fossil fish with preserved skeletons, 59 specimens could be identified at species level, 18 specimens were determinable only up to the genus level and the others were not identifiable (Supplemental material Table S1, sheet 1). Two new genera, each represented with two species, were identified (Fig. 4). In the following descriptions, specimens are designated by the prefix GRC or NHMW followed by their serial number; ‘/’ indicates the presence of part/counterpart, while ‘p’ and ‘cp’ indicate that only the part or the counterpart is present. The presence of sagitta (s), lapillus (l), both sagitta and lapillus (s+l) or both sagitta and asteriscus (s+a) *in situ* are also indicated.

## Systematic palaeontology

Order **Cyprinodontiformes** Berg, 1940  
 Suborder **Cyprinodontoidei** Gill, 1865  
 Family **Valenciidae** Parenti, 1981  
 Genus †*Miovalencia* gen. nov.

**Type species.** †*Miovalencia bugojnensis* gen. et sp. nov.

**Other species.** †*Miovalencia chios* (Malz, 1978) from the same locality as the type species. Otoliths of †*M. chios* are also known from the Middle Miocene (Langhian) Nenita Beds from the Chios Island, Greece, from where Malz (1978) had described them as †*Aphanius chios* Malz, 1978. Another otolith-based species of †*Miovalencia* is †*M. angulosa* (Steurbaut, 1978) from the Lower Miocene (Aquitanian) of south-west France (Steurbaut, 1978, as *Cyprinodontidarum*). See section ‘Otoliths of Valenciidae’ for details.

**Stratigraphical range.** Lower Miocene (Aquitanian) to Middle Miocene (Langhian).

**Diagnosis.** †*Miovalencia* gen. nov. shares with other valenciids the synapomorphic characters described by Parenti (1981) and Costa (2012a): (i) slender dorsal process of maxilla, extending over ascending process of premaxilla (Fig. 5A), and (ii) neural spine of PU 2 (= penultimate vertebra) about three times wider than

neural spine of PU 4 (Fig. 6A, B). Further characters shared with valenciids include long ascending process of premaxilla (Fig. 5A), conical jaw teeth arranged in multiple rows and posteriorly positioned unpaired fins (Fig. 4A, B, Table 1).

†*Miovalencia* gen. nov. exhibits slightly lower modes concerning both total vertebrae (26) and dorsal-fin rays and pterygiophores (10) than those seen in †*Wilsonilebias* gen. nov. (27 and 11, respectively), and the range of the same counts indicates that †*Miovalencia* gen. nov. has slightly fewer vertebrae (25–28) than the remaining valenciids (27–31), and slightly fewer dorsal-fin rays and pterygiophores (9–11) than seen in †*Prolebias* (12–13). In addition, its range of anal-fin rays (12–14) tends to be slightly lower than in †*Prolebias* (14–16) (Tables 1, 2). Moreover, †*Miovalencia* gen. nov. can be distinguished from *Valencia*, †*Aphanolebias*, †*Francolebias*, †*Prolebias* and †*Wilsonilebias* gen. nov. by the following unique combination of osteological characters: (i) broad pelvic bone, width about 65% of length (Fig. 7B, Table 1) (*vs* 50% in *Valencia* and †*Prolebias*); (ii) long, slender 1st dorsal-fin pterygiophore (Fig. 8A, C) (*vs* short and robust in †*Wilsonilebias* gen. nov., Fig. 8B, D); (iii) 1st dorsal-fin pterygiophore unfused from 2nd pterygiophore (Fig. 8A3) (*vs* being fused in †*Francolebias*); (iv) short anterior anal-fin pterygiophores, not reaching middle portion of adjacent haemal spine (Fig. 9A) (*vs* long anterior anal-fin pterygiophores, reaching beyond middle portion of adjacent haemal spine in †*Francolebias* and †*Wilsonilebias* gen. nov., Fig. 9B); (v) posterior anal-fin pterygiophores gradually diminishing in size (Fig. 9A) (*vs* similar in length to preceding ones in †*Wilsonilebias* gen. nov., Fig. 9B); (vi) unmodified haemal spines above anal fin (Fig. 9A) (*vs* widened in putative males of †*Francolebias* and †*Wilsonilebias* gen. nov., Fig. 9B); (vii) totally fused hypural plates, with suture visible (Fig. 6A, B) (*vs* unfused in †*Prolebias*, and *vs* partially fused in †*Aphanolebias* and †*Wilsonilebias* gen. nov., Fig. 6C, D); (viii) premaxilla ascending process with robust base (Fig. 5A) (*vs* slender base in †*Wilsonilebias*, Fig. 5B); (ix) premaxilla ascending process long and robust (Fig. 5A) (*vs* short and elongate in †*Aphanolebias*); (x) retroarticular elongated (Fig. 5A) (*vs* short in *Valencia*, †*Prolebias*, †*Francolebias*); and (xi) opercle slender, relatively narrow (Fig. 5A) (*vs* triangular and wide in †*Wilsonilebias* gen. nov., Fig. 5B).

Moreover, the sagitta of †*Miovalencia* gen. nov. shows morphometric and morphological traits that are significantly different to the sagittae of other Valenciidae (Welch-ANOVA test with Games-Howell post-hoc,  $p < 0.001$ ): five and four otolith variables separate it from *Valencia* and †*Prolebias*, respectively, while three and two otolith variables discriminate it from †*Aphanolebias* and †*Wilsonilebias*, respectively

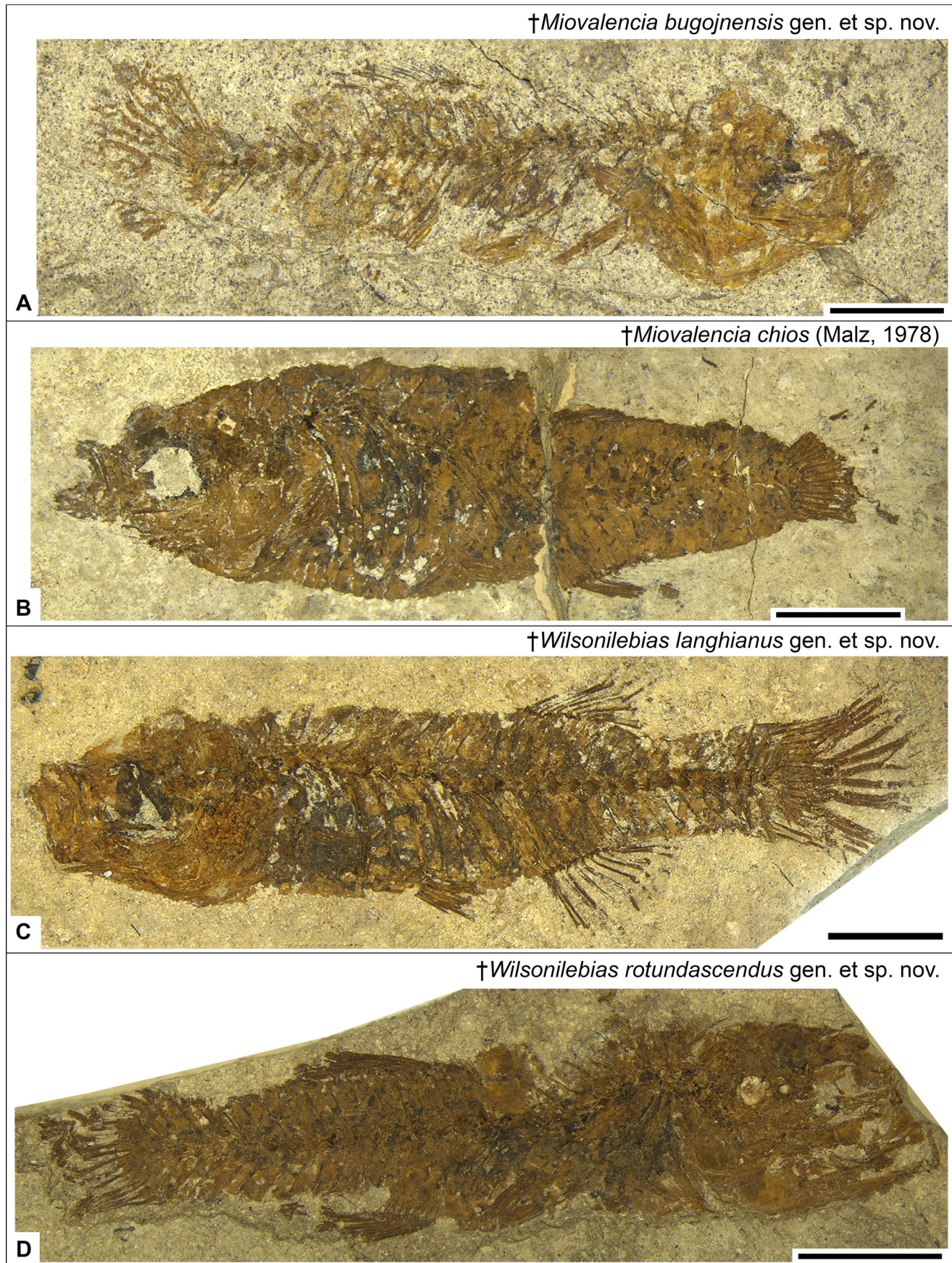
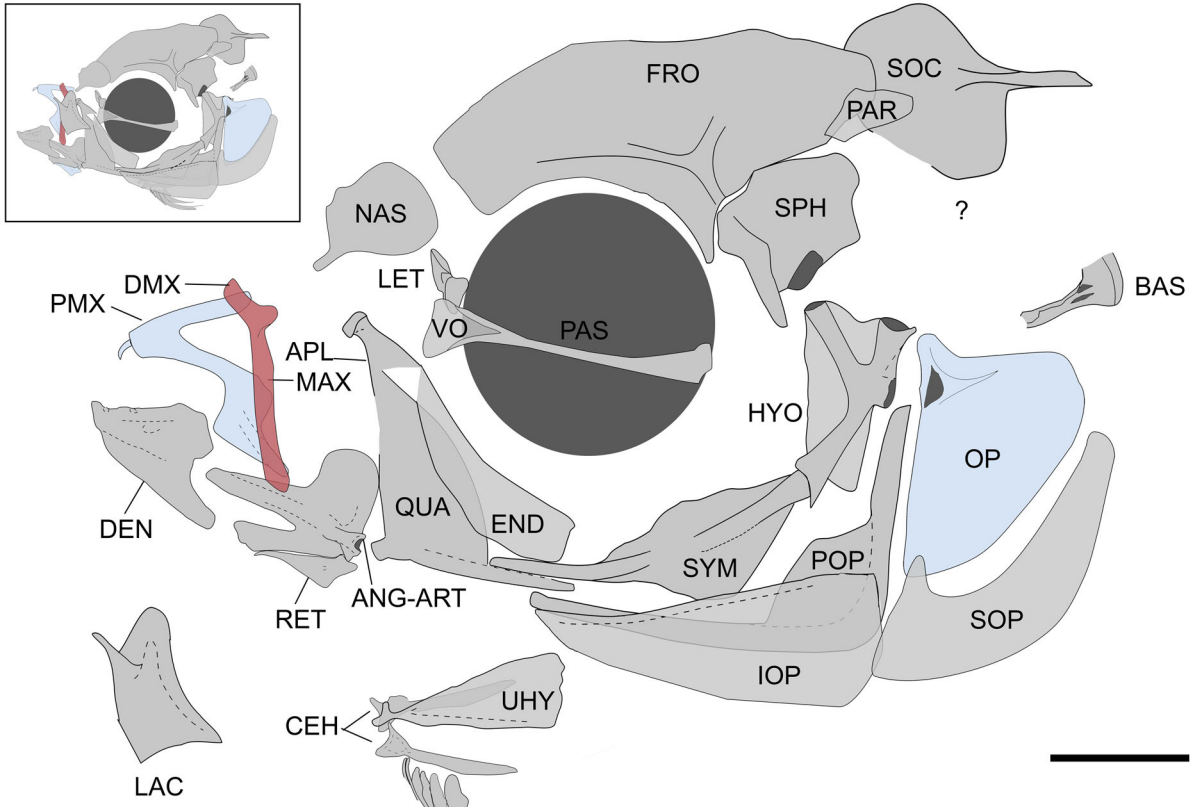
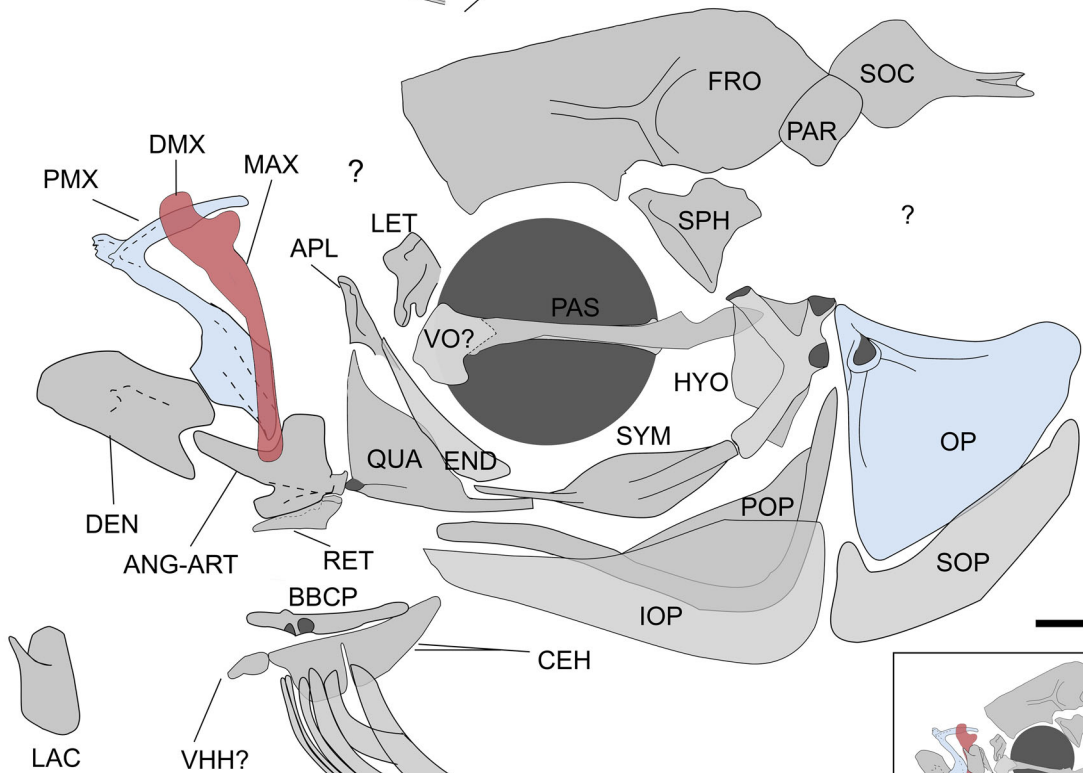


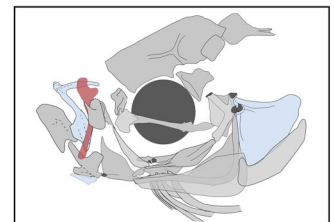
**Figure 4.** **A, C, D**, holotypes of the three new valenciid species from the Bugojno Basin and **B**, the newly defined skeleton-type. **A**, GRC 011.2 (part). **B**, GRC 204 (counterpart). **C**, GRC 004 (counterpart). **D**, GRC 236.2 (part). Scales = 5 mm.



A †*Miovalencia* gen. nov.



B †*Wilsonilebias* gen. nov.



(Tables 3, 4). Furthermore, the presence of a shallow, straight or slightly ascending sulcus separates the sagitta of †*Miovalencia* gen. nov. from both †*Aphanolebias* (sulcus distinctively curved ventrally at its end, see Fig. 12M–P) and †*Wilsonilebias* gen. nov. (sulcus deep and slightly S-shaped, see Fig. 11A1, B1, C, E1–I1). Additionally, †*Miovalencia* gen. nov. lacks a clear constriction between ostium and cauda (*vs* being present in †*Wilsonilebias* gen. nov.) (Fig. 12A–F). Also the lapillus of †*Miovalencia* gen. nov. displays some taxonomic characteristics including a rounded-rectangular to crescent shape (Fig. 13D, E), *vs* a rounded-rhomboid to drop-shape in †*Wilsonilebias* gen. nov. (Fig. 13F, G) and *vs* a rectangular-trapezoid shape in *Valencia* (Fig. 13A–C). Unfortunately, the lapillus is not known for †*Prolebias*, †*Francolebias* and †*Aphanolebias*.

**Etymology.** The name refers to the Miocene temporality of the new taxon and its similarity with the extant genus *Valencia*. †*Miovalencia* gen. nov. is feminine.

**Remarks.** In the following descriptions, we provide ranges and mean values  $\pm$  standard deviation (SD) for body or bone measurements, and ranges and modal numbers (modes) for meristic counts. In addition, means  $\pm$  SD for all measurements and modes for all counts are listed in Table 1. The underlying details of measurements and counts can be found in Supplemental material Table S1, sheet 1. Comparative meristic data and otolith data from other Valenciidae used for the diagnosis of the new genus are presented in Tables 2 and 3.

**General description.** †*Miovalencia* gen. nov. is a small-sized fish, its SL is between 15.9 and 42.7 mm (mean  $28.3 \pm 6.9$  mm). Head moderately large (HL  $32.3 \pm 2.5\%$  SL, HD  $77.4 \pm 11.3\%$  HL). Snout moderately long (preorbital length  $30.8 \pm 3.4\%$  HL), eyes relatively small (ED  $26.7 \pm 2.8\%$  HL), body moderately deep (BD  $22.4 \pm 3.4\%$  SL). Dorsal and anal fin posteriorly positioned on body, dorsal-fin origin slightly in front of anal-fin origin (predorsal distance  $62.8 \pm 2.6\%$  SL, preanal distance  $66.0 \pm 2.0\%$  SL). Dorsal fin consisting of (9)10–11 rays and pterygiophores each, anal fin composed of 12–13(14) rays and 11–12(13)

pterygiophores. Pectoral fin comprising 9–14 rays and placed relatively low-set at body. Pelvic fin composed of 5–7 rays and positioned closer to anal fin than to pectoral fin (pectoral-pelvic distance  $15.4 \pm 1.7\%$  SL, pelvic-anal distance  $14.6 \pm 1.0\%$  SL). Vertebral column with 25–28 vertebrae of which 10–11 are abdominal and 15–17 caudal. Caudal peduncle relatively long and slender (CPL  $23.5 \pm 1.7\%$  SL, CPD  $13.5 \pm 1.7\%$  SL). Caudal fin palette-shaped, number of principal rays is 15–17. Body and head covered by cycloid scales. The saccular otoliths (sagittae) are of triangular, almost symmetrical shape with a rostrum that is longer than the antirostrum (Table 3, Fig. 10A1–K1, L, M). The lapilli are rounded to crescent shape with the sulculus not continuing to the linea basalis (Fig. 10A2–I2, K2). The single asteriscus is bean-shaped with a deep fossa acustica bounded by two walls (Fig. 10J2).

**Neurocranium and orbital series.** In most specimens, the neurocranium and skull were poorly preserved, or the preservation only allowed to identify a few bones. Thus, we present here a composite skull reconstruction (Fig. 5A, see also Supplemental material Fig. S3), which is based on the details seen in the specimens GRC 003, 016/032, 197, 199, 204, 211, 262, and TPC 001.

The frontal bones are long, broad, and slightly narrowing posteriorly; their lateral rims border the supra-orbital area and, in some specimens, it was possible to identify the parietal bone (Supplemental material Fig. S4a). A disarticulated nasal bone with a possible medial extension was discernible in specimen GRC 003 (Supplemental material Fig. S4c), while a broad, rectangular-shaped lacrimal is exhibited in specimens GRC 047 and GRC 016/032 (Fig. 5A). The parasphenoid crosses the eye at the lower half, narrowing slightly in the middle and widening posteriorly. The vomer has a triangular fan shape. The supraoccipital has a rounded anterior body and a long posterior process (Fig. 5A, visible in GRC 199), but if the latter is bifurcated it is impossible to discern. In some specimens, parts of the basioccipital were visible.

**Jaws.** The jaw joint is situated anterior to the orbit. The premaxilla has a long ‘S’-shaped ramus and a long ascending process, which is broad at its base and

**Figure 5.** Skull reconstruction of **A**, †*Miovalencia* gen. nov. and **B**, †*Wilsonilebias* gen. nov. Skull has been disarticulated for better view of each bone, inset shows reconstruction of articulated skull. Dark grey shading depicts articular faces and foramina; red shading indicates synapomorphic character for Valenciidae; light blue shading shows differences between genera. **Abbreviations:** ANG-ART, angulo-articular; APL, autopalatine; BAS, basioccipital; BRAR, branchiostegal rays; BBP, basibranchial plate; CEH, ceratohyal; DEN, dentary; DMX, dorsal process of the maxilla; END, endopterygoid; FRO, frontal; HYO, hyomandibular; IOP, interopercle; LAC, lachrymal; LET, lateral ethmoid; MAX, maxilla; NAS, nasal; OP, opercle; PAR, parietal; PAS, parasphenoid; PMX, premaxilla; POP, preopercle; QUA, quadrate; RET, retroarticular; SOC, supraoccipital; SOP, subopercle; SPH, sphenotic; SYM, symplectic; UHY, urohyal; VHH, ventral hypohyal; VO, vomer; ?, non-identified. Scale = 2 mm.

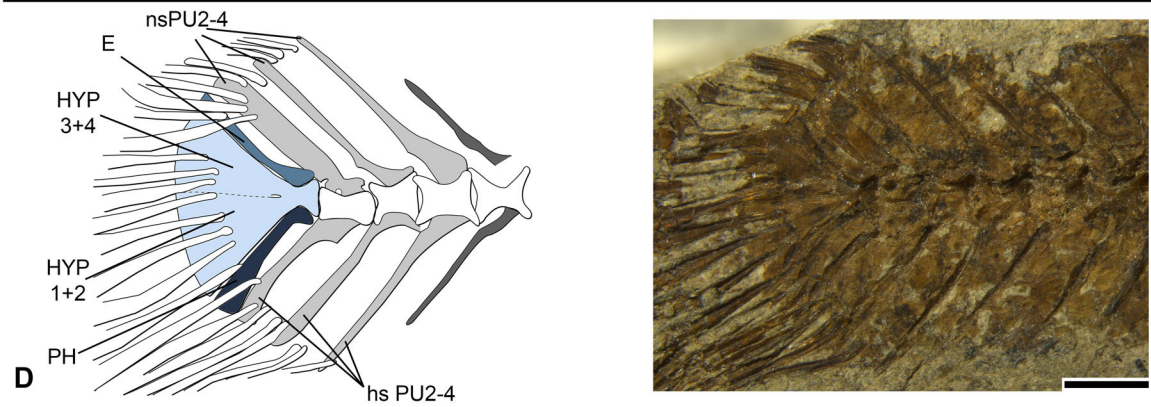
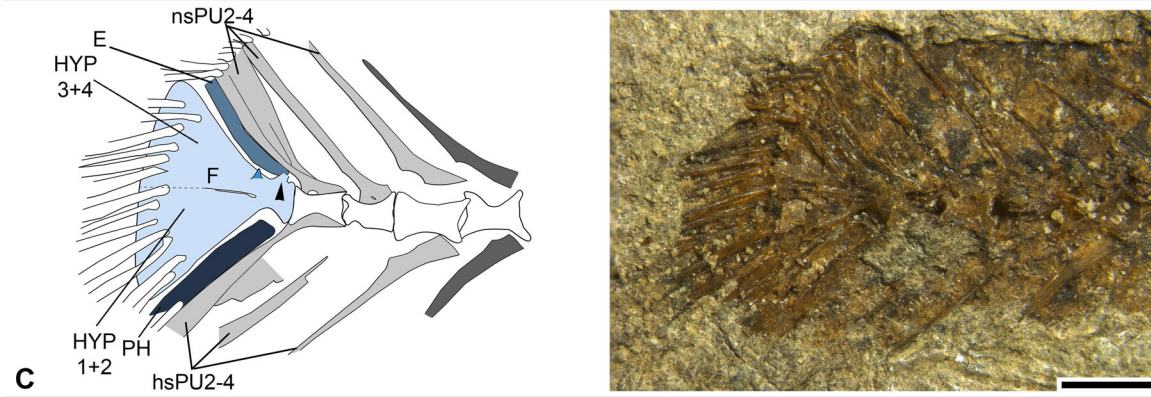
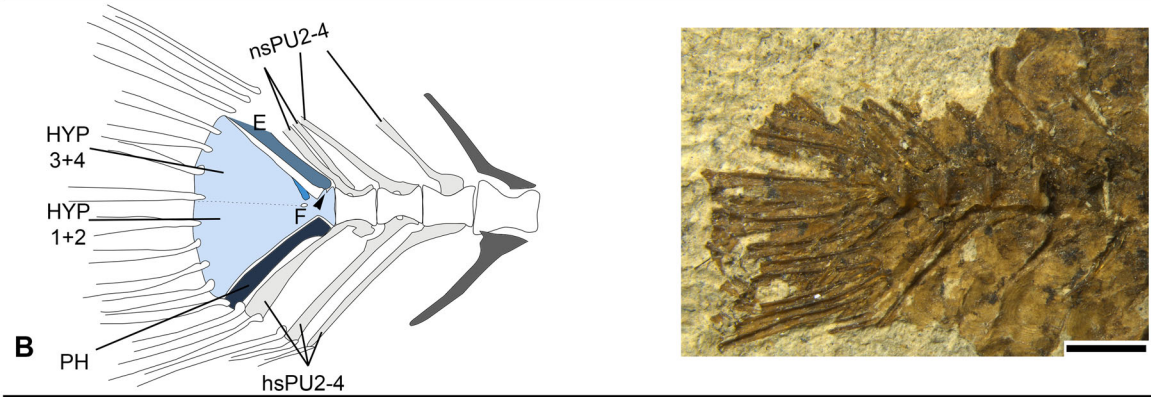
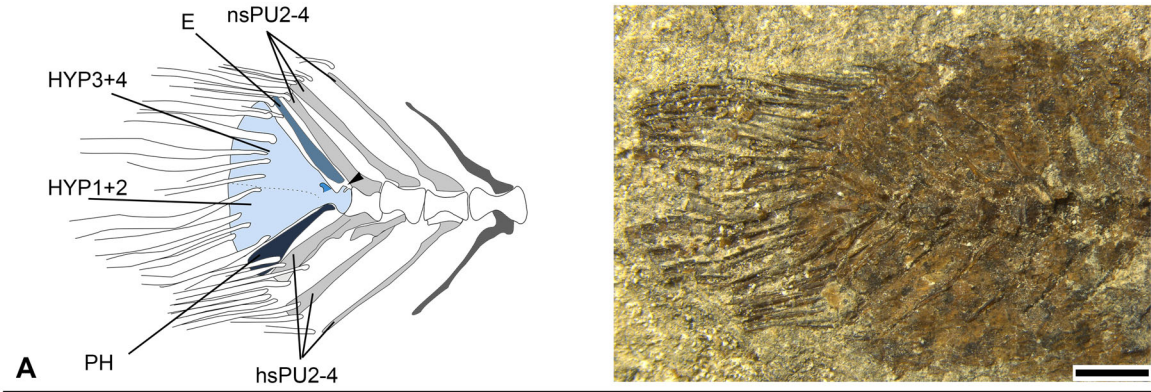
**Table 1.** Morphometric, meristic and osteological characters of the new genera and species from the Bugojno Basin. Total number of specimens belonging to paratypes are given in parentheses. Number of specimens that could be used for the respective character are provided in subscripted parentheses. For the meristic counts, modal numbers were provided if possible. For raw data see [Supplemental material Table S1](#), sheet 1. For measurements and counts see [Fig. 3A](#) and [Supplemental material Figs S1, S2](#).

Genus	† <i>M. bugojnensis</i>		† <i>M. chios</i> (Malz., 1978)		† <i>Miovalencia</i> gen. nov.		† <i>W. langhianus</i>		† <i>W. rotundascendus</i>		† <i>Wilsonilebias</i> gen. nov.	
	Holotype	Paratypes (21)	Holotype	Paratypes (7)	† <i>Miovalencia</i> sp. (8)	Genus (38)	Holotype	Paratypes (16)	Holotype	Paratypes (11)	† <i>Wilsonilebias</i> sp. (5) and cf. specimens (5)	Genus (39)
Species	GRC 011/069		GRC 204		† <i>Miovalencia</i> sp. (8)		GRC 004		GRC 236.2		† <i>Wilsonilebias</i> sp. (5) and cf. specimens (5)	
SL (mm)	31.0	26.2±6.6 <sub>(7)</sub>	32.0	33.5±13.4 <sub>(2)</sub>	27.9±5.9 <sub>(3)</sub>	28.3±6.9 <sub>(14)</sub>	34.9	22.8±6.7 <sub>(5)</sub>	26.8	26.8±2.5 <sub>(3)</sub>	28.0±NA	26.7±5.7 <sub>(13)</sub>
Morphometric characters as percentage of SL (mean±SD <sub>(n)</sub> )												
Prenasal length	66.8	66.8±2.0 <sub>(7)</sub>	65.8	65.0±NA	64.1±1.4 <sub>(3)</sub>	66.0±2.0 <sub>(13)</sub>	65.2	65.4±1.0 <sub>(5)</sub>	65.1	65.0±1.4 <sub>(3)</sub>	66.9±1.6 <sub>(2)</sub>	65.3±1.5 <sub>(12)</sub>
Predorsal length	60.0	63.3±3.2 <sub>(7)</sub>	64.4	62.2±2.6 <sub>(2)</sub>	62.2±1.2 <sub>(3)</sub>	62.8±2.6 <sub>(14)</sub>	63.8	60.7±1.5 <sub>(4)</sub>	62.9	63.1±4.8 <sub>(2)</sub>	62.9±1.4 <sub>(3)</sub>	62.2±2.2 <sub>(11)</sub>
Prepelvic length	51.4	52.2±2.3 <sub>(6)</sub>	52.4	51.5±1.3 <sub>(2)</sub>	51.0±1.2 <sub>(2)</sub>	51.8±1.7 <sub>(12)</sub>	49.5	51.2±1.8 <sub>(5)</sub>	51.0	52.1±3.9 <sub>(3)</sub>	50.4±0.5 <sub>(2)</sub>	51.1±2.2 <sub>(12)</sub>
Prepectoral length	37.2	36.8±2.2 <sub>(6)</sub>	35.6	35.0±1.1 <sub>(2)</sub>	38.1±NA	36.5±1.9 <sub>(11)</sub>	34.7	35.6±1.9 <sub>(5)</sub>	35.7	37.2±5.7 <sub>(3)</sub>	34.8±1.0 <sub>(2)</sub>	36.0±2.9 <sub>(12)</sub>
Caudal peduncle length	21.7	23.3±1.6 <sub>(6)</sub>	23.2	22.9±1.0 <sub>(2)</sub>	25.8±1.0 <sub>(2)</sub>	23.5±1.7 <sub>(12)</sub>	23.6	23.5±0.9 <sub>(5)</sub>	23.9	25.0±2.6 <sub>(3)</sub>	22.3±2.3 <sub>(3)</sub>	23.6±1.8 <sub>(13)</sub>
Pectoral–pelvic distance	14.3	15.3±1.8 <sub>(6)</sub>	16.7	16.5±2.4 <sub>(2)</sub>	13.7±NA	15.4±1.7 <sub>(11)</sub>	14.8	15.8±2.7 <sub>(5)</sub>	15.9	14.9±3.0 <sub>(3)</sub>	16.3±1.6 <sub>(3)</sub>	15.4±2.3 <sub>(13)</sub>
Pelvic–anal distance	15.1	14.8±1.0 <sub>(6)</sub>	13.5	15.1±NA	13.8±0.8 <sub>(2)</sub>	14.6±1.0 <sub>(11)</sub>	16.2	14.8±1.1 <sub>(5)</sub>	13.6	12.8±2.7 <sub>(3)</sub>	15.1±0.1 <sub>(2)</sub>	14.2±1.9 <sub>(12)</sub>
Head length (HL)	33.1	32.2±2.1 <sub>(7)</sub>	30.0	32.5±NA	33.2±4.3 <sub>(3)</sub>	32.3±2.5 <sub>(13)</sub>	31.1	32.5±1.4 <sub>(5)</sub>	32.8	34.1±4.0 <sub>(3)</sub>	32.4±1.1 <sub>(2)</sub>	32.9±2.2 <sub>(12)</sub>
Body depth	24.1	22.2±3.8 <sub>(7)</sub>	24.8	21.0±NA	22.0±4.7 <sub>(3)</sub>	22.4±3.4 <sub>(13)</sub>	22.1	17.8±1.6 <sub>(4)</sub>	20.0	21.3±3.6 <sub>(2)</sub>	18.9±3.8 <sub>(3)</sub>	19.3±2.7 <sub>(11)</sub>
Minimal caud. peduncle depth	13.6	13.2±1.8 <sub>(6)</sub>	13.4	12.8±NA	14.9±2.8 <sub>(2)</sub>	13.5±1.7 <sub>(11)</sub>	14.7	12.1±1.5 <sub>(5)</sub>	13.2	12.7±2.8 <sub>(3)</sub>	11.6±1.3 <sub>(3)</sub>	12.4±1.8 <sub>(13)</sub>
Pelvic fin length	8.8	7.4±1.2 <sub>(6)</sub>	7.5	7.8±NA	7.2±NA	7.5±1.0 <sub>(10)</sub>	NA	7.6±1.3 <sub>(5)</sub>	7.6	7.5±0.1 <sub>(2)</sub>	5.6±NA	7.4±1.2 <sub>(9)</sub>
Pectoral fin length	12.3	10.4±NA	16.9	NA	14.8±NA	13.6±2.8 <sub>(4)</sub>	18.5	11.7±0.3 <sub>(2)</sub>	NA	12.3±4.3 <sub>(2)</sub>	10.4±2.4 <sub>(2)</sub>	12.5±3.4 <sub>(7)</sub>
Anal fin length	NA	13.4±1.9 <sub>(4)</sub>	NA	NA	NA	13.4±1.9 <sub>(4)</sub>	NA	13.5±NA	NA	NA	NA	13.5±NA
Dorsal fin length	NA	12.6±2.0 <sub>(3)</sub>	NA	13.5±NA	NA	12.8±1.7 <sub>(4)</sub>	NA	11.8±NA	17.6	17.3±3.2 <sub>(2)</sub>	18.7±NA	15.9±3.2 <sub>(5)</sub>
Anal-fin base	12.1	10.3±1.0 <sub>(6)</sub>	11.3	12.6±NA	9.8±1.3 <sub>(2)</sub>	10.7±1.2 <sub>(11)</sub>	11.6	11.3±1.3 <sub>(5)</sub>	10.9	10.2±1.5 <sub>(3)</sub>	10.7±0.6 <sub>(2)</sub>	11.1±1.4 <sub>(12)</sub>
Dorsal-fin base	14.9	11.0±1.0 <sub>(6)</sub>	10.9	11.4±2.3 <sub>(2)</sub>	9.5±0.2 <sub>(2)</sub>	11.1±1.7 <sub>(12)</sub>	11.1	11.7±0.6 <sub>(3)</sub>	12.8	10.8±2.3 <sub>(2)</sub>	11.4±2.4 <sub>(3)</sub>	11.4±1.4 <sub>(10)</sub>
Morphometric characters as percentage of HL (mean±SD <sub>(n)</sub> )												
Preorbital length	27.4	31.8±2.4 <sub>(5)</sub>	35.4	30.2±NA	25.3±NA	30.8±3.4 <sub>(9)</sub>	NA	28.7±5.2 <sub>(3)</sub>	28.7	28.2±NA	31.6±0.2 <sub>(2)</sub>	29.1±3.5 <sub>(7)</sub>
Eye diameter	NA	27.0±3.2 <sub>(5)</sub>	27.0	28.7±NA	23.5±NA	26.7±2.8 <sub>(8)</sub>	NA	28.0±5.9 <sub>(3)</sub>	25.5	30.7±NA	25.1±9.5 <sub>(2)</sub>	27.5±5.5 <sub>(7)</sub>
Head depth	71.7	77.9±13.2 <sub>(7)</sub>	88.8	76.4±NA	74.7±12.0 <sub>(3)</sub>	77.4±11.3 <sub>(13)</sub>	76.0	65.6±2.6 <sub>(5)</sub>	75.1	82.3±21.8 <sub>(2)</sub>	70.2±1.5 <sub>(2)</sub>	70.5±9.8 <sub>(11)</sub>
Meristic characters (mode/min-max <sub>(n)</sub> )												
Dorsal-fin rays and pt.	11	(9)10–11 <sub>(11)</sub>	10	(9)10 <sub>(3)</sub>	10–11 <sub>(3)</sub>	10	11	10–11 <sub>(12)</sub> <sub>(5)</sub>	11	(9)10 <sub>(2)</sub>	10	11
Anal-fin rays	>13	12–13 <sub>(10)</sub>	13	13 <sub>(2)</sub>	12–13 <sub>(2)</sub>	(9)10–11 <sub>(17)</sub>	13	13	12	13 <sub>(1)</sub>	10–11 <sub>(6)</sub>	(9)10–12 <sub>(15)</sub>
Anal pt.	13	11–12 <sub>(8)</sub>	12	12 <sub>(3)</sub>	11–12 <sub>(2)</sub>	12–13 <sub>(14)</sub> <sub>(16)</sub>	12	12	12	12 <sub>(1)</sub>	12 <sub>(5)</sub>	12–13 <sub>(17)</sub>
Pelvic-fin rays	6	6 <sub>(6)</sub>	6	6	6 <sub>(3)</sub>	11–12 <sub>(13)</sub> <sub>(14)</sub>	7	6	6	6–7 <sub>(2)</sub>	6 <sub>(4)</sub>	11–12 <sub>(15)</sub>
Pectoral-fin rays	11	13	13	11 <sub>(1)</sub>	13	5–7 <sub>(14)</sub>	15	5–7 <sub>(8)</sub>	NA	14 <sub>(2)</sub>	12	5–7 <sub>(16)</sub>
Caudal-fin rays at HYP plate	7	9–14 <sub>(7)</sub>	5	7 <sub>(1)</sub>	7 <sub>(1)</sub>	9–14 <sub>(13)</sub>	7–8	8–14 <sub>(8)</sub>	NA	8 <sub>(1)</sub>	9–12 <sub>(4)</sub>	8–15 <sub>(15)</sub>
Caudal fin prin. rays	NA	16–17 <sub>(1)</sub>	>12.0	15–16 <sub>(2)</sub>	15–16 <sub>(1)</sub>	5–9 <sub>(11)</sub>	16–17	7–9 <sub>(6)</sub>	NA	NA	(14)16 <sub>(3)</sub>	7–9 <sub>(13)</sub>
						15–17 <sub>(5)</sub>	14–17 <sub>(4)</sub>	17	NA	NA	16	14–17 <sub>(8)</sub>

(Continued)

**Table 1.** (Continued).

Genus	† <i>Miovalencia</i> gen. nov.				† <i>Wilsonilebias</i> gen. nov.							
	† <i>M. bugojnensis</i>		† <i>M. chios</i> (Malz, 1978)		† <i>W. langhianus</i>		† <i>W. rotundascendens</i>					
Species	Holotype GRC 011/069	Paratypes (21)	Holotype GRC 204	Paratypes (7)	† <i>Miovalencia</i> sp. (8)	Genus (38)	Holotype GRC 004	Paratypes (16)	Holotype GRC 236.2	Paratypes (11)	† <i>Wilsonilebias</i> sp. (5) and cf. specimens (5)	Genus (39)
Caudal-fin dorsal pro. rays	NA	5 (1)	NA	5 (1)	5 (1)	5 (3)	6	4-6 (3)	NA	NA	5-6 (2)	6
Caudal-fin ventral procurrent rays	NA	5 (1)	NA	5 (1)	NA	5 (2)	6	3	NA	NA	4-6 (2)	6
Total vertebrae	26-27	26-27 (9) 10-11 (9)	27	26-28 (3)	25-26 (3)	(25)26-28 (17) 10-11 (6)	28	27	27	26-28 (2)	27	27
Abdominal vertebrae	10-11	10-11 (9)	11	11	10-11 (2)	10-11 (6)	12	10-11 (6)	11	10 (1)	26-27 (5) (10)11 (3)	11
Caudal vertebrae	16	16	16	16	16	16	16	16	16	16	16 (5)	16
Precural vertebrae	3	3	3	3 (2)	3 (2)	3	3	3 (7)	3	15-16 (3) 3 (3)	3 (5)	15-16 (19) 3 (17)
Other morphometry-osteological characters (mean ± SD <sub>(n)</sub> )												
pAL/pDL	1.1	1.1 ± 0.0 (7)	1.0	1.0 ± NA	1.0 ± 0.0 (3)	1.0 ± 0.0 (13)	1.0	1.1 ± 0.0 (5)	1.1	1.0 ± 0.0 (2)	1.1 ± 0.0 (3)	1.0 ± 0.1 (12)
Pelvic W/L ratio (%)	54.9	NA	76.8	70.6 ± NA	68.2 ± 7.5 (3)	67.8 ± 8.6 (6)	NA	67.3 ± 6.9 (6)	NA	77.2 ± 11.0 (2)	68.5 ± 8.2 (3)	69.0 ± 8.0 (11)
2Dr/2Ar ratio	Na	0.9 ± 0.2 (3)	0.5	NA	1.3 ± NA	0.9 ± 0.3 (5)	0.5	0.7 ± 0.1 (2)	1.0	0.9 ± NA	0.8 ± 0.0 (2)	0.8 ± 0.2 (7)
3Dr/3Ar ratio	0.6	0.5 ± 0.1 (3)	0.5	NA	0.8 ± NA	0.5 ± 0.1 (6)	0.4	1.0 ± 0.2 (3)	1.1	1.0 ± NA	0.8 ± 0.1 (2)	0.9 ± 0.3 (8)
ns-PU2/ns-PU4 ratio	2.9	2.9 ± 0.6 (5)	NA	NA	2.8 ± NA	2.9 ± 0.5 (7)	2.7	4.0 ± 1.3 (5)	4.2	1.9 ± NA	3.1 ± 0.4 (5)	3.4 ± 1.0 (13)
hs-PU2/hs-PU4 ratio	3.8	2.8 ± 0.8 (4)	2.3	NA	3.2 ± NA	2.8 ± 0.7 (7)	3.0	3.0 ± 0.6 (4)	3.4	NA	3.1 ± 0.3 (4)	3.1 ± 0.4 (10)



tapered distally (Fig. 5A, Supplemental material Fig. S3). The maxilla is a straight rod-like bone with a slight curve in the posterior border of the distal portion; its dorsal process is long, slender and somewhat flattened (Supplemental material Fig. S4b). The dentary is long and deep, with a slightly concave lower margin; a medial process is not present (Fig. 5A). The angulo-articular has a long ventral process running almost parallel to the main body of this bone, the coronoid process is large and rounded (Fig. 5A). The retroarticular runs along the ventral process of the angulo-articular; its articular head is shorter than its body (Fig. 5A, Supplemental material Fig. S4b). Both upper and lower jaws possess multiple rows of conical teeth of different sizes (Supplemental material Fig. S5a).

#### Suspensorium, opercular apparatus and hyoid arch.

The quadrate has a triangular shape and bears a slender posteroventral process. The relatively long endopterygoid extends along its posterior margin and anteriorly, it overlaps the ventral portion of the autopalatine, which is slightly bent anteriorly and has a hammer-like head (Fig. 5A). The symplectic is composed of a rod with a bony lamella dorsally and ventrally, which results in its feather-shape. The hyomandibular presents a small posteroventral extension; its articular condyles to the opercle, the pterotic and sphenotic fossae are well preserved (Fig. 5A).

The opercular series is partially well preserved (GRC 177, GRC 199). The preopercle has a boomerang shape, with a convex thin lamella in the middle portion (Fig. 5A); its lower arm extends along the posterior process of the quadrate, while its upper arm, which is almost of similar length, runs along the anterior border of the opercle. The large interopercle has a straight ventral margin and an overall triangular to trapezoidal shape. The opercle is elongate-triangular and slightly longer than wide; the articular facet to the hyomandibular is preserved in multiple specimens. The subopercle is half-moon shaped, its posterior margin reaches behind the mid-height of the opercle.

The preservation of the hyoid arch is poor; however, a complete, triangle-shaped urohyal is visible in specimen GRC 197. It bears a straight ventral border and the articulation process is directed anterodorsally (Fig. 5A). Six branchiostegal rays are recognizable in few

specimens; the two first rays are very thin, while the next ones are more robust (Fig. 5A).

**Pharyngeal jaws.** The pharyngeal jaws were poorly preserved, while straight or slightly curved pharyngeal teeth of different sizes were well visible. In the most posterior internal row of the pharyngeal jaw, the teeth usually reveal an indentation below their crown or a blunt cusp (Supplemental material Fig. S5b5, 8, 11).

Possible 3rd and 4th pharyngobranchials are visible in specimen GRC 177. They show a semi-circular (to drop) shape with a small process and narrow anteromedially; multiple teeth and alveoli that appear to be arranged in rows are recognizable (not figured).

**Axial skeleton.** The vertebral column is composed mostly of 26 vertebrae (rarely 25 or 27–28), of which 10 or 11 are abdominal and 16 (15–17) are caudal. The neural spines of the first three to four vertebrae are flattened and broadened. The neural arch of the first vertebra is relatively shorter than that of the other ones, but it is not possible to discern whether it is completely closed or not. The neural spines of the caudal vertebrae below the dorsal fin have a slight curvature to the head region (Fig. 8A). Nine pairs of ribs are present, starting from the 2nd vertebra. Epipleural ribs were not identifiable.

**Pectoral girdle and fins.** The cleithrum is long with a broadened upper part (well visible in GRC 199, Fig. 7A). Of the post-temporal, only the dorsal tip of the dorsal process is preserved (specimen GRC 007). A possible supra-cleithrum was identifiable in specimen GRC 261.1; it has a bottle shape with a narrower dorsal portion (Fig. 7A). The scapula is posterior to the cleithrum, and bears an elongate scapular foramen (Fig. 7A). The coracoid is of long-triangular shape with a slightly rounded ventral margin. Four poorly preserved radials are recognizable (GRC 011). In some specimens, a long, slender postcleithrum 3 is noticeable (Fig. 7A). The number of pectoral-fin rays is 9–14, the pectoral-fin length is 10.4–16.9% SL ( $13.6 \pm 2.8\%$  SL).

**Pelvic girdle and fins.** The pelvic bone is triangular; its maximum width is 54.9–76.8% of its length ( $67.8 \pm 8.6\%$ ). The anterior margin is rounded and the medial process appears to be short; the presence of an ischial process can be seen in multiple specimens, but

**Figure 6.** Caudal skeleton reconstruction of the four valenciid species from the Bugojno Basin. **A**, †*Miovalencia bugojnensis* gen. et sp. nov. (holotype GRC 177, drawing and photo). **B**, †*M. chios* (skeleton-type GRC 204, drawing and photo). **C**, †*Wilsonilebias langhianus* gen. et sp. nov. (paratype GRC 179 mirrored, drawing and photo). **D**, †*W. rotundascendus* gen. et sp. nov. (holotype GRC 236.2, drawing and photo). Black arrowheads point to prezygapophysis. **Abbreviations:** **E**, epural (blue-grey); **F**, fenestra/anterior gap of hypural plate; **hsPU**, haemal spine of preural vertebrae (light grey); **HYP**, hypural plates (light blue); **nsPU**, neural spine of preural vertebrae (light grey); **PH**, parhypural (dark blue). Scale bars = 1 mm.

**Table 2.** Meristic characters (ranges) of extant and fossil genera and species of Valenciidae. Data for *V. hispanica* from this study, for †*V. arcasensis* from Gaudant et al. (2015), for †*P. stenoura* from Gaudant (2012), for †*F. delphinensis* from Gaudant (1989), for †*F. aymardi* from Gaudant (1988), for †*F. rhenanus* from Gaudant (1981b), for †*F. arvernensis* from Gaudant (2016), and for †*A. meyeri* from Reichenbacher and Gaudant (2003).

	† <i>V.</i>		Genus		† <i>Prolebias</i>		† <i>Francolebias</i>		Genus		† <i>Aphanolebias</i>	
	<i>hispanica</i>	<i>arcasensis</i>	<i>Valencia</i>	<i>stenoura</i>	<i>delphinensis</i>	<i>aymardi</i>	<i>rhenanus</i>	<i>arvernensis</i>	<i>Francolebias</i>	<i>meyeri</i>		
Dr	10	11–12	10–12	12–13	9–10	9–10	9–11	10–11	9–11	9–11	10	
Dpt	10–11	11	10–11	12	9–10	8–9	9–11	9–10	8–11	9–10	9–10	
Ar	13–>14	12	12–14	14–16	11–12	12	12–13	11–13	11–13	11–13	11–14	
Apt	12–14	12	12–14	14–15	10–11	11	11–12	10–12	10–12	10–12	10–12	
Pelr	NA	NA	NA	6	6	6	6	6	6	6	6–7	
Pecr	12–13	16	12–16	15	14–15	13–14	13	14–15	13–15	13–15	12–15	
Cprnr	17	NA	17	10	12	11	12	12	11–12	11–12	15–16	
Dpror	7	NA	7	8–9	7–10	6–9	7–8	8–9	6–10	6–10	NA	
Vpror	8–7	NA	7–8	8–9	8–9	6–9	7–8	8–9	7–9	7–9	NA	
TV	30	28	28–30	30–31	27–28	27–28	28–29	30–31	27–31	27–31	28–29	
aV	13–14	12	12–14	11–12	NA	10–11	12	NA	10–12	10–12	NA	
cV	16–17	16	16–17	18	17–18	17–18	16–17	18–19	17–19	17–19	15	
PU	3–4	NA	3–4	3	3	3	3	3	3	3	3	

**Abbreviations:** Apt, anal-fin pterygiophores; Ar, anal-fin rays; Av, abdominal vertebrae; Cprnr, caudal-fin principal rays (branched and articulated to hypural bone in †*Prolebias* and †*Francolebias*); cV, caudal vertebrae; Dpror, caudal-fin dorsal procurent rays; Dpt, dorsal-fin pterygiophores; Dr, dorsal-fin rays; Pecr, pectoral-fin rays; Pelr, pelvic-fin rays; PU, preural vertebrae; TV, total vertebrae; Vpror, caudal-fin ventral procurent rays. For sources and data see Supplemental material Table S1, sheet 2.

does not appear to be very long (Fig. 7B). The pelvic fin consists of 5–7 rays and is relatively short (length 5.5–9.0% SL, 7.5 ± 1.0% SL).

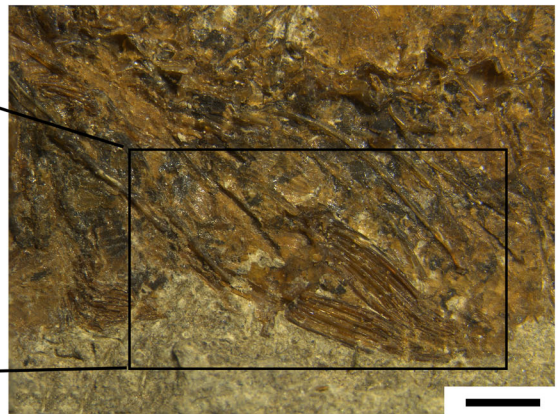
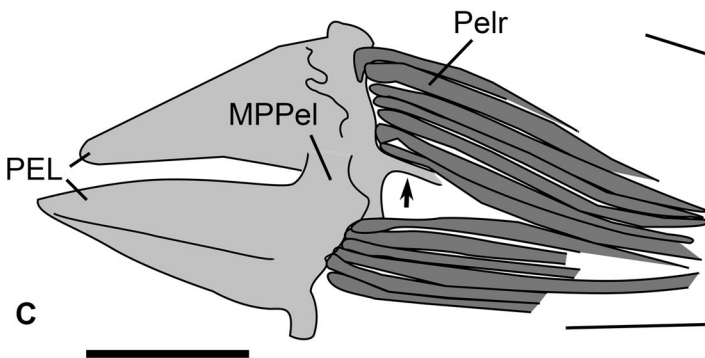
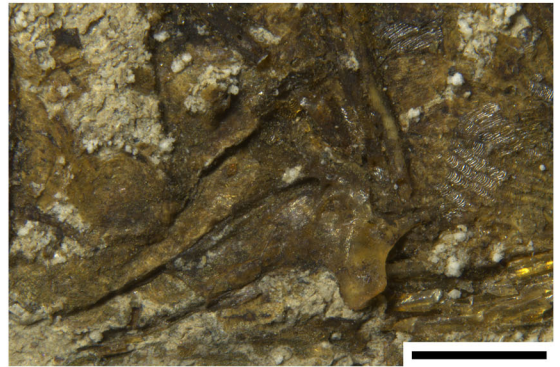
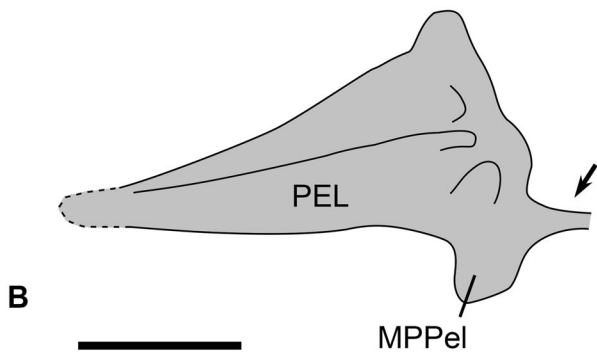
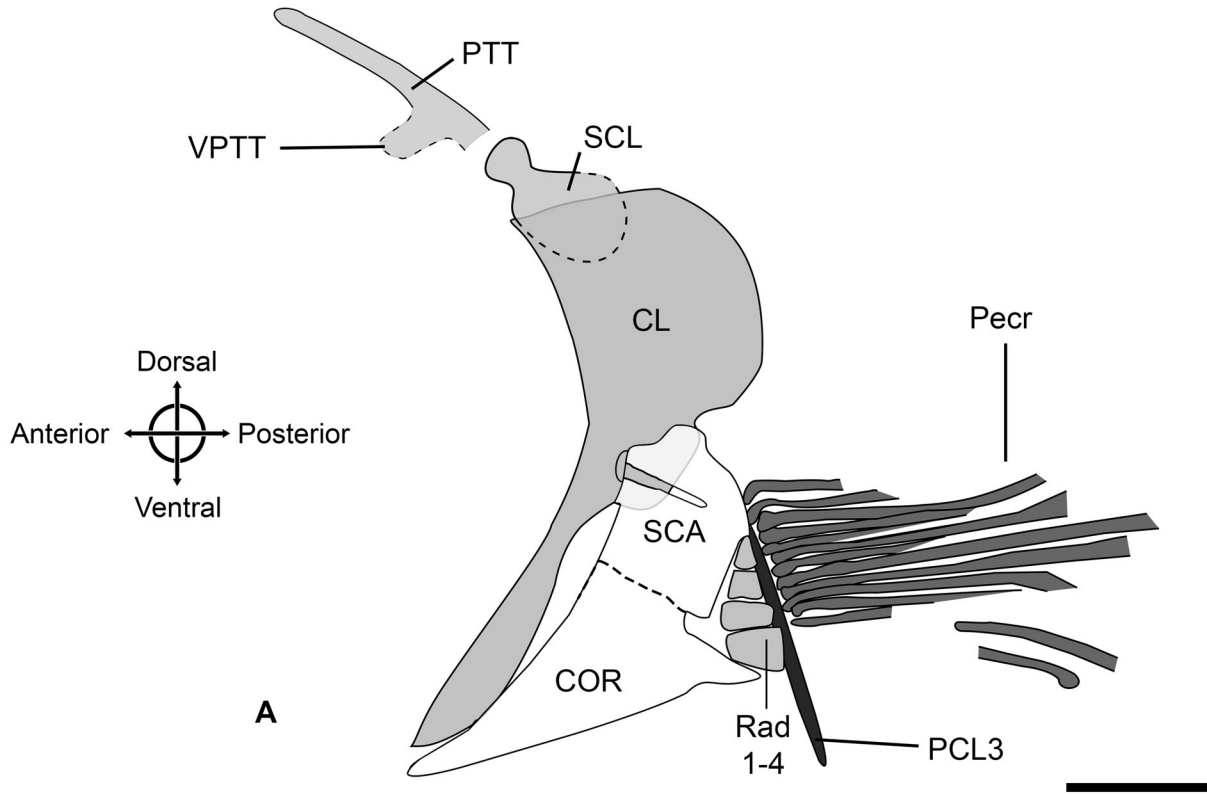
**Dorsal and anal fins.** The dorsal fin consists of (9)10–11 rays and pterygiophores. The first pterygiophore is deeply split into two long, rod-shaped bones, with an enlarged bone lamella between them and also behind the second rod, giving the first pterygiophore a triangular shape (Fig. 8A1–A3, C). The following pterygiophores are also long and display a thin bony lamella associated to the main rod-like structure (Fig. 8A1, A2). The dorsal-fin length is relatively short (10.6–14.2% SL, 12.8 ± 1.7% SL), with its base measuring 9.3–14.9% SL (11.1 ± 1.7% SL).

The number of anal-fin rays is 12–13, and the number of supporting pterygiophores is usually 11–12 (rarely 13). The first anal-fin pterygiophore is thin and reaches the middle portion of the haemal spine of the second caudal vertebra (Fig. 9A); the following pterygiophores gradually diminish in size. A small thin lateral bone expansion is recognizable at the first up to the fourth pterygiophore. The anal-fin length is slightly longer than that of the dorsal fin (11.1–15.5% SL, 13.4 ± 1.9% SL), its base being 8.6–12.6% SL (10.7 ± 1.2% SL).

**Caudal fin and skeleton.** The caudal fin comprises 15–17 principal rays and five dorsal and ventral procurent rays. Neural and haemal spines of three preural vertebrae (PU 2–4) contribute to the support of the caudal-fin rays (Fig. 6A, B). Both the neural and haemal spine of PU 2 are mostly about three times wider than the corresponding spines of PU 4 (nsPU2/nsPU4 ratio 2.9 ± 0.5; hsPU2/hsPU4 ratio 2.8 ± 0.7). The haemal spine of PU 2 has a thin bony expansion anteriorly.

The caudal skeleton is composed of the terminal centrum, which is fused to a fan-shaped hypural plate (Fig. 6A, B). The terminal centrum bears anteriorly a dorsally projecting prezygapophysis, while the posterodorsal margin of the terminal centrum presents a spine-shaped lateral process. The hypural plate is typically fused, but in some specimens a very small foramen is visible anteriorly between the upper and lower hypural plates (Fig. 6B), while in others only a thin suture is evident (Fig. 6A). There is one straight epural, with a slightly widened or slightly rounded proximal portion that is almost in contact with the anterior margin of the terminal centrum. The parhypural is usually in contact or overlapping the posteroventral end of the terminal centrum. Its proximal portion is rounded or rectangular, while it broadens distally.

**Scales.** The entire body is covered with scales. Head scales are present and are larger than body scales. Flank scales are of rounded to ovate shape and present 7 to 8



radii in †*M. bugojnensis* gen. et sp. nov., and up to 14 radii in †*M. chios* (Supplemental material Fig. S7a, b).

**Pigmentation.** Specimen TPC 001 displays the preserved original pigmentation patterns, with three clear dark stripes in the peduncle area (Supplemental material Fig. S8). Other individuals show spots all over the body, principally in the dorsal region, which may also relate to the original pigmentation.

**Otoliths.** The sagittae are triangular-shaped (Fig. 10A1–K1, L, M); the length-height index is 1.04–1.35 (1.16 ± 0.07). The antirostrum is clearly shorter than the rostrum (AL 7.7 ± 2.6%, RL 16.3 ± 3.2%). The posterior margin may exhibit a clear posteroventral angle, resulting in a symmetric appearance. The excisura angle is mostly around 90° (93.2 ± 13.6). The sulcus is straight (†*M. bugojnensis* gen. et sp. nov.), slightly ascending (†*M. chios*) or slightly bent posteriorly (†*M. angulosa*). The ostium is usually slightly wider than the cauda. A shallow or well-developed crista superior is present.

The lapilli (Figs 10A2–I2, K2, 13D, E) are rounded-to crescent-shaped, with the sulculus running from the extremum anterior along the lateral margin to the extremum posterior. The posterior section of the lateral margin is almost straight, while the medial margin can be rounded (typical for †*M. bugojnensis* gen. et sp. nov., Fig. 13D) or can create a corner at the medial edge (typical for †*M. chios*, Fig. 13E). The linea basalis is not profound or not visible. The single asteriscus that was preserved in one specimen (GRC 261) is bean-shaped with a straight dorsoanterior margin and rounded ventrally (Fig. 10J2).

#### †*Miovalencia bugojnensis* gen. et sp. nov.

(Figs 4A, 6A, 8A, 9A, 10A–H, 12A, 13D; Supplemental material Figs S5a6, S5b3–12, S7a)

**Etymology.** The name refers to the Bugojno Basin, where this species was found.

**Type material.** Holotype: GRC 011.2/069.1 (s + 1). Twenty-one paratypes: GRC 007cp (s), GRC 019p (s), GRC 021/022 (s + 1), GRC 038.5/038.1 (s), GRC 038.3/038.6 (s), GRC 038.2/038.4 (s + 1), GRC 045.2/045.1 (s + 1), GRC 047.2/047.1 (s), GRC 055 (s + 1), GRC 177.2/177.1 (s + 1); GRC 182.1/182.2 (s + 1), GRC

197.1/197.2 (s + 1), GRC 199cp (s + 1), GRC 206.2/206.1 (s + 1), GRC 211.1/211.2 (s + 1), GRC 214.2/2114.1 (l), GRC 245.2/245.1 (s), GRC 246cp (s + 1), GRC 256.2/256.1 (s + 1), GRC 259cp (s + 1), NHMW 001p (s). Except for GRC 055, which is preserved in dorsal view, all type specimens are preserved in lateral view.

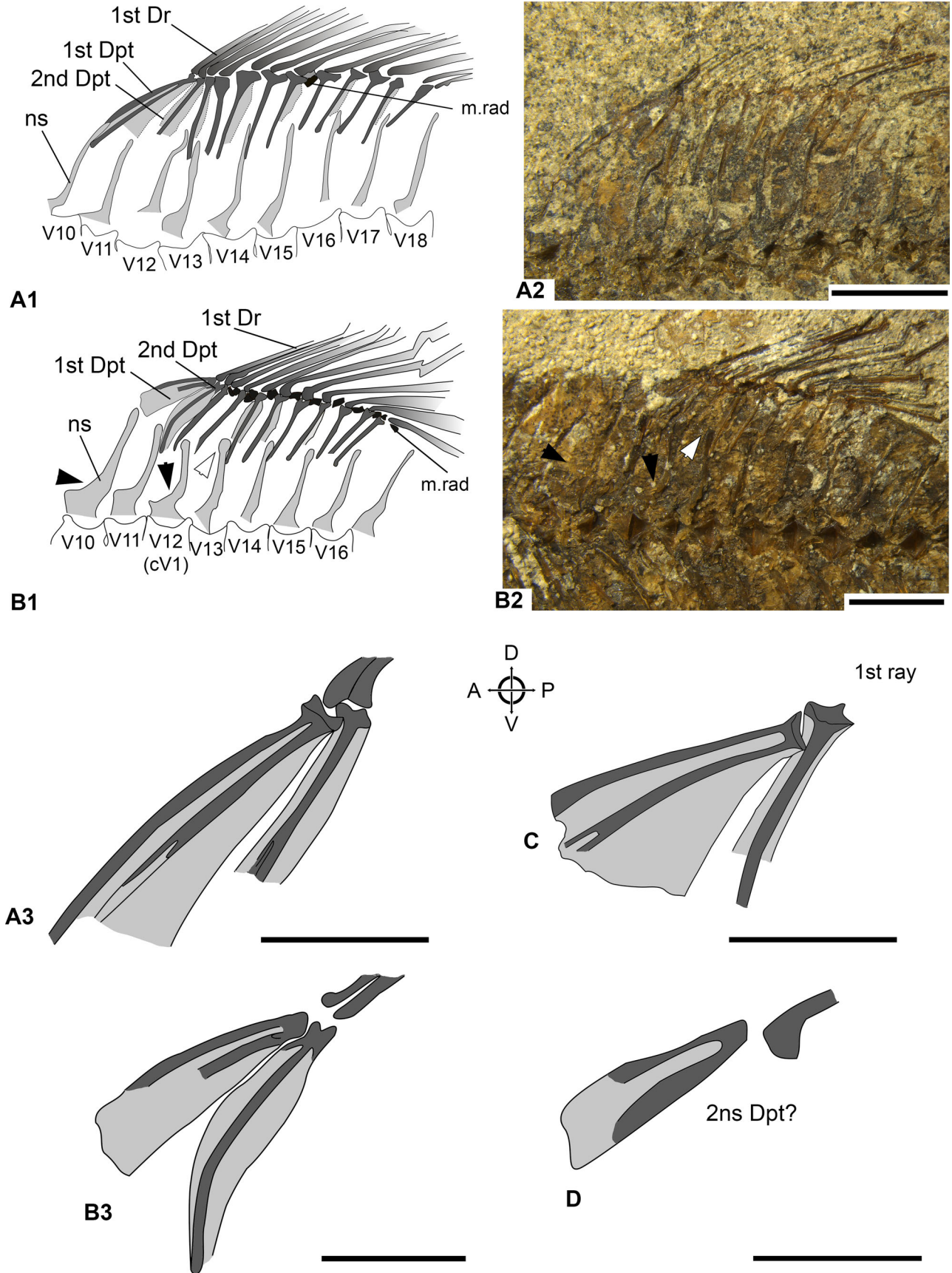
**Type locality and age.** Gračanica, Bugojno Basin, Bosnia and Herzegovina; Middle Miocene (Langhian), 14.8–14.55 Ma.

**Differential diagnosis.** †*Miovalencia bugojnensis* gen. et sp. nov. differs from the only other skeleton-based species †*M. chios* in the narrow, rectangular-shaped bony lamella of the 1st dorsal-fin pterygiophore (vs wide, triangular-shaped; see Fig. 8A3 vs 8C), and also in the relatively small, rounded scales with 7–8 radii (vs relatively big, ovate scales with roughly 14 radii; see Supplemental material Fig. S7a vs 7B). Sagitta morphometry is not different between the two species (Table 3), but the sulcus is mostly straight in †*M. bugojnensis* gen. et sp. nov. (Figs 10A1–H1, 12A), whereas the sulcus is mostly slightly ascending in †*M. chios* (Figs 10I1–K1, L, M, 12B, C). Moreover, the lapillus of †*M. chios* is rounded or rounded-rectangular (Figs 10A2–H2, 13D), whereas the lapillus displays a crescent shape with a clear corner at the medial edge in †*M. chios* (Figs 10I2, K2, 13E).

From the otolith-based species †*M. angulosa*, the sagittae of †*M. bugojnensis* gen. et sp. nov. can be discriminated by a significantly greater relative rostrum height (R 43.2 ± 3.9% vs 35.0 ± 4.1%, Welch–ANOVA test with Games–Howell post-hoc,  $p < 0.05$ ) and a tendency to possess a smaller relative antirostrum height (A 26.9 ± 4.8% vs 33.0 ± 7.4%) (Table 3). Additionally, the sulcus shape in †*M. bugojnensis* gen. et sp. nov. is straight, whereas it is terminally slightly bent in †*M. angulosa* (Fig. 12D).

**General description.** Same as for the genus, except for the characters mentioned in the differential diagnosis. For morphometric and meristic characters see Table 1, for otolith morphometry see Table 3.

**Figure 7.** A, pectoral and B, C, pelvic girdle reconstructions for †*Miovalencia* gen. nov. and †*Wilsonilebias* gen. nov. from the Bugojno Basin. A, pectoral girdle and fin based on both new genera (specimens GRC 004, 196.1, 199, 261). B, right pelvic bone based on †*M. chios* (specimen GRC 016/032, drawing and photo). C, both pelvic bones based on †*W. rotundascendus* gen. et sp. nov. (holotype GRC 236.2, drawing and photo). Arrows indicate the ischial process. **Abbreviations:** CL, cleithrum; COR, coracoid; MPPel, medial process of the pelvic; SCA, scapula; SCL, supra-cleithrum; PCL3, postcleithrum 3; PECr, pectoral-fin rays; PEL, pelvic bone; PELr, pelvic-fin rays; PTT, post-temporal; Rad, radials of pectoral girdle; VPTT, ventral process of the post-temporal. Scale = 1 mm.



†*Miovalencia chios* (Malz, 1978) (comb. nov.)

(Figs 4B, 6B, 7B, 8C, 10I–M, 12B, C, 13E;

Supplemental material Figs S3, S4a, S4c, S5b2, S7b)

\*1978 *Aphanius* (*Aphanius*) *chios* n. sp. Malz: p. 458–459, fig. 1f, pl. 1, figs 8, 9, pl. 2, figs 10, 11, pl. 3, figs 24, 25 (otoliths only).

2004 *Aphanolebias chios* (Malz, 1978); Reichenbacher, Gaudant, et al.: p. 51.

2009 *Aphanius chios* Malz, 1978; Reichenbacher and Kowalke: p. 45, figs 3k–n.

**Remark.** In the initial diagnosis of ‘*Aphanius*’ *chios*, which was solely based on otoliths, Malz (1978) mentioned that the otoliths are characterized by a convex ventral margin that curves upwards to a short rostrum (Fig. 12C) and assumed that they document a relatively small species. Among the skeleton-based specimens of †*Miovalencia* gen. nov., seven specimens exhibited otoliths *in situ* that are similar to those described and figured by Malz (1978) and later also by Reichenbacher and Kowalke (2009). Like the otoliths from the Chios Island, the otoliths have a slightly convex ventral margin terminating in a short, slightly rounded or blunt rostrum, the antirostrum is slightly pointed and shorter than the rostrum, the excisura is ‘V’-shaped and narrow, the sulcus is shallow with a wide ostium and the cauda rises posteriorly and terminates with a tapering point (Figs 10I1–K1, L, M, 12B). Only their length-height index is slightly higher than in the otoliths from the Chios Island ( $1.2 \pm 0.09$  vs  $1.13 \pm 0.02$ ) (Table 3). Due to their similarities with the otoliths of ‘*Aphanius*’ *chios* Malz, 1978, these otoliths from the Bugojno Basin were classified as †*M. chios* (Malz, 1978).

**New material.** 7 specimens: GRC 003.2/003.1 (s), GRC 016/032 (s+1), GRC 058.1/058.3 (s+1); GRC 185.2/185.1 (s), GRC 204.1/204.2 (s+1), GRC 229.1/229.2 (s+1), GRC 261.2/261.1 (s+a). Specimen GRC 204 is selected as the skeleton-type of this species.

**Further material.** Specimen SNSB-BSPG 2024 I 80 (skeleton with sagitta), shown in Supplemental material Fig. S8).

**Type locality and age.** Middle Miocene (Langhian) Nenita Beds from the Chios Island, Greece (Malz, 1978).

**Differential diagnosis.** As described above, the skeleton of †*M. chios* differs from that of †*M. bugojnensis* gen. et sp. nov. in a wide-triangular (vs elongate) bony lamella of the 1st dorsal-fin pterygiophore (Fig. 8C vs 8A3). The scales of †*M. chios* are relatively large and ovate (vs round in †*M. bugojnensis* gen. et sp. nov.) and possess about 14 radii (vs 7–8) (Supplemental material Fig. S7b vs S7a). The otoliths of †*M. chios* differ from those of †*M. bugojnensis* gen. et sp. nov. in the slightly ascending sulcus of the sagitta (Figs 10I1–K1, L, M, 12B, C), and a lapillus that has a crescent shape characterized by a medial edge (Figs 10I2, K2, 13E). Furthermore, the sagitta of †*M. chios* differs from the sagitta of †*M. angulosa* (Fig. 12D) in a tendency towards a smaller antirostrum height ( $A 26.4 \pm 4.5\%$  vs  $33.0 \pm 7.3\%$ ), a greater rostrum height ( $R 42.5 \pm 4.5\%$  vs  $35.0 \pm 4.1\%$ ), and the slightly ascending sulcus (vs terminally bent). For further figures of †*M. angulosa* see Steurbaut (1978, figs 11–18) and Reichenbacher and Kowalke (2009, fig. 3a–d).

**General description.** Same as for the genus, except for the characters mentioned in the differential diagnosis. For morphometric and meristic characters see Table 1, for otolith morphometry see Table 3.

†*Miovalencia* sp.

(Fig. 5A, Supplemental material Fig S4b)

**Material.** Eight specimens: GRC 001 (s+1), GRC 005 (s), GRC 010 (s), GRC 048, GRC 049, GRC 217 (s+1), GRC 242 (s), GRC 249 (s+1).

**Remark.** These specimens are either partially preserved skeletal remains or the skeleton is complete but poorly preserved. Some of them show that the posterior anal-fin pterygiophores are decreasing in size. The specimens are assigned to †*Miovalencia* gen. nov. because their otoliths preserved *in situ* (sagittae or lapilli or both) display the typical shape of that genus, but the otoliths are too poorly preserved to allow species identification.

Genus †*Wilsonilebias* gen. nov.

**Type species.** †*Wilsonilebias langhianus* gen. et sp. nov.

**Figure 8.** A1, A2, B1, B2, dorsal fin skeleton and A3, B3, C, D, close-up of 1st and 2nd pterygiophores of the four valenciid species from the Bugojno Basin. A, †*Miovalencia bugojnensis* gen. et sp. nov. (holotype GRC 011/069.1). B, †*Wilsonilebias langhianus* gen. et sp. nov. (holotype GRC 004.1/004.2; black arrows indicate curvature in neural spines, white arrows indicate modified spines). C, †*M. chios* (specimen GRC 016/032). D, †*W. rotundascendus* gen. et sp. nov. (holotype GRC 236.2). **Abbreviations:** A, anterior; cV1, first caudal vertebra; D, dorsal; Dpt, dorsal-fin pterygiophore; Dr, dorsal-fin ray; m.rad, middle radial; ns, neural spine; P, posterior; V, ventral; V10–18, vertebra number. Scale bar = 2 mm in A1, A2, B1, B2, and 1 mm in A3, B3, C, D.

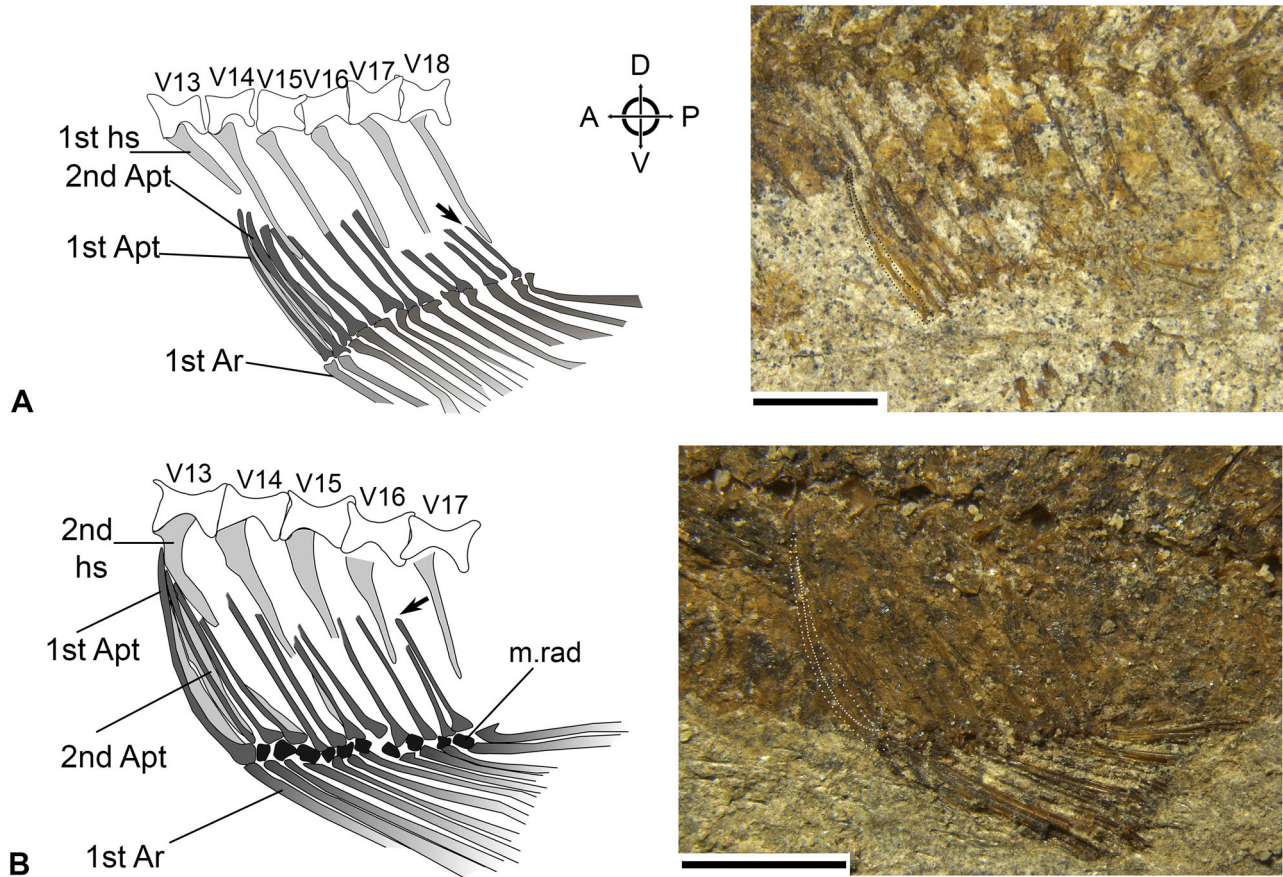


**Figure 9.** Anal fin skeleton of †*Miovalencia* gen. nov. and †*Wilsonilebias* gen. nov. from the Bugojno Basin. **A**, based on †*M. bugojnensis* gen. et sp. nov. (holotype GRC 011/069.1 mirrored, drawing and photo); **B**, based on †*W. langhianus* gen. et sp. nov. (paratype GRC 179, drawing and photo). **Abbreviations:** A, anterior; Apt, anal-fin pterygiophore; Ar, anal-fin ray; D, dorsal; hs, haemal spine; m.rad, middle radial; P, posterior; V, ventral; V13–18, vertebra number. Scale bar = 2 mm. Note that the pterygiophores are partially only preserved as imprints and therefore not well detectable in the photos; to facilitate understanding the first pterygiophore is indicated in each photo.

**Other species.** †*Wilsonilebias rotundascendus* gen. et sp. nov. from the same locality and strata of the type species.

**Diagnosis.** †*Wilsonilebias* gen. nov. shares with other valenciids the synapomorphic characters described by Parenti (1981) and Costa (2012a): (i) slender dorsal process of maxilla, extending over ascending process of premaxilla (Fig. 5B), and (ii) neural spine of PU 2 about three times wider than neural spine of PU 4 (Fig. 6C, D). Additionally, †*Wilsonilebias* gen. nov. shares with other valenciids: long ascending process of premaxilla (Fig. 5B, Supplemental material Fig. S4d), conical jaw teeth arranged in multiple rows and posteriorly positioned unpaired fins (Fig. 4C, D).

†*Wilsonilebias* gen. nov. can be distinguished from other valenciid genera by the following unique combination of osteological characters: (i) broad pelvic bone, width about 69% of length (Fig. 7C, Table 1) (*vs* 50%

in *Valencia* and †*Prolebias*; (ii) relatively short, robust 1st dorsal-fin pterygiophore (Fig. 8B, D) (*vs* long, slender in †*Miovalencia* gen. nov.); (iii) 1st dorsal-fin pterygiophore unfused from 2nd pterygiophore (Fig. 8B, D) (*vs* fused in †*Francolebias*); (iv) long anterior anal-fin pterygiophores, reaching proximal portion of adjacent haemal spine (Fig. 9B) (*vs* short and not reaching beyond middle portion of haemal spine in *Valencia*, †*Prolebias*, †*Miovalencia* gen. nov.); (v) long posterior anal-fin pterygiophores, similar in length to preceding ones, last ones still reaching middle portion of haemal spines (Fig. 9B) (*vs* gradually diminishing, last ones not reaching the haemal spines in *Valencia*, †*Prolebias* and †*Miovalencia* gen. nov.); (vi) widened or robust haemal spines above anal fin in putative males (Fig. 9B) (*vs* unmodified in all other valenciids except †*Francolebias*); (vii) partially fused hypural plate, anteriorly with elongated fenestra (Fig. 6C, D) (*vs* unfused in †*Prolebias*; *vs* fused or with suture in

**Table 3.** Comparison of sagittal morphometry between the four species from the Bugojno Basin and previously described otoliths of Valenciidae. All values given as percentage of otolith length (DL, ML, al, r) or otolith height (a, r) except angle measurements for the excisura (E).

	n	L-H	DL	ML	a	r	al	rl	E
† <i>M. bugojnensis</i>	24	1.07-1.29 (1.15 ± 0.06)	77.9-90.6 (84.4 ± 3.2)	72.6-87.7 (79.5 ± 3.6)	11.5-32.1 (26.9 ± 4.8)	34.9-49.6 (43.2 ± 3.9)*	1.6-13.2 (7.8 ± 2.8)	10.3-24.3 (16.2 ± 2.9)	65.0-121.7 (89.9 ± 13.8)
† <i>M. chios</i> (Bugojno Basin)	10	1.10-1.32 (1.20 ± 0.09)*	79.3-86.7 (83.0 ± 2.5)	72.5-81.9 (78.1 ± 3.3)	21.8-34.0 (27.2 ± 4.8)	35.7-47.3 (43.1 ± 3.8)	5.0-14.4 (8.0 ± 3.19)	13.2-21.9 (17.9 ± 3.5)	74.4-107.8 (91.1 ± 12.8)
† <i>M. chios</i> (Chios, Greece)	6	1.11-1.15 (1.13 ± 0.02)*	79.4-87.6 (82.8 ± 2.9)	74.3-88.8 (79.6 ± 5.2)	20.7-30.2 (25.2 ± 4.0)	34.3-50.0 (41.6 ± 5.7)	4.6-10.0 (7.3 ± 2.2)	7.5-19.3 (8 ± 4.3)	83.0-132.0 (102.2 ± 16.8)
† <i>M. angulosa</i>	4	1.04-1.19 (1.14 ± 0.07)	82.6-90.7 (86.3 ± 3.6)	78.7-84.9 (82.4 ± 2.7)	23.1-40.7 (33.0 ± 7.4)	29.5-39.3 (35.0 ± 4.1)*	4.9-10.9 (8.6 ± 2.7)	12.9-19.3 (14.9 ± 3.0)	72.6-104.7 (91.4 ± 13.8)
† <i>Miovalencia</i> (all species)	50	<b>1.04-1.35</b> (1.16 ± 0.07)	<b>73.2-90.7</b> (83.8 ± 3.5)	<b>72.5-88.8</b> (79.5 ± 3.5)	<b>11.5-40.7</b> (27.3 ± 5.1)	<b>29.5-50.0</b> (41.4 ± 4.6)	<b>1.6-14.4</b> (7.7 ± 2.4)	<b>7.5-24.3</b> (16.2 ± 3.0)	<b>65.0-132.0</b> (93.2 ± 13.6)
† <i>W. langhianus</i>	19	1.03-1.30 (1.16 ± 0.08)	79.4-90.2 (83.7 ± 3.1)	70.4-86.4 (78.7 ± 3.7)	21.4-41.3 (33.0 ± 5.3)	34.0-43.7 (38.7 ± 3.1)*	5.1-14.0 (9.4 ± 2.4)	9.1-22.6 (17.6 ± 3.7)	68.0-119.4 (86.6 ± 15.0)
† <i>W. rotundascendus</i>	13	1.06-1.22 (1.13 ± 0.04)	78.6-88.5 (84.3 ± 3.5)	71.3-86.5 (80.5 ± 4.6)	9.9-42.9 (28.8 ± 8.5)	31.2-39.8 (35.9 ± 2.8)*	1.4-17.1 (6.8 ± 4.2)	10.0-24.0 (15.4 ± 3.9)	52.2-120.7 (91.8 ± 17.6)
† <i>Wilsonilebias</i> (all species)	43	<b>1.03-1.34</b> (1.16 ± 0.07)	<b>74.8-91.8</b> (82.9 ± 4.1)	<b>70.4-86.5</b> (78.7 ± 4.2)	<b>9.9-43.9</b> (31.7 ± 6.5)	<b>31.2-45.3</b> (38.7 ± 3.4)	<b>1.4-17.1</b> (8.4 ± 3.4)	<b>9.1-27.0</b> (17.0 ± 4.0)	<b>52.2-120.7</b> (88.2 ± 14.3)
† <i>Prolebias symmetricus</i>	7	<b>0.92-1.04</b> (0.97 ± 0.04)	<b>69.4-89.1</b> (79.8 ± 6.3)	<b>78.0-88.2</b> (82.2 ± 3.7)	<b>11.0-20.3</b> (14.7 ± 3.7)	<b>36.6-49.7</b> (42.7 ± 4.1)	<b>0.1-5.0</b> (1.8 ± 1.9)	<b>6.5-16.5</b> (12.1 ± 3.3)	<b>123.2-155.6</b> (142.8 ± 12.4)
† <i>Francolebias rhenanus</i>	1	<b>1.15</b>	<b>80.1</b>	<b>82.5</b>	<b>31.3</b>	<b>39.2</b>	<b>5.3</b>	<b>14.9</b>	<b>126.0</b>
† <i>A. meyeri</i>	33	1.03-1.48 (1.26 ± 0.10)	74.0-97.4 (81.8 ± 5.7)	71.1-92.1 (80.4 ± 5.5)	14.0-38.7 (23.6 ± 5.8)	28.6-49.8 (37.7 ± 5.2)	2.5-14.8 (6.6 ± 2.9)	8.5-27.2 (17.8 ± 5.0)	71.0-136.0 (100.0 ± 17.2)
† <i>A. konradi</i>	12	0.93-1.17 (1.08 ± 0.08)	83.2-91.3 (87.1 ± 2.4)	82.7-90.8 (87.6 ± 2.6)	19.6-32.5 (25.0 ± 4.6)	27.4-47.0 (34.7 ± 5.0)	2.0-7.5 (5.0 ± 1.9)	6.3-13.6 (9.8 ± 2.4)	107.0-145.0 (124.8 ± 12.4)
† <i>A. gubleri</i>	5	1.08-1.24 (1.16 ± 0.06)	85.7-97.3 (93.0 ± 4.4)	90.9-100.0 (96.4 ± 3.4)	18.9-30.3 (25.8 ± 4.3)	24.2-36.1 (28.7 ± 4.6)	2.4-4.5 (2.9 ± 0.9)	4.8-8.0 (6.3 ± 1.3)	135-160 (140.0 ± 11.2)
† <i>A. sarmaticus</i>	3	1.14-1.34 (1.23 ± 0.10)	80.2-82.4 (80.9 ± 1.2)	82.3-86.4 (84.3 ± 2.1)	24.4-27.1 (25.9 ± 1.4)	33.1-38.9 (35.7 ± 2.9)	2.9-4.3 (3.6 ± 0.7)	8.8-10.6 (10.0 ± 1.0)	127.7-131.3 (129.2 ± 1.9)
† <i>A. bettinae</i>	7	1.09-1.27 (1.18 ± 0.06)	75.5-85.8 (81.7 ± 3.6)	67.7-77.6 (74.9 ± 3.5)	35.0-45.1 (41.2 ± 4.3)	34.7-45.6 (40.1 ± 4.1)	10.3-16.4 (13.5 ± 2.3)	19.5-27.0 (22.8 ± 2.8)	59.8-94.0 (73.5 ± 11.4)
† <i>Aphanolebias</i> (all species)	61	<b>0.93-1.48</b> (1.20 ± 0.11)	<b>74.0-97.4</b> (83.8 ± 5.8)	<b>67.7-100.0</b> (82.8 ± 7.2)	<b>14.0-45.1</b> (26.3 ± 7.5)	<b>24.2-49.8</b> (36.5 ± 5.6)	<b>2.0-16.4</b> (6.6 ± 3.7)	<b>4.8-27.2</b> (15.3 ± 6.3)	<b>59.8-160.0</b> (107.1 ± 23.5)
<i>V. hispanica</i>	20	0.94-1.24 (1.08 ± 0.09)	80.9-93.5 (87.6 ± 3.0)	83.6-95.0 (89.3 ± 3.3)	13.7-95.9 (22.8 ± 17.8)	24.3-41.4 (31.3 ± 4.1)	0.0-8.5 (2.5 ± 2.1)	2.9-11.5 (6.4 ± 2.5)	122.0-165.0 (145.4 ± 12.8)
<i>V. letournexi</i>	18	1.01-1.22 (1.12 ± 0.07)	76.1-100.3 (87.2 ± 5.9)	80.8-96.1 (85.9 ± 3.8)	22.1-35.8 (29.5 ± 3.6)	30.8-47.6 (39.4 ± 3.6)	2.7-14.0 (7.1 ± 3.3)	4.6-15.2 (10.7 ± 2.9)	91.0-154.0 (121.6 ± 17.0)
<i>V. robertae</i>	13	1.12-1.43 (1.29 ± 0.08)	72.8-88.1 (80.8 ± 5.2)	72.2-84.6 (78.4 ± 4.3)	13.4-43.4 (28.4 ± 8.0)	34.1-43.9 (39.4 ± 3.0)	1.9-15.2 (6.3 ± 3.7)	9.9-19.4 (15.1 ± 3.0)	58.0-127.0 (101.4 ± 17.4)
† <i>V. arcasensis</i>	1	1.19	85.0	86.0	18.0	33.7	5.1	10.7	123.0
† <i>V. reichenbacherae</i>	4	1.02-1.11 (1.07 ± 0.04)	85.5-91.1 (89.5 ± 2.7)	82.6-87.0 (85.4 ± 1.9)	25.5-30.9 (27.4 ± 2.4)	30.3-37.7 (33.4 ± 3.1)	6.2-9.2 (7.5 ± 1.2)	10.4-13.0 (11.3 ± 1.2)	92.4-110.0 (99.6 ± 7.8)
<i>Valencia</i> (all species)	57	<b>0.94-1.43</b> (1.14 ± 0.11)	<b>72.8-100.3</b> (86.0 ± 5.3)	<b>72.2-96.1</b> (85.4 ± 5.4)	<b>13.4-95.9</b> (26.3 ± 11.7)	<b>24.3-47.6</b> (35.9 ± 5.2)	<b>0.0-15.2</b> (5.3 ± 3.5)	<b>2.9-19.4</b> (10.2 ± 4.2)	<b>58.0-165.0</b> (123.8 ± 23.2)

Values show ranges for left and right otoliths combined, mean values ± standard deviation are given in brackets. Values in bold indicate the sagitta morphometry of the respective genus. n is the total number of otoliths. \* after mean values indicates significant difference between species or, in case of †*M. chios*, between populations ( $p < 0.05$ ). For sagittae measurements see Fig. 3C. **Abbreviations:** a, antirostrum height; al, antirostrum length; DL, dorsal length; E, excisura angle; L-H, length-height index; ML, medial length; r, rostrum length; rl, rostrum length. For raw data see [Supplemental material Table S1](#), sheets 1 and 3.

**Table 4.** Significant differences in otolith morphology between genera of Valenciidae (Welch–ANOVA test with Games–Howell post-hoc,  $p < 0.05$  and  $p < 0.001$  (the latter is indicated in bold)).

	n	† <i>Miovalencia</i> gen. nov.	† <i>Wilsonilebias</i> gen. nov.	† <i>Prolebias</i>	† <i>Aphanolebias</i>	<i>Valencia</i>
† <i>Miovalencia</i> gen. nov.	53	<b>X</b>				
† <i>Wilsonilebias</i> gen. nov.	35	a, r	<b>x</b>			
† <i>Prolebias</i>	7	<b>L-H, a, al, E</b>	<b>L-H, a, al, rl, E</b>	<b>x</b>		
† <i>Aphanolebias</i>	57	<b>ML, r, E</b>	ML, a, E	<b>L-H, a, r, al, E</b>	<b>x</b>	
<i>Valencia</i>	57	<b>ML, r, al, rl, E</b>	DL, ML, al, <b>rl, E</b>	<b>L-H, a, r, al</b>	<b>rl, E</b>	<b>x</b>

Grey shading indicates that cells are left empty to avoid repetition. **Abbreviations:** a, antirostrum height; al, antirostrum length; DL, dorsal length; E, excisura angle; L-H, length-height index; ML, medial length; r, rostrum height; rl, rostrum length. For details see Table 3.

†*Francolebias*, †*Miovalencia* gen. nov. and *Valencia*), (viii) premaxilla ascending process with slender base (Fig. 5B) (*vs* robust base in *Valencia* and †*Miovalencia* gen. nov.); (ix) premaxilla ascending process long (Fig. 5B) (*vs* short in †*Aphanolebias*); (x) retroarticular elongated (Fig. 5B) (*vs* short in *Valencia*, †*Prolebias*, †*Francolebias*); and (xi) opercle wide-triangular (Fig. 5B) (*vs* slender in †*Miovalencia* gen. nov.). Moreover, the modal number of total vertebrae in †*Wilsonilebias* gen. nov. (27) is slightly higher than in †*Miovalencia* gen. nov. (26), and the range of that count indicates that †*Wilsonilebias* gen. nov. has slightly fewer vertebrae (25–28) than the remaining valenciids (28–31). In addition, its number of dorsal-fin rays and pterygiophores (10–12) appears slightly lower than in †*Prolebias* (12–13), and slightly higher than in †*Francolebias* (8–11) and †*Aphanolebias* (9–10). Finally, its range of anal-fin pterygiophores (11–12) is lower than in *Valencia* (12–14) and †*Prolebias* (14–15) (Tables 1, 2).

Additionally, the sagitta of †*Wilsonilebias* gen. nov. shows morphometric and morphological traits that are significantly different to the sagittae of other Valenciidae (Welch–ANOVA test with Games–Howell post-hoc,  $p < 0.001$ ): five otolith variables differentiate †*Wilsonilebias* gen. nov. from *Valencia* and †*Prolebias*, respectively, while three and two otolith variables discriminate it from †*Aphanolebias* and †*Miovalencia*, respectively (Table 4). Furthermore, the sagitta of †*Wilsonilebias* gen. nov. differs from that of the other Valenciidae in the presence of a deep sulcus (*vs* shallow in all other Valenciidae), a slight to pronounced ‘S’-shape of the sulcus (*vs* straight in †*Prolebias*, †*Francolebias* and *Valencia*, *vs* straight and slightly ascending posteriorly in †*Miovalencia* gen. nov., and *vs* straight with cauda ventrally bent in †*Aphanolebias*). Also the lapillus of †*Wilsonilebias* gen. nov. is characteristic. It has a rhomboid to drop-shape (Fig. 13F, G), whereas it is rounded-rectangular to crescent shaped in †*Miovalencia* gen. nov. (Fig. 13D, E) and rectangular shaped in *Valencia* (Fig. 13A–C). The sulculus continues to a distinct linea basalis (*vs* indistinct linea basalis in †*Miovalencia* gen. nov. and *Valencia*), which borders

the posteromedial part of the lapillus and separates the very bulged part of the lapillus from a more flattened area (Figs 11, 13F, G). As mentioned above, the lapillus is not known for †*Prolebias*, †*Francolebias* and †*Aphanolebias*.

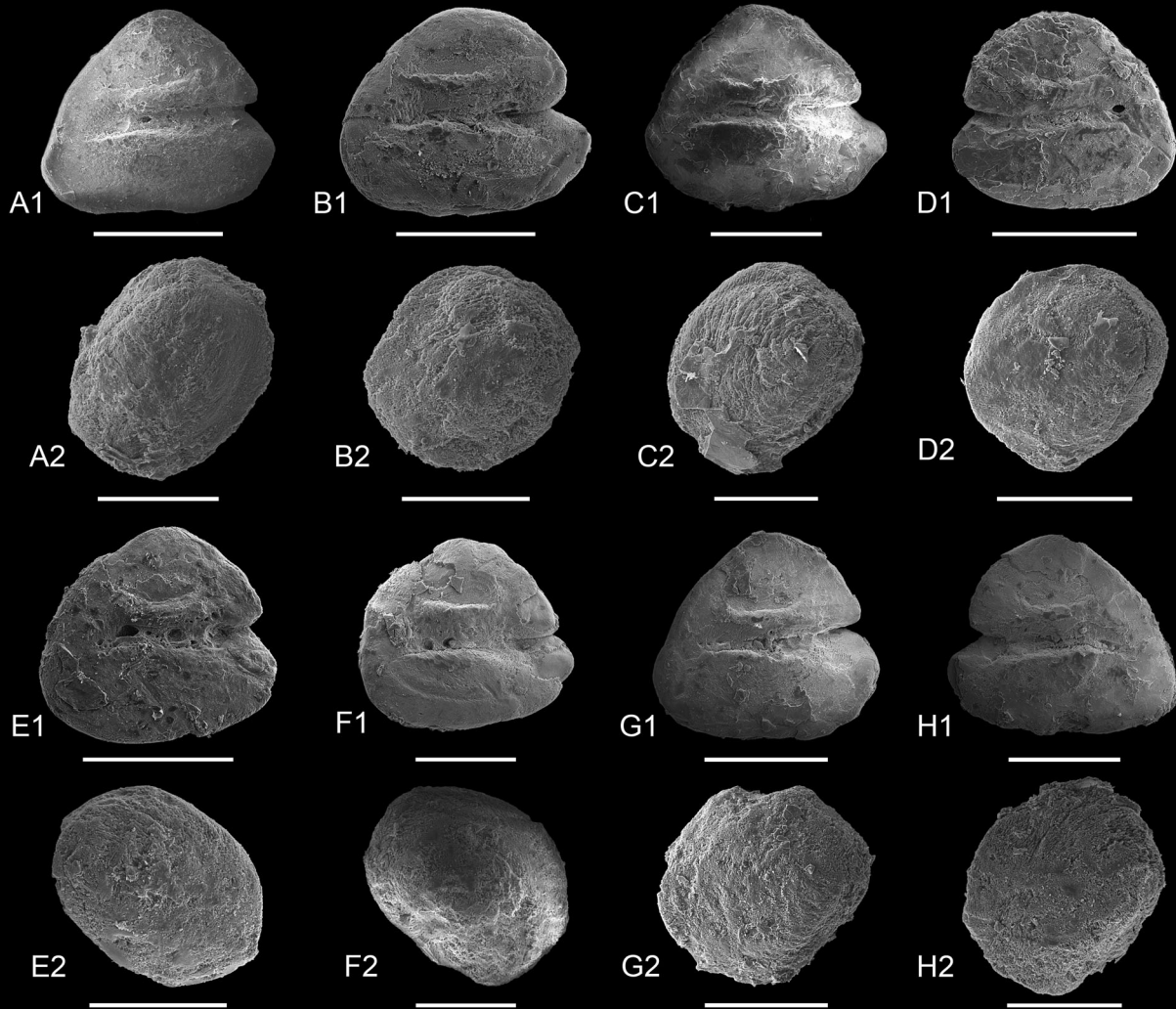
**Etymology.** The genus name honours Wilson J. E. M. Costa (Federal University of Rio de Janeiro, Brazil) for his meticulous work on the morphology, osteology and phylogenetic relationships of many extant and fossil cyprinodontiform genera and species. The Greek word ‘lebias’ is a common second element in cyprinodontiform generic names. †*Wilsonilebias* gen. nov. is masculine.

**Stratigraphical range.** Middle Miocene (Langhian).

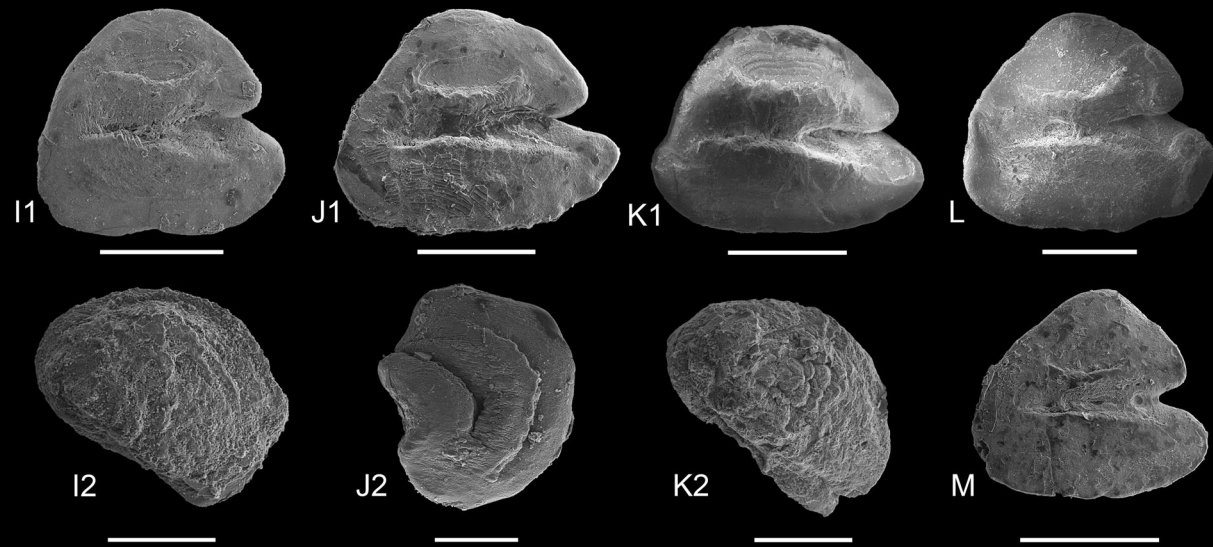
**Remarks.** As for †*Miovalencia* gen. nov., we provide ranges and mean values  $\pm$  SD for body or bone measurements and ranges and modal numbers (modes) for meristic counts in the following descriptions. Means  $\pm$  SD for all measurements and modes for all counts are additionally listed in Table 1 and the underlying details of measurements and counts can be found in Supplemental material Table S1, sheet 1. Comparative meristic data and otolith data from other Valenciidae used for the diagnosis of the new genus are presented in Tables 2 and 3.

**General description.** †*Wilsonilebias* gen. nov. is a small-sized fish, its SL ranges from 15.3 to 34.9 mm (mean  $26.9 \pm 5.5$  mm). Head moderately large and relatively slender (HL  $32.9 \pm 2.2\%$  SL, HD  $70.5 \pm 9.8\%$  HL). Snout about one third of head length (preorbital length  $29.1 \pm 3.5\%$  HL), eyes relatively small (ED  $27.5 \pm 5.5\%$  HL). Body slightly elongated (BD  $19.3 \pm 2.7\%$  SL), dorsal and anal fins posteriorly positioned on body, dorsal fin opposite to anal fin or slightly in front of anal fin (predorsal distance  $62.2 \pm 2.2\%$  SL, preanal distance  $65.3 \pm 1.5\%$  SL). Dorsal fin composed of (9)10–12 rays and same number of pterygiophores, anal fin comprising 12–13 rays supported by 11–12 pterygiophores. Pectoral fin placed relatively low-set at body and consisting of 8–15 rays. Pelvic fin

†*Miovalencia bugojnensis* gen. et sp. nov.



†*M. chios* (Malz, 1978)



encompassing 5–7 rays and slightly closer to anal fin than to pectoral fin (pectoral–pelvic distance  $15.8 \pm 2.3\%$  SL, pelvic–anal distance  $14.2 \pm 1.9\%$  SL). Vertebral column composed of 25–28 vertebrae of which 10–12 are abdominal and 15–16 are caudal. Caudal peduncle relatively long and slender (CPL  $23.6 \pm 1.8\%$  SL, CPD  $12.4 \pm 1.8\%$  SL). Caudal fin palatte-shaped, number of principal rays 14–17. Body and head covered by cycloid scales. The saccular otoliths (sagittae) show an elongate- or rounded-triangular shape with a slender, upwards curved rostrum, a robust, short antirostrum and a relatively narrow excisura (Fig. 11A1, B1, C, E1–K1, L–N). The sulcus is clearly deepened and slightly ‘S’-shaped, in some specimens with a crenulated lower margin. The lapillus has a rhomboid shape, with the sulculus continuing to the clear linea basalis, and a thickened ventral surface (Fig. 11A2, B2, D, E2–J2). The single asteriscus is elongate-bean-shaped with a deep fossa acustica bounded by two walls, and a pronounced concavity at the anterior margin (Fig. 11K2).

**Neurocranium and orbital series.** This area is usually distorted and poorly preserved, but a composite skull reconstruction based on the details seen in several specimens is possible (GRC 002, 004, 006, 178, 188.1, 233, 236.2) (Fig. 5B, see also Supplemental material Fig. S6). The frontal bones are relatively broad and long, with the lateral rim enclosing the orbit and a supra-orbital canal in the posterior area; also the sphenotic is recognizable (Fig. 5B). A parietal bone could be discerned in specimen GRC 188.1 (Fig. 5B), while it was not possible to identify the nasal bone. The lacrimal was partially preserved in specimen GRC 188.1, it shows an elongated-rectangular shape (Fig. 5B). The lateral ethmoid appears to be robust and is usually in close contact to the vomer and parasphenoid. The latter crosses at middle to lower half of the orbit and expands posteriorly (Fig. 5B). The supraoccipital has a rounded (diamond) shaped anterior body and a slightly bifurcated posterior process (Fig. 5B). The basioccipital is poorly preserved and details are not recognizable.

**Jaws.** The jaw joint region is placed anterior to the orbit (Fig. 5B, Supplemental material Fig. S6). The premaxilla shows a curved, anteriorly slim and posteriorly widened ramus and a long, slender ascending process, slightly tapering towards its tip (Fig. 5B, Supplemental material Fig. S4d). The maxilla is a robust, slightly

curved bone with an elongated ventral process (only visible in medial view) and a relatively long dorsal process (Fig. 5B). The bones of the lower jaw are usually broken or pressed together, allowing little observation on the details of these bones. The dentary seems to be long, with an almost straight lower border, a medial process is not developed. The angulo-articular shows a relatively short ventral process that runs parallel to the retroarticular, its coronoid process is rectangular-shaped with slightly rounded edges (Fig. 5B). The retroarticular is well preserved. It has an elongated-triangular shape, an articular head that is smaller than the body, and its dorsal surface adjoins the ventral process of the angulo-articular (Fig. 5B, Supplemental material Fig. S4f). Both the premaxilla and the dentary bear multiple rows of conical teeth of different sizes (Supplemental material Fig. S5c).

**Suspensorium, opercular apparatus and hyoid arch.**

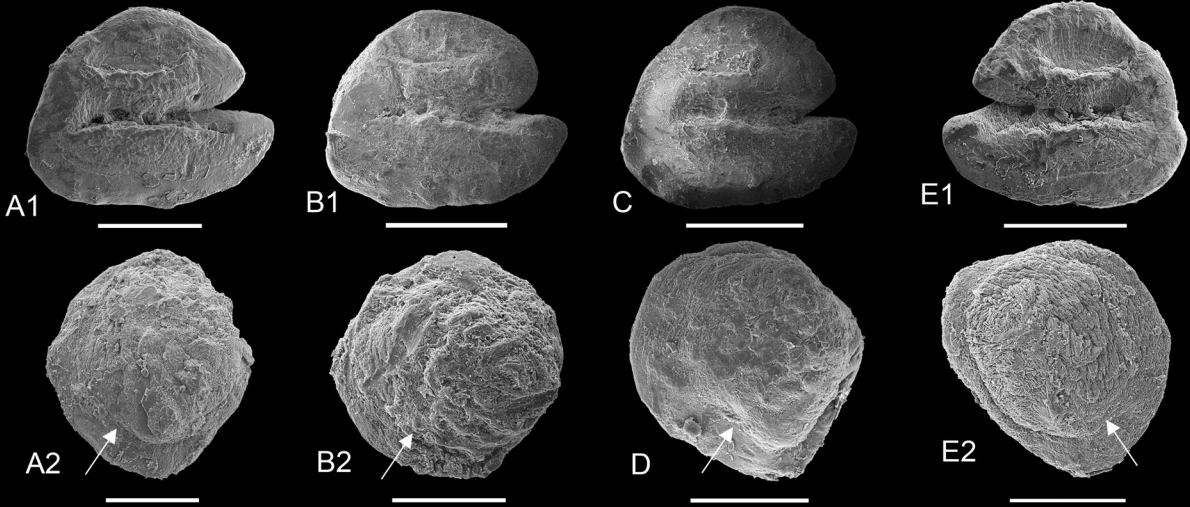
The quadrate has a narrow triangular shape. The endopterygoid is positioned at the posterior rim of the quadrate and has a broad ventral portion. The autopalatine shows an anteriorly bent head and is ventrally in contact with the quadrate and endopterygoid. The symplectic is leaf-shaped with a dorsal and ventral bony lamella and a main body that articulates anteriorly with the quadrate and posteriorly with the hyomandibular. The hyomandibular displays well-preserved upper and posterior condyles and a small posteroventral process (Fig. 5B).

The preopercle is as described for †*Miovalencia* gen. nov., with a lamella between the lower and upper arm. The ventral border of the interopercle is well defined and extends parallel to the lower arm of the preopercle (Fig. 5B). The opercle has a broad-triangular shape, with a concave upper margin, the articular facet for the hyomandibular is visible in its anterodorsal corner (Fig. 5B). The subopercle is long, slender, and half-moon shaped.

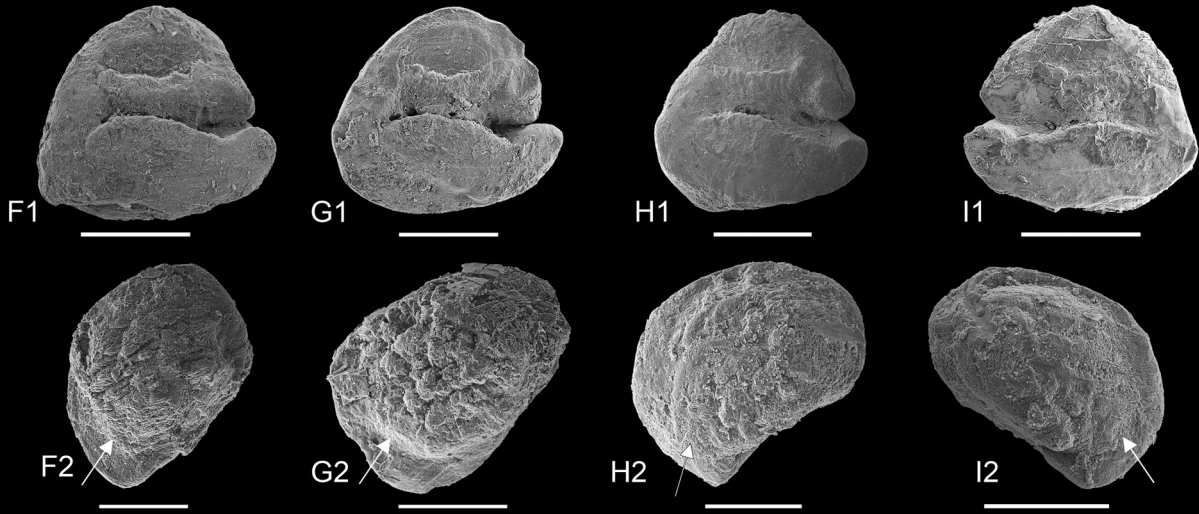
The hyoid bar is moderately well preserved. The anterior ceratohyal is relatively broad, the posterior ceratohyal is broad and becomes slender in its posterior-most part. The ceratohyal seem to be associated with a longish, slightly triangular-shaped ventral hypohyal (specimens GRC 215, GRC 236.2, Fig. 5B). A well-preserved basibranchial plate with the articular fossae for the hypobranchial in its anterior region is visible in specimen GRC 006 (Fig. 5B). Six branchiostegal rays could be counted, the first two are thin, and the four posterior ones are broader (Fig. 5B).

**Figure 10.** Sagittae (suffix 1), lapilli (suffix 2, except J2) and asteriscus (J2) preserved *in situ* in the species of †*Miovalencia* gen. nov. from the Bugojno Basin. A–H, †*M. bugojnensis* gen. et sp. nov. (A, GRC 038-2; B, GRC 182; C, GRC 177; D, GRC 019; E, GRC 055; F, GRC 206; G, GRC 021; H, GRC 197). I–M, †*M. chios* (I, GRC 204; J, GRC 261; K, GRC 229; L, GRC 003; M, GRC 185). Scale bars for sagittae = 0.5 mm; for lapilli and asteriscus = 0.2 mm.

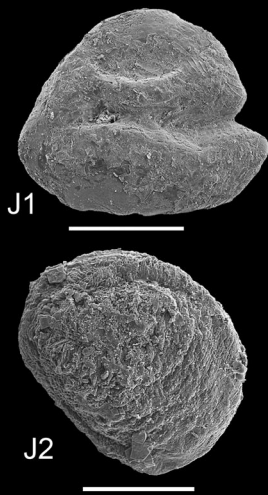
†*W. langhianus* gen. et sp. nov.



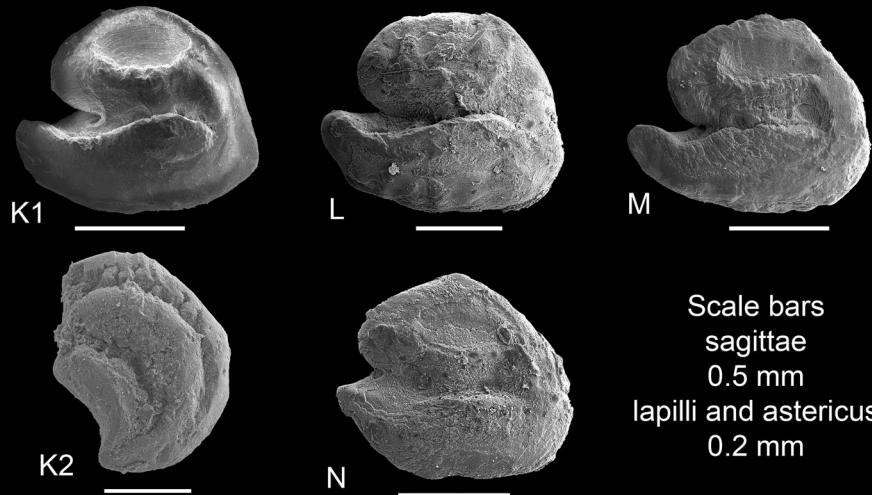
†*W. rotundascendus* gen. et sp. nov.



†*W. cf. langhianus*



†*W. cf. rotundascendus*



Scale bars  
sagittae  
0.5 mm  
lapilli and astericus  
0.2 mm

**Pharyngeal jaws.** The pharyngeal jaws, with multiple pharyngeal teeth *in situ*, are preserved in anatomical position in several specimens. The teeth are conical, with a very small shoulder below the curved tip (Supplemental material Fig. S5d3). At the posterior part of the pharyngeal plate some teeth are compressed, with a straight crown and a very small indentation (Supplemental material Fig. S5d1, 4). While it is difficult to discern the cerato- and pharyngobranchials (e.g. specimens GRC 012, 216), a boomerang-shaped 5th ceratobranchial is recognizable in specimen GRC 004 (not figured).

**Axial skeleton.** The vertebral column is mostly composed of 25–28 (mode 27) vertebrae including 10–12 (mode 11) abdominal vertebrae and 15–16 (mode 16) caudal vertebrae. The first vertebra has a short neural spine. The following three vertebrae (V2 to V4) have flat and broad neural spines, in V2 the spine is wider than tall (specimens GRC 002, 004). The neural spines of the last abdominal vertebra (V11) and of the first caudal vertebrae (V12, V13) are associated with the dorsal-fin pterygiophores and show a slightly anteriorly curved shape (Fig. 8B). In some specimens, the haemal spines (sometimes also the neural spines) opposite to the anal-fin are particularly robust and display a blunt distal end (Fig. 9B, i.e. specimens GRC 018, 189, 233, 236.1). Around 10 rib pairs, starting from the 2nd vertebra, are associated to the abdominal vertebrae. Epipleurals could not be identified.

**Pectoral girdle and fins.** The pectoral girdle is particularly well preserved in specimen GRC 196.1 (Fig. 7A, Supplemental material Fig. S4e). The cleithrum is curved with a broad plate in the dorsal area and narrows ventrally. The post-temporal has a thin rod-shaped dorsal process and an ossified ventral process (best visible in specimens GRC 004 and 018, see Supplemental material Fig. S4e). A slightly rounded to rectangular scapula and a triangular-shaped coracoid are discernible, but a clear division between both is not recognizable. The scapula has a thin, elongated scapular foramen in its upper part. Four radials articulate with the pectoral rays, the first (upper) is triangular and small, the second has a trapezoidal shape, and the third and fourth ones are more rectangular and larger in size. They are overlapped by a thin rod-like bone, a possible postcleithrum

3. The pectoral fin has 8–15 rays; its length is 9.3–18.5% SL ( $12.5 \pm 3.4\%$  SL).

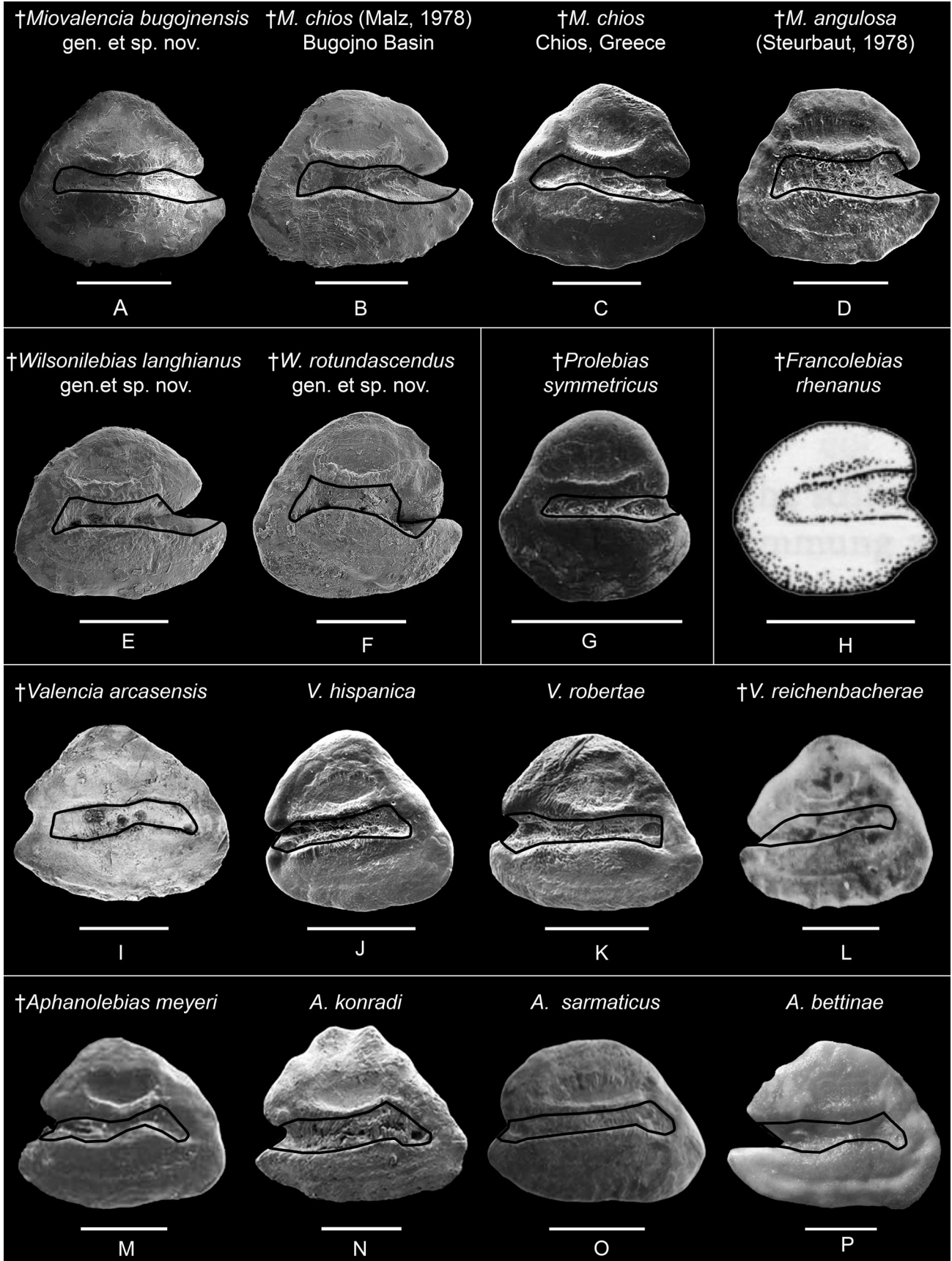
**Pelvic girdle and fins.** The pelvic bone is a broad, triangular-shaped bone with a rectangular medial process and a partially visible ischial process (Fig. 7C). The pelvic bone width is about 70% of its length, with the posterior portion being broader than the anterior part. The pelvic fin comprises 5–7 rays and is relatively short ( $6.5\text{--}9.1\%$  SL,  $7.4 \pm 1.2\%$  SL).

**Dorsal and anal fins.** The dorsal fin is composed of (9)10–12 rays supported by the same number of pterygiophores (Fig. 8B). The first pterygiophore is robust, has a broad articulating head and is deeply split into two bones (Fig. 8B, D), the next pterygiophore is also robust and close to the first one (Fig. 8B). The third pterygiophore is longer than the preceding ones, and the following pterygiophores only slightly decrease in length and width (Fig. 8B1). The dorsal-fin length is 11.8–19.5% SL ( $15.9 \pm 3.2\%$  SL), its base measuring 9.2–13.9% SL ( $11.4 \pm 1.4$  SL).

The anal fin comprises 12–13 rays, supported by 11–12 pterygiophores (Fig. 9B). In all specimens, the anal-fin pterygiophores are relatively long. In putative male specimens (GRC 179, 189, 233), the first anal-fin pterygiophore is relatively broad and reaches the haemal arch of the first or second caudal vertebra. In the same specimens, also the last anal-fin pterygiophore is long (almost equal in length to the preceding ones, Fig. 9B). In putative females (GRC 192, 247) the pterygiophores are also long, reaching beyond the middle of the haemal spines, but the last one is much shorter. Anal-fin length measurements were mostly not possible to take as the distal part of the rays were not preserved, but based on specimen GRC-033 seems to be around 13.5% of the SL. The anal-fin base is almost equal to the dorsal fin base ( $8.6\text{--}13.6\%$  SL,  $11.1 \pm 1.4\%$  SL).

**Caudal fin and skeleton.** The caudal fin comprises 14–17 principal rays and six dorsal and ventral procurent rays. Neural and haemal spines of three preural vertebrae (PU 2–4) are involved in the support of the caudal-fin rays. PU 2 is characterized by expanded, blade-shaped neural and haemal spines, which are close to the epural and parhypural (Fig. 6C). The width of these spines is about three to four times greater than the width of the corresponding spines of PU 4 (nsPU2/nsPU4 ratio  $3.4 \pm 1.0$ ; hsPU2/hsPU4 ratio  $3.1 \pm 0.4$ ).

**Figure 11.** Sagittae (suffix 1, C, L–N), lapilli (D, suffix 2, except K2) and asteriscus (K2) preserved *in situ* in the species of †*Wilsonilebias* gen. et sp. nov. from the Bugojno Basin. A–E, †*W. langhianus* gen. et sp. nov. (A, GRC 179; B, GRC 233; C, GRC 196.1; D, GRC 188.1; E, GRC 236.1). F–I, †*W. rotundascendus* gen. et sp. nov. (F, GRC 247; G, GRC 215; H, GRC 192; I, GRC 205). J, †*W. cf. langhianus* (GRC 216). K–N, †*W. cf. rotundascendus* (K, GRC 002; L, GRC 219; M, GRC 226; N, GRC 210).



The caudal skeleton is composed of the terminal centrum and a fan-shaped hypural plate (Fig. 6C, D). The terminal centrum bears anteriorly a dorsally projecting prezygapophysis, while at the posterodorsal edge of the terminal centrum is another small, lateral, spiny process. The hypural plate is anteriorly unfused, i.e. it shows a thin elongated gap (fenestra) narrowing posteriorly and indicating the boundary between the upper and lower hypural plate. The epural is slightly curved and has a plank- or rod-like shape. The parhypural is broad with a rectangular head that is in contact with the dorsoventral portion of the terminal centrum, but not overlapping it.

**Scales.** Round scales can be recognized all over the body, but they are poorly preserved. Only in specimen GRC 236.2 are flank scales better preserved; they display a ‘U’-shape with about 6 to 7 radii (Supplemental material Fig. S7c). The scales on the head are larger than the flank scales.

**Pigmentation.** Pigmentation is not very well preserved except for possible dark dots across the body in some specimens.

**Otoliths.** The sagitta has a rounded-triangular to trapezoidal shape (Fig. 11A1, B1, C, E1–K1, L–N). The ventral rim is straight to rounded, followed by a moderately long, anteriorly curving and slender rostrum (RL  $17.4 \pm 4.0\%$ ). The antirostrum is rounded and relatively short (AL  $8.4 \pm 3.4\%$ ). The sulcus is slightly to distinctively ‘S’-shaped (best visible along its lower margin), owing to the presence of a constriction between the relatively wider ostium and the relatively narrower cauda; the cauda is slightly bent at its end. The excisura is deep, but narrow. A thick crista superior, which delimits a deeply depressed dorsal area, adjoins the sulcus.

The lapillus has a thick ventral surface and a rhomboid to rounded-trapezoid shape with a very curved medial margin (Fig. 11A2, B2, D, E2–J2). The sulculus usually continues to a clear linea basalis. One asteriscus was possible to extract (GRC 002). It has an elongate bean-like-like shape with a straight anterodorsal margin, a concave anteroventral margin and a narrowing ventral tip (Fig. 11K2). The fossa acustica is deep and bounded by two walls.

### †*Wilsonilebias langhianus* gen. et sp. nov.

(Figs 4C, 6C, 8B, 9B, 11A–E, 12E, 13F;  
Supplemental material Figs S4d, S4f, S6)

**Etymology.** The name refers to the stratigraphical age (Langhian) of this new species.

**Type material.** Holotype: GRC 004.2/004.1 (s+l). 16 paratypes: GRC 012.2/012.1 (s+l), GRC 033.1/033.2 (s+l), GRC 036 (s+l), GRC 063.1/063.2 (s+l), GRC 064.1/064.2 (s+l), GRC 173p (s), GRC 179.2/179.1 (s+l), GRC 188.1cp (l), GRC 195.2Bp (s+l), GRC 196.1p (s), GRC 207 (s+l), GRC 223.1A/223.3A (s+l), GRC 233cp (s+l), GRC 236.1 (s+l), GRC 238.1B/238.2B (s+l), GRC 262/180 (s+l).

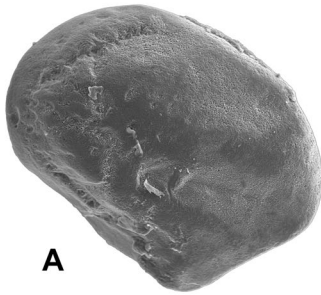
**Referred specimens.** One specimen (GRC 216cp (s+l)) is referred to as †*W.* cf. *langhianus* because its sagitta and lapillus are similar to those of the type specimens, but also display some similarity to the sagitta and lapillus of †*W. rotundascendus* gen. et sp. nov.

**Type locality and age.** Gračanica, Bugojno Basin, Bosnia and Herzegovina; Middle Miocene (Langhian), about 14.8–13.8 Ma.

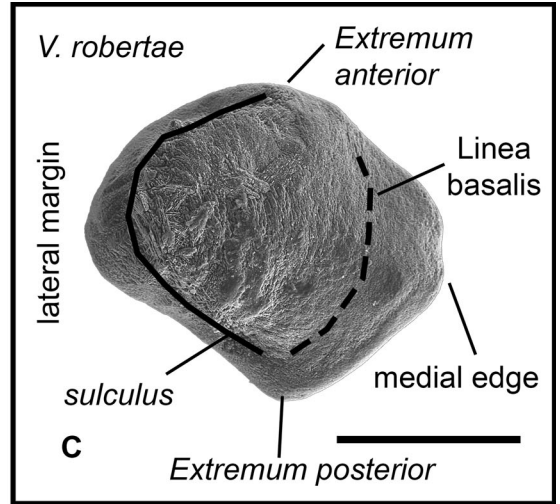
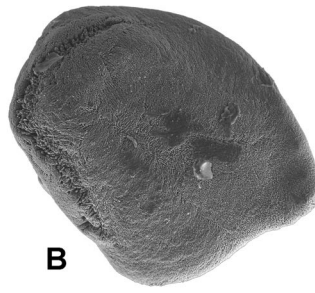
**Differential diagnosis.** Some specimens of †*Wilsonilebias langhianus* gen. et sp. nov. display a PU 2 with proximally curved neural and haemal spines (GRC 012, 033, 063, 179, see Fig. 6C) (not seen in †*W. rotundascendus* gen. et sp. nov.). Apart from that, the discrimination between †*W. langhianus* gen. et sp. nov. and its congener, †*W. rotundascendus* gen. et sp. nov., is based on differences in the morphology of both the sagitta and the lapillus. Compared to its congener, the sagitta of †*W. langhianus* gen. et sp. nov. has an elongated-triangular shape (*vs* rounded-triangular), a relatively straight posteroventral portion (*vs* mostly rounded and sometimes protruding), a rostrum that is only slightly curved (*vs* moderately to strongly curved), a more opened excisura (*vs* almost closed), a moderately deep sulcus (*vs* deeply incised), a weak constriction between ostium and cauda (*vs* clear constriction), and a shallow crista inferior (*vs* marked) (Fig. 11A1, B1, C, E1). In addition, it has a significantly greater relative rostrum height (R  $38.7 \pm 3.1\%$  *vs*  $35.9 \pm 2.8\%$ ,  $p < 0.05$ ), and also tends to have a slightly greater relative antirostrum height and length (A  $33.0 \pm 5.3\%$  *vs*  $28.8 \pm 8.5\%$ , AL  $9.4 \pm 2.4\%$  *vs*  $6.8 \pm 4.2\%$ ). Furthermore, the sagitta

**Figure 12.** Comparison of the otoliths between species of †*Miovalencia* gen. nov., †*Wilsonilebias* gen. nov. and previously described fossil and extant Valenciidae. **A, B**, GRC 177, GRC 261. **C, D**, from Reichenbacher and Kowalke (2009, fig. 3k and, mirrored, 3b). **E, F**, GRC 179, GRC 215. **G**, from Reichenbacher (2000, pl. 1, fig. 5). **H**, from Weiler (1963, fig. 18, mirrored). **I, J, K**, from Gaudant *et al.* (2015, fig. 9a, b, f). **L**, from Rückert-Ülkümen (2006, fig. 7: 10). **M**, from Reichenbacher and Gaudant (2003, fig. 3: 1). **N**, from Jost *et al.* (2006, fig. 11a). **O**, from Reichenbacher *et al.* (2019, fig. 3a). **P**, from Bradić-Milinović *et al.* (2021, fig. 4: 9A). All scales = 0.5 mm.

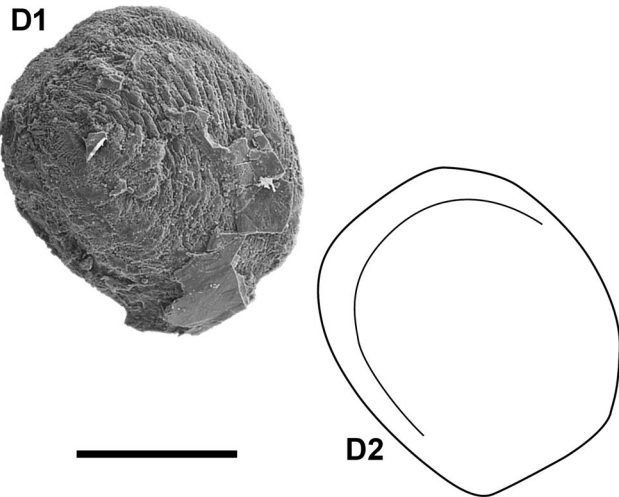
*Valencia hispanica*



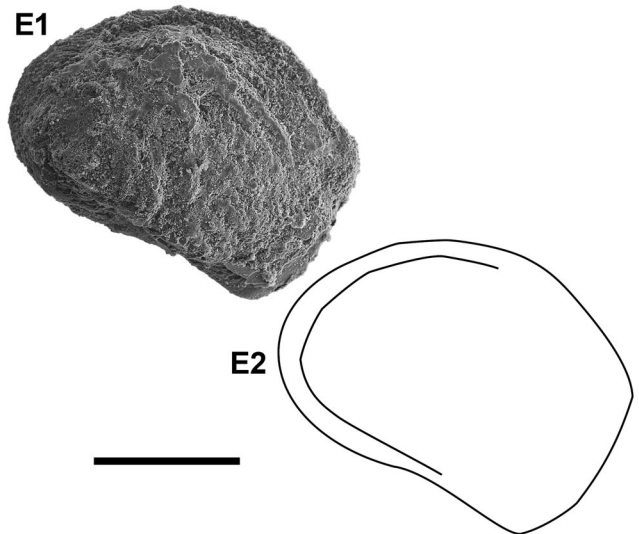
*V. letourneuxi*



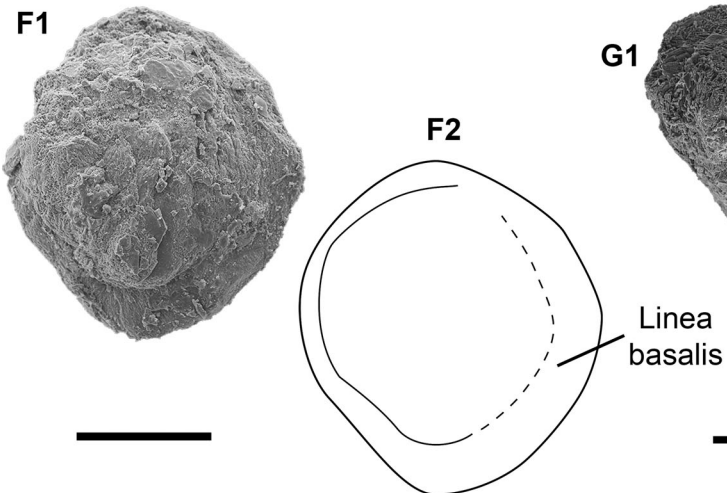
†*Miovalencia bugojnensis* gen. et sp. nov.



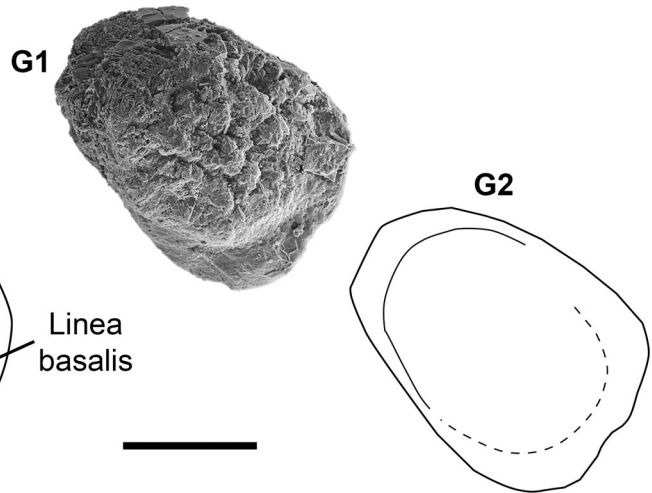
†*M. chios* (Malz, 1978)



†*Wilsonilebias langhianus* gen. et sp. nov.



†*W. rotundascendus* gen. et sp. nov.



of some specimens of †*W. langhianus* gen. et sp. nov. shows a slightly crenulated lower margin of the cauda (see Fig. 11B1, C), which is not observed in the sagittae of †*W. rotundascendus* gen. et sp. nov. The lapillus of †*W. langhianus* gen. et sp. nov. is characterized by a roundish to rhomboid shape (*vs* mostly ovate) and a less coarse ventral surface (Fig. 11A2, B2, D, E2).

**General description.** Same as for the genus, except characters mentioned in the differential diagnosis. For morphometric and meristic characters see Table 1, for otolith morphometry see Table 3.

†*Wilsonilebias rotundascendus* gen. et sp. nov.

(Figs 4D, 7C, 8D, 6D, 11F–I, 12F, 15G;  
Supplemental material Figs S4e, S5d, S7c)

**Etymology.** The name *rotundascendus* refers to the rounded, ascending rostrum of the sagitta of this species.

**Type material.** Holotype: GRC 236.2p (s+1). 11 Paratypes: GRC 018.1/018.2 (s+1), GRC 178.2/178.1 (s+1), GRC 189.1/189.2 (s+1), GRC 192.2/192.1 (s+1), GRC 205.2/205.1 (s+1), GRC 215.2/215.1 (s+1), GRC 237.2p (s+1), GRC 239cp (l), GRC 244.2/244.1 (s+1), GRC 247p (s+1), GRC 255cp (s).

**Referred specimens.** Four specimens (GRC 226.1/226.2 (s), GRC 002cp (s+a), GRC 219.1/291.2 (s), GRC 210 (s)) are referred to as †*W. cf. rotundascendus* because their sagittae showed a more elongated and slenderer rostrum than the sagittae of the holotype and paratypes (Fig. 11K1, L–N).

**Type locality and age.** Gračanica, Bugojno Basin, Bosnia and Herzegovina; Middle Miocene (Langhian), about 14.8–13.8 Ma.

**Differential diagnosis.** As described in the differential diagnosis of †*W. langhianus* gen. et sp. nov., none of the specimens of †*W. rotundascendus* gen. et sp. nov. displays a PU 2 with proximally curved neural and haemal spines that are very close to the epural and parhypural. Apart from that, †*W. rotundascendus* gen. et sp. nov. can be differentiated from its congener based on differences in the morphology of both the sagitta and the lapillus. Its sagitta has a rounded-triangular shape (*vs* elongated-triangular in †*W. langhianus* gen. et sp. nov.), a mostly rounded and sometimes protruding

posteroventral portion (*vs* relatively straight), a moderately to strongly curved rostrum (*vs* slightly curved), an almost closed excisura (*vs* opened), a deeply incised sulcus (*vs* moderately deep), a clear constriction between ostium and cauda (*vs* weak), and a marked crista inferior (*vs* shallow) (Fig. 11F1–I1). In addition, †*W. rotundascendus* gen. et sp. nov. has a significantly smaller relative rostrum height (R  $35.9 \pm 2.8\%$  *vs*  $38.7 \pm 3.1\%$ ,  $p < 0.05$ ), and also tends to have a smaller antirostrum height and length (A  $28.8 \pm 8.5\%$  *vs*  $33.0 \pm 5.3\%$ , AL  $6.8 \pm 4.2\%$  *vs*  $9.4 \pm 2.4\%$ ). The lapillus of †*W. rotundascendus* gen. et sp. nov. is characterized by a mostly ovate shape (*vs* roundish to rhomboid) and a coarser ventral surface (Fig. 11F2–I2).

**General description.** As for genus, except characters mentioned in the differential diagnosis. For morphometric and meristic characters see Table 1, for otolith morphometry see Table 3.

†*Wilsonilebias* sp.

(Fig. 5B, Supplemental material Fig. S4d)

**Material.** Five specimens (GRC 006 (s+1), GRC 030 (s), GRC 035 (s), GRC 066 (s+1), GRC 238.A (s+1)).

**Remark.** These specimens could be assigned to †*Wilsonilebias* gen. nov. because their posterior anal-fin pterygiophores were not decreasing in size, and/or because the neural and haemal spines of PU2 were positioned close to the epural and parhypural, respectively, and/or because their otoliths preserved *in situ* (sagittae or lapilli or both) display the typical shape of that genus. However, the otoliths are too poorly preserved to allow species identification.

**Unclassified material**

102 specimens were not possible to identify to genus or species level. Most of them (79) were poorly preserved and no otolith or diagnostic characters were recognizable. Among the remainder, 10 specimens, of which four had otoliths *in situ*, could be included in both body morphometry and at least some meristic counts, and a further 13 specimens, of which nine had otoliths, allowed some meristic counts, but no body measurements. These specimens have a mean SL of 28.9 mm (21.9–34.0 mm), their morphometric and meristic characters have similar ranges to the values in the species

←  
**Figure 13.** Terminology of the lapillus and lapillus morphology (in ventral view) of the three extant species of *Valencia* (A–C) and the four fossil species from the Bugojno Basin (D–G). For better comparison, each lapillus is shown as right lapillus (left lapilli were mirrored). A, SNSB-BSPG-13 (mirrored). B, SNSB-BSPG-130a (mirrored). C, SNSB-BSPG-573. D, GRC 177 (mirrored). E, GRC 204. F, GRC 179. G, GRC 215 (mirrored). Scale = 0.2 mm.

described above, and their otoliths were too poorly preserved to allow genus or species identification (for details of data see Supplemental material Table S1, sheet 1).

### Fossil otoliths of Valenciidae

The new material from Bugojno Basin required attention with respect to the abundant fossil record of previously described valenciid taxa based on otoliths (sagittae). Of the genus *Valencia*, one otolith-based species and one skeleton-based species with otolith *in situ* are known (see Table 5 for species names and references). The genus †*Aphanolebias* contains four otolith-based species and one species recorded based on both skeletons with otoliths *in situ* and isolated otoliths (Table 5). Additionally, as described in the systematic section, we assign two otolith-based species, initially described as *Aphanius* or *Aphanolebias*, to †*Miovalencia* gen. nov. One of these species is ‘*Aphanius*’ *chios* from the Middle Miocene of the Chios Island (Greece) (Malz, 1978). The otoliths of the type material of this species show remarkable similarity in the general outline and sulcus shape to the otoliths of this taxon from the Bugojno Basin (Fig. 12B, C), but differ slightly in their lower length-height index (L-H  $1.13 \pm 0.02$  vs  $1.20 \pm 0.09$ ,  $p < 0.05$ ; Table 3). This difference may be related to ontogenetic variation as the otoliths in the Bugojno Basin population are larger than those from the Chios island, which could account for their slightly

more elongated shape. The second species is ‘*Cyprinodontidarum*’ *angulosus* Steurbaut, 1978 from the Lower Miocene of the Aquitaine Basin (south-western France). It was transferred to †*Aphanolebias* by Reichenbacher, Gaudant, et al. (2004), and subsequently considered as *Aphanius* by Reichenbacher and Kowalke (2009). In the original description of this species, Steurbaut (1978) noted that it bears similarities with ‘*Aphanius germaniae*’ Weiler, 1963 (now †*Aphanolebias meyeri*, see Reichenbacher & Gaudant, 2003). We tentatively reclassify this species to †*Miovalencia* gen. nov. because its otoliths show a straight to slightly ascending sulcus without clear distinction between ostium and cauda (Fig. 12C), as seen in †*Miovalencia* gen. nov. (Fig. 12A, B), and the sulcus does not show a clearly curved cauda at the end, as is characteristic for †*Aphanolebias* (Fig. 12M–P). Nonetheless, the sagitta of †*M. angulosa* exhibits a relatively low rostrum height, which differentiates it against †*M. bugojnensis* gen. et sp. nov. ( $R\ 43.2 \pm 3.9$  vs  $35.0 \pm 4.1$ ,  $p < 0.05$ ) and also, albeit not significantly, against †*M. chios* (Table 3). Perhaps the lower rostrum height is attributed to the stratigraphically older appearance of †*M. angulosa* in the Early Miocene, compared to the rest of †*Miovalencia* gen. nov. species, which come from the Middle Miocene.

Additionally, we tried to find otoliths of †*Prolebias* (in the definition of Costa, 2012a) and †*Francolebias*, of which no otoliths have previously been described. Examination of the abundant skeletal type material of

**Table 5.** Fossil species of Valenciidae described based on isolated otoliths (ot) and otoliths preserved *in situ* (sk + ot). Bold indicates re-assignments based on the present study.

Previously described fossil otoliths of Valenciidae	References (authors of species marked by an asterisk)	Figured in this study
<i>Valencia arcasensis</i> (sk + ot)	*Gaudant et al. (2015)	Fig. 12I
<i>Valencia reichenbacherae</i> (ot)	*Rückert-Ülkümen (2006)	Fig. 12L
<i>Aphanolebias bettinae</i> (ot)	*Bradić-Milinović et al. (2021)	Fig. 12P
<i>Aphanolebias gubleri</i> (ot)	*Reichenbacher (1993, as <i>Aphanius</i> ); Reichenbacher, Böhme, et al. (2004)	
<i>Aphanolebias konradi</i> (ot)	*Reichenbacher (1988, as <i>Aphanius</i> ); Reichenbacher, Böhme, et al. (2004)	Fig. 12N
<i>Aphanolebias meyeri</i> (sk + ot, ot)	*Agassiz (1839, as <i>Lebias</i> ); Reichenbacher and Gaudant (2003); Reichenbacher, Gaudant, et al. (2004)	Fig. 12M
<i>Aphanolebias sarmaticus</i> (ot)	*Reichenbacher et al. (2019)	Fig. 12O
<b><i>Miovalencia angulosa</i></b> (ot)	*Steurbaut (1978, as genus <i>Cyprinodontidarum</i> ); Reichenbacher et al. (2004, as <i>Aphanolebias</i> ), Reichenbacher and Kowalke (2009, as <i>Aphanius</i> )	Fig. 12D
<b><i>Miovalencia chios</i></b> (sk + ot, ot)	*Malz (1978, as <i>Aphanius</i> ); Reichenbacher, Gaudant, et al. (2004, as <i>Aphanolebias</i> ), Reichenbacher and Kowalke (2009, as <i>Aphanius</i> )	Fig. 12B, C
<i>Prolebias symmetricus</i> (ot)	*Weiler, 1963, as Otol. ( <i>Cyprinodontidarum symmetricus</i> ); Reichenbacher and Weidmann (1992, as <i>Palaeolebias symmetricus</i> )	Fig. 12G
<b><i>Francolebias rhenanus</i></b> (sk, ot)	*Gaudant (1981b, as <i>Prolebias</i> ); Weiler (1963, as <i>Prolebias</i> sp.)	Fig. 12H

†*Prolebias stenoura* in the NHMUK collection revealed one specimen (NHMUK PV P 76303) with an otolith *in situ* (Fig. 1A1). Although the otolith is not completely preserved it is recognizable that it has a high-ovate shape. This shape sets it clearly apart from the otoliths of *Valencia*, †*Aphanolebias* and †*Francolebias* (see below), and, moreover, make it reminiscent of the otolith-based species *Palaeolebias symmetricus* (Weiler, 1963) (Fig. 12G), known from the lower Oligocene of both southern Germany and southern France (Reichenbacher & Philippe, 1997; Weiler, 1963), thus from the same stratigraphical interval as †*P. stenoura*. Taking into account both its otolith shape and stratigraphical age, we consider *Palaeolebias symmetricus* as a species of †*Prolebias* (the taxon name *Prolebias* Sauvage, 1874 has priority over *Palaeolebias* Reichenbacher & Weidmann, 1992). Accordingly, the otoliths of †*Prolebias* would be characterized by an ovate shape and a short rostrum (Figs 1A1, 12G). Whether other otolith-based species of †*Palaeolebias*, as described in Reichenbacher and Weidmann (1992), should also be transferred to †*Prolebias* requires further research and will be the topic of a future study.

Furthermore, our search for possible otoliths of †*Francolebias* resulted in the observation that the otolith identified in Weiler (1963) as ‘*Prolebias* sp.’ (Figs 1B1, 12H) comes from the same strata (Upper Pechelbronn Beds, lower Oligocene) as the skeleton-based species †*Francolebias rhenanus* (see Gaudant, 1981b). In addition, both ‘*Prolebias* sp.’ and †*F. rhenanus* originate from the southern Upper Rhinegraben, and the respective localities, that is the drilling ‘Grißheim 2’ (‘*Prolebias* sp.’) and the quarry Kleinkems (†*F. rhenanus*) are only 25 km apart from each other (see Gaudant 1981b; Weiler, 1963). Since no other cyprinodontiform species are known from the Upper Pechelbronn Beds, we interpret ‘*Prolebias* sp.’ *sensu* Weiler (1963) as representing the sagitta of †*F. rhenanus* (Gaudant, 1981b). Accordingly, †*Francolebias* has an almost circular sagitta with a small, slightly pointed rostrum (see Figs 1B1, 12H).

Moreover, we used sulcus morphology, otolith morphometry and statistical tests to characterize the otoliths of each valenciid genus including the two new genera described here, with the exception of †*Francolebias* of which only one otolith is known. Nevertheless, †*Francolebias* shows a markedly rounded otolith, with a wide excisura and straight sulcus, which does not resemble any of the other genera.

The statistical tests (Welch–ANOVA with Games–Howell post-hoc,  $p < 0.001$  or  $p < 0.05$ ) reveal significant differences between †*Prolebias* and each of the other Valenciidae in the length–height index and the relative

antirostrum height ( $p < 0.001$ , Tables 3, 4); for further significantly different otolith variables between †*Prolebias* and the remainder see Table 4. The otoliths of *Valencia* and †*Aphanolebias* can be distinguished by two to five otolith variables from the other genera (Table 4), and the otoliths of †*Aphanolebias* differ from all others in their particular sulcus, characterized by a ventrally bent cauda (Fig. 12M–P). Finally, significant differences can be seen in the excisura angle, except between †*Miovalencia* gen. nov. and †*Wilsonilebias* gen. nov., and between †*Prolebias* and *Valencia* (Table 4).

## Phylogenetic results

**Results of the unconstrained phylogenetic analysis.** A cladistic parsimony analysis was performed based on the newly prepared dataset composed of 116 characters and 44 species without constraints and under implied weights ( $K = 12$ ). The analysis was performed two times with different outgroup species. With *Oryzias matanensis* (belontiiform) as outgroup, the analysis resulted in three equally parsimonious trees of 305 steps (CI = 0.455, RI = 0.756) of which the strict consensus is shown in Fig. 14A. Bootstrap support (500 repetitions) is moderate to good for some families (those being Pantanodontidae, Anablepidae, Fundulidae), but not for Valenciidae and Procatopodidae, which are not recovered as monophyletic. The general tree topology is similar to that obtained by Costa (2012a). The valenciid taxa of Costa’s (2012a) matrix, i.e. *V. hispanica*, *V. robertae* [as *V. letourneuxi* in Costa], †*Prolebias stenoura*, †*Francolebias delphinensis* and †*F. aymardi*, plus the newly added *V. letourneuxi* cluster together. However, contrary to Costa (2012a), the three *Valencia* species form a polytomy with a clade including †*Prolebias* + †*Francolebias*. Notably, this clade does not include the newly added fossil valenciids: †*Aphanolebias* is placed as sister to *Aplocheilus panchax* (Hamilton, 1822) (Aplocheiloidei), whereas †*Miovalencia* gen. nov., retrieved as monophyletic, is placed as sister to a polytomy containing †*F. rhenanus*, two members of the family Anablepidae, †*Wilsonilebias* gen. nov., which is not monophyletic, and †*F. arvernensis*. A second analysis with *Melanotaenia affinis* (atheriniform) as outgroup, resulted in three trees of 301 steps (CI = 0.458, RI = 0.760), of which the strict consensus is shown in Supplemental material Fig. S9a. Both analyses yielded similar results, with only minor differences in bootstrap support.

## Results of the constrained phylogenetic analysis.

Using the same dataset, we also performed an implied weights maximum parsimony analysis using the latest molecular phylogenies (Bragança *et al.*, 2018; Piller *et al.*, 2022) as scaffold for the extant clades, while the

fossil taxa were left unconstrained as floaters. As in the unconstrained analysis, we performed two analyses, each with different outgroup species. With *O. matanensis* as outgroup, the analysis resulted in 24 equally parsimonious trees of 344 steps (Fit = 13.1511, CI = 0.403, RI = 0.669) of which the strict consensus tree is shown in Fig. 13B. Almost all families show relatively good (>80) bootstrap support (500 repetitions), except Valenciidae and Procatopodidae, while both the Old World clade and the relationships among its families (Procatopodidae, Valenciidae, Aphaniidae) reveal low support values. Notably, the three species of *Valencia* are included in a polytomy with a clade comprising all fossils of the Valenciidae except †*Aphanolebias*, which is retrieved in a polytomy with †*Eurolebias* and present-day Aphaniidae (Fig. 14B). Within the clade with the extant *Valencia* and most valenciid fossils, †*Miovalencia* gen. nov. is monophyletic, †*Francolebias* and †*Wilsonilebias* gen. nov. are not monophyletic, but

grouped in a clade that is sister to †*Prolebias stenoura*, and this entire group is sister to †*Miovalencia* gen. nov. (Fig. 14B). The analysis with *M. affinis* as outgroup resulted in 48 trees of 340 steps (CI = 0.405, RI = 0.703), of which the strict consensus is shown in Supplemental material Fig. S9b. Both analyses have similar results with slight differences in bootstrap support, and only show difference in the polytomy formed by †*Wilsonilebias* gen. nov. species, †*Francolebias rhenanus* and †*F. arvernensis*.

## Discussion

### Systematic position of the new killifish genera from the Bugojno Basin

The position of the new genera from the Bugojno Basin within the order Cyprinodontiformes is supported by two synapomorphies recognized by Costa (2012b) and Parenti

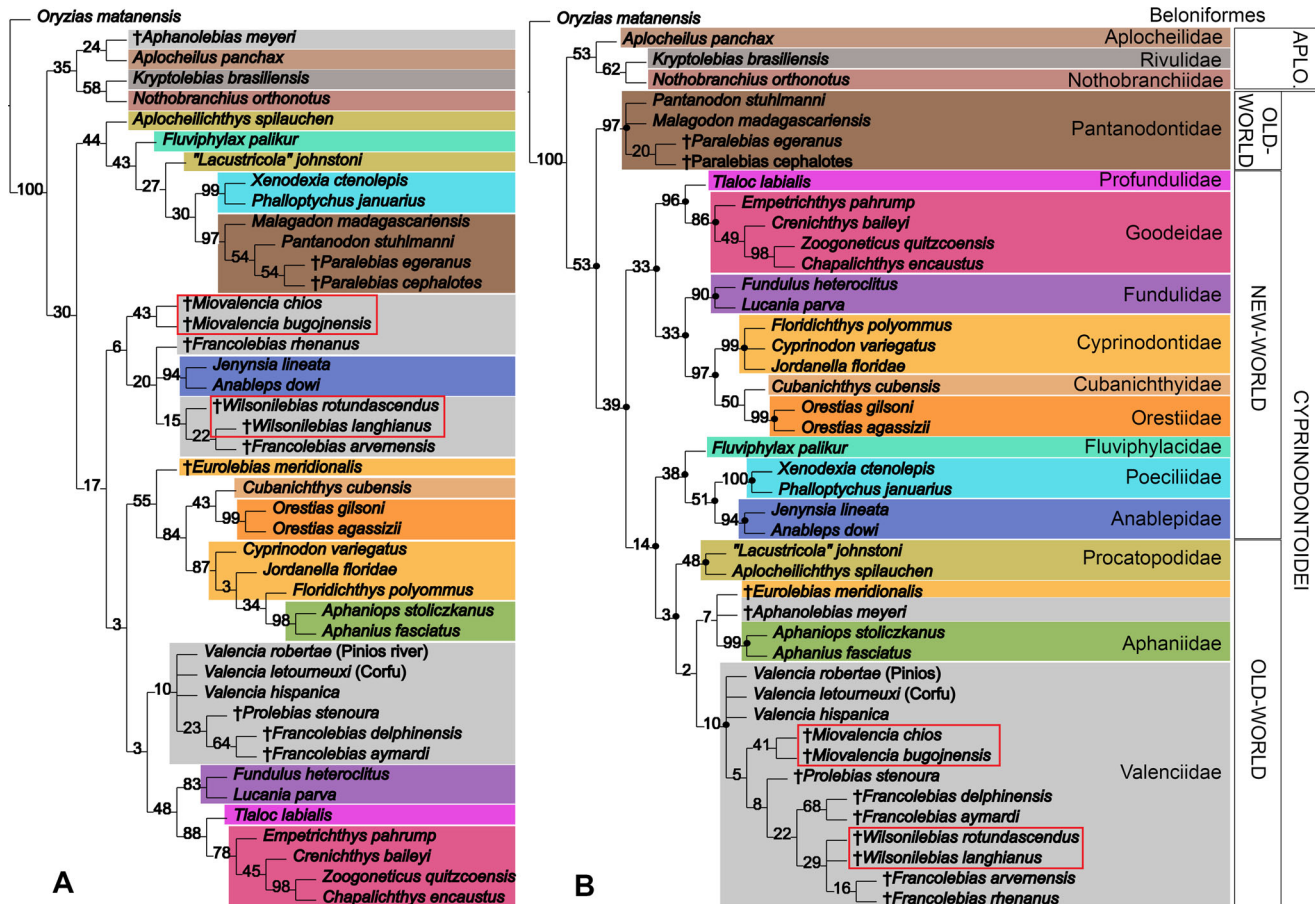


**Figure 14.** **A**, unconstrained and **B**, constrained maximum parsimony tree of 43 species of Cyprinodontiformes using implied weight ( $K = 12$ ), with absolute bootstrap values. **A**, strict consensus of three equally parsimonious trees (TL = 305, CI = 0.455, RI = 0.756). **B**, strict consensus of 24 equally parsimonious trees (TL = 344, CI = 0.403, RI = 0.669) using as molecular scaffold the molecular phylogenies of Bragança et al. (2018) and Piller et al. (2022); constrained nodes are indicated with a black circle, fossils (†) were left as floaters. Shading colours refer to families, the fossil species from the Bugojno Basin are highlighted by a red box. For details of analysis data see Supplemental material Table S1, sheets 4–6.

(1981): the first pleural rib is articulating on the parapophysis of the second vertebra and the caudal fin skeleton is symmetrical, with one epural mirroring the parhypural. Placement within the suborder Cyprinodontoidei was determined based on the presence of characteristics specific for the Cyprinodontoidei (Altner & Reichenbacher, 2015; Costa, 1998; Parenti, 1981). These include: a broad, deep dentary; an anteriorly bent head of the autopalatine; a spine-like process in the dorsoposterior portion of the terminal centrum; and neural and haemal spines of preural 2 and 3 that are wider than the spines of preural 4 and preceding caudal vertebrae.

The family Valenciidae was diagnosed by Parenti (1981) based on a single synapomorphy, i.e. the presence of an elongated dorsal process of the maxilla (Table 6, Fig. 15A, B). The same process is trapezoid in Aphaniidae (Fig. 15C, D) and rounded in Procatopodidae (Fig. 15E, F). Although rarely preserved, as it is very fragile and usually pushed underneath the premaxilla, the identification of a narrow and elongated dorsal process of the maxilla was possible in some of the studied specimens of †*Miovalencia* gen. nov. and †*Wilsonilebias* gen. nov. Moreover, Costa (2012a) proposed two further synapomorphies for the Valenciidae, i.e. distinctively thicker anal-fin rays than dorsal-fin rays, and a PU 2-neural spine that is three to four times wider than the PU 4-neural spine (Table 6). Considering these synapomorphies and the synapomorphy introduced by Parenti (1981), Costa (2012a) could classify †*Prolebias stenoura*, †*Francolebias delphinensis* and †*F. aymardi* as members of Valenciidae and retrieved them together with *Valencia* as a monophyletic group.

However, we found it difficult to assess what is meant by ‘distinctively’ thicker anal-fin rays. Based on Costa (2012a, fig. 2c), †*Francolebias delphinensis* shows somewhat thicker anal-fin rays, but †*Prolebias stenoura* does not (Costa, 2012a, fig. 2a). In the studied specimens of †*Miovalencia* gen. nov. and †*Wilsonilebias* gen. nov., as well as in *Valencia hispanica*, the anal-fin rays were equal to slightly thicker than the dorsal-fin rays (Table 1), but we would not interpret them as ‘distinctively’ thicker. The other synapomorphy introduced by Costa (2012a), i.e. presence of a PU 2-neural spine that is three to four times wider than that of PU 4, could be observed in several specimens of †*Wilsonilebias* gen. nov. and †*Miovalencia* gen. nov. (Table 1). Notably, our specimens of *V. hispanica* (ZSM 15451, 15453, 15454) showed some variability in this trait as the width of their PU 2-neural spine was 1.6, 2.5 and 3.0 times the width of the PU 4-neural spine (Supplemental material Table S1, sheet 2, column AS). That this character shows some variability was also observed in other killifish taxa (Altner & Reichenbacher, 2015).

Furthermore, both Costa (2012a) and Gaudant (2016) highlighted additional shared characteristics among the fossil species of †*Prolebias*, †*Francolebias* and *Valencia* which can help to distinguish them from the members of the two other Old World families, the Aphaniidae and Procatopodidae. These characters encompass (i) a long and narrow ascending process of the premaxilla; (ii) jaws with conical teeth arranged in multiple rows, (iii) posteriorly positioned unpaired fins; and (iv) origin of the dorsal fin slightly behind the anal fin origin (Table 6). The same combination of characters is visible in the specimens from the Bugojno Basin and confirms that they cannot belong to Aphaniidae, and together with the presence of a pelvic fin that is closer to the anal than to the pectoral fin, also differentiates them from the Procatopodidae (Table 6). Additionally, the pelvic fin of the specimens from the Bugojno Basin has no hook-like rays which, together with its position relatively nearer to the anal fin, is clearly different from the pelvic fin of the single fossil genus of the family Pantanodontidae, the genus †*Paralebias* Gaudant, 2013 (Gaudant, 2013; Rosen, 1965). Furthermore, their teeth arrangement is different from the European genus †*Eurolebias* (?Cyprinodontidae), which has large teeth in the outer row and few small teeth in the internal row near the symphysis (Costa, 2012a; Gaudant, 1978).

### Discussion of the phylogenetic results

Phylogenetic analysis with fossils is always a complicated task as morphology-based groups can be related to each other due to convergent evolution (Lee & Palci, 2015) or missing data (Mongiardino Koch *et al.*, 2021). This is also clearly visible in the results of our unconstrained phylogenetic analysis, in which the relationships between the families, as it has been established based on molecular work, are not resolved (Fig. 14A). Additionally, Valenciidae is not monophyletic in the unconstrained tree, as †*Wilsonilebias* gen. nov., two species of †*Francolebias* (†*F. rhenanus*, †*F. arvernensis*) are in a clade with the Anablepidae Garman, 1895. Most Anablepidae are viviparous, reproduce by internal fertilization, and possess an anal fin that is modified into a gonopodium (Meyer & Lydeard, 1993; Parenti, 1981). Both †*Wilsonilebias* gen. nov. and †*Francolebias* are, amongst others, characterized by specific modifications in the anal-fin skeleton; though their grouping with Anablepidae could be due to convergence in the modifications of the anal-fin and adjacent structures.

A molecular scaffold approach, as we used in the constrained analysis, is frequently used to incorporate fossils and extant taxa in the same analysis, in particular when total evidence data is not available (Darlim *et al.*, 2022; Paterson *et al.*, 2020; Springer *et al.*, 2001). With the molecular

**Table 6.** Character presence-absence of the genera of the family Valenciidae (dark green), Aphaniidae (light green), and Procatopodidae (beige). Data from Costa (1998, 2012a, 2012b), Reichenbacher and Gaudant (2003), and Gaudant (1978, 1981b, 1988, 1989, 2012, 2013, 2016), and this study.

	<i>Valencia</i>	† <i>Prolebias</i>	† <i>Aphanolebias</i>	† <i>Francolebias</i>	† <i>Wilsonilebias</i> gen. nov.	† <i>Miovalencia</i> gen. nov.	Aphaniidae	Procatopodidae
Synapomorphy	+	+	?	+	+	+	0	0
Narrow, equally wide DMX as VMX (vs wider)								
Anal rays distinctively thicker (vs equal/slightly thicker)	+?	+	?	+	0	0	0	0
nsPU2 width 3-4 times that of PU4 (vs equal/slightly wider)	v	+	?	+	+	+	0	0
Shared								
Long premaxillary ascending process (ASC) (vs short)	+	+	+	+	+	+	0	0?
Truncate, rectangular ASC (vs narrow, triangular)	+	+	?	+	+	+	0	+
Maxilla ventral process well developed (vs rudimentary)	+	?	?	?	+	+	0	v
Jaw dentition in multiple rows (vs one row)	+	+	+	+?	+	+	0	+
Conical jaw teeth (vs tricuspid)	+	+	+	+	+	+	0v	+
Pelvic fin position closer to anal (vs closer to pectoral)	+	+	+	+	+	+	+	0
Dorsal-fin origin opposing/behind anal fin origin (vs in front)	+	+	+	+	+	+	v	v

For osteological or otolith characters see Figs 3, 5–12, Supplemental material Figs S2, S4, and Supplemental material Table S1, sheets 4 and 5. + = presence, 0 = absence, ? = unknown condition or uncertainty because of different observations in previous works/in our study, v = variable character state.

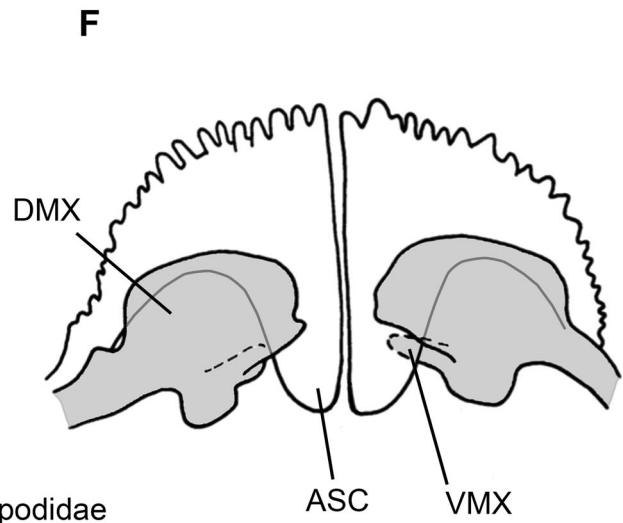
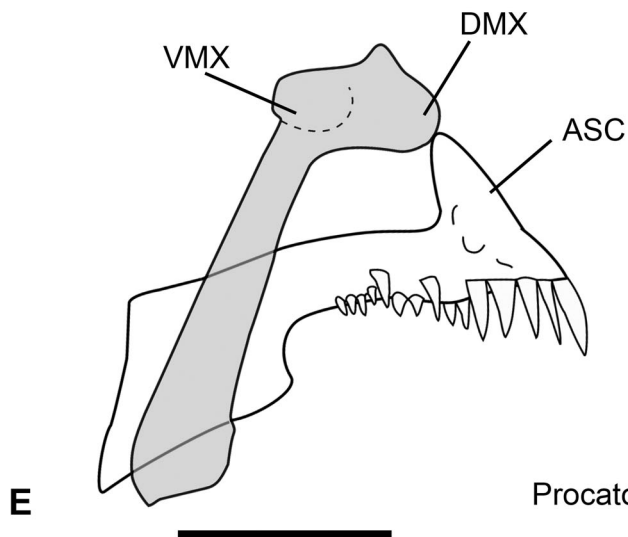
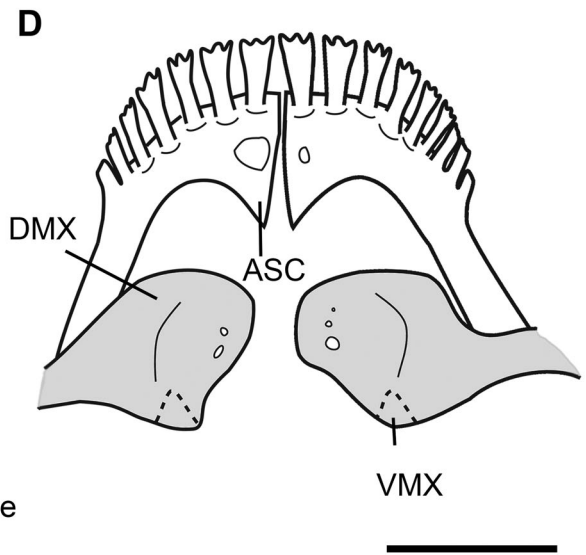
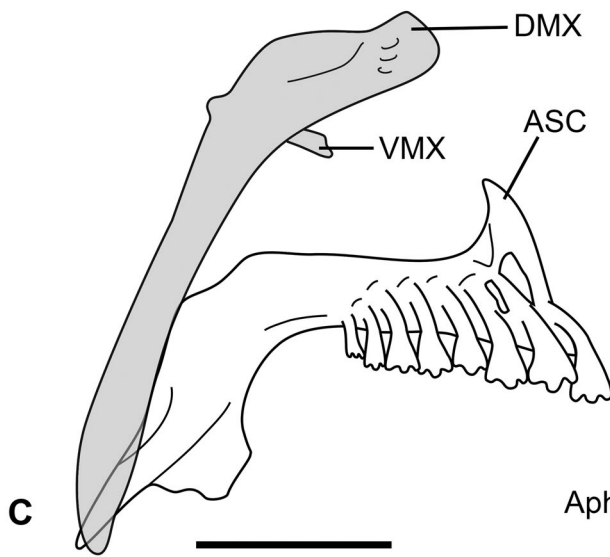
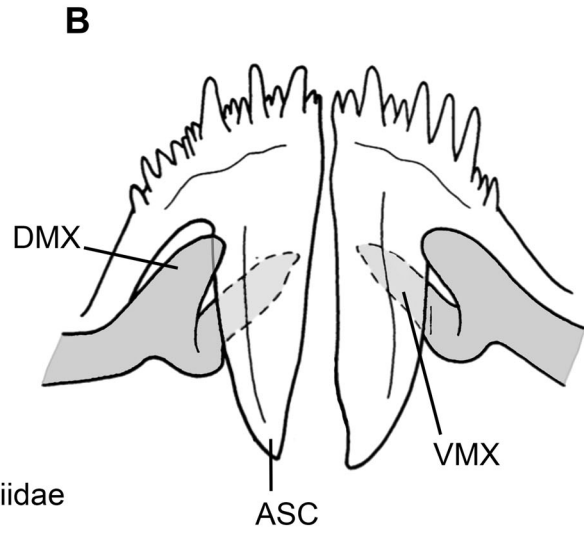
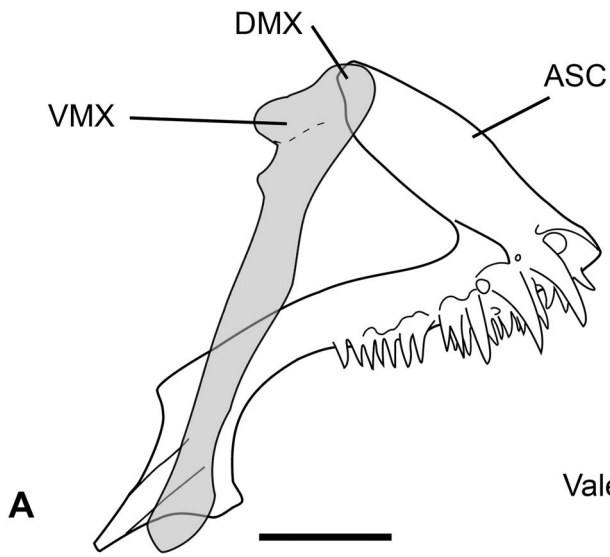


**Table 7.** Character presence-absence of the genera of the family Valenciidae. See Table 6 for literature sources and symbols.

		<i>Valencia</i>	† <i>Prolebias</i>	† <i>Aphanolebias</i>	† <i>Francolebias</i>	† <i>Wilsonilebias</i> gen. nov.	† <i>Miovalencia</i> gen. nov.
Genus combination	Robust premaxilla ASC base ( <i>vs</i> slender)	+	?	?	?	0	+
	Retroarticular elongated ( <i>vs</i> short)	0	0	?	0	+	+
	Parietal present ( <i>vs</i> not present)	+	0	?	0?	?	+
	Ventral process of posttemporal ossified ( <i>vs</i> unossified)	0	+	?	+	+	?
	Deep body depth around 28–30% SL ( <i>vs</i> slender)	0	0	+	v	0	0
	Broad pelvic bone 70% w/l ( <i>vs</i> slender, 50% w/l)	0	0	?	+	+	+
	Dorsal/anal fin position about 70% SL ( <i>vs</i> 60– 65% SL)	+	0	+	0	0	0
	1st and 2nd dorsal pterygiophore fused ( <i>vs</i> unfused)	0	0	?	+	0	0
	1st dorsal ptery. with broad triangle shape ( <i>vs</i> not expanded)	0	?	?	?	0	+
	Anal-fin ptery. reaching haemal arch ( <i>vs</i> up to distal portion)	0	0	?	+	+	0
	Haemal spines above anal- fin modified in putative males ( <i>vs</i> unmodified)	0	0	0	+	+	0
	Anal-fin posterior ptery. long ( <i>vs</i> diminishing, short)	0	0	?	v	+	0
	Hypurals fused/suture visible ( <i>vs</i> unfused/ partially fused*)	+	0	0*	v	0*	+
	Parhypural overlapping/ contact TC ( <i>vs</i> not articulating)	+	+	+	+	0	+
	Sagitta otolith triangular shape ( <i>vs</i> rounded)	+	0	+	0	+	+
	Sagitta sulcus straight ( <i>vs</i> bent posteriorly)	+	+	0	+	v	+

scaffold, both †*Miovalencia* gen. nov. and †*Wilsonilebias* gen. nov. were resolved within Valenciidae. The species of †*Miovalencia* gen. nov. formed a monophyletic group, but the species of †*Wilsonilebias* gen. nov. formed a polytomy with the same two species with which they were grouped in the unconstrained analysis, i.e. †*F. rhenanus* and †*F. arvernensis*. The type species of †*Francolebias*, i.e. †*F.*

*delphinensis*, and †*F. aymardi* are resolved as sister group to this polytomy (Fig. 14B). This suggests that †*Francolebias* is paraphyletic and needs revision. A possible hypothesis is that †*F. rhenanus* and †*F. arvernensis*, both of which had been interpreted as †*Francolebias* by Gaudant (2016) and not by Costa (2012a), actually represent further species of †*Wilsonilebias* gen. nov.

**Figure 15.** Upper jaw reconstruction of **A, B**, Valenciidae, **C, D**, Aphaniidae and **E, F**, Procatopodidae in lateral (**A, C, E**) and dorsal views (**B, D, F**). **A, B**, *Valencia hispanica* (**A**, ZSM 2070, **B**, modified from Parenti (1981, fig. 5d). **C, D**, *Aphaniops stoliczkanus* (specimens **C**, BSPG 2024 VII 4 (22) and **D**, BSPG 2024 VII 4 (6) from Al Bahayez, Oman; see Herbert Mainero et al., 2023). **E**, ‘*Lacustricola johnstoni* (SAIAB 35820) redrawn from Bragança et al. (2020, fig. 6n mirrored). **F**, ‘*Aplocheilichthys johnstoni* modified from Parenti (1981, fig. 35c). **Abbreviations:** ASC, ascending process of the premaxilla; **DMX**, dorsal process of the maxilla; **VMX**, ventral process of the maxilla. Scales = 1 mm.

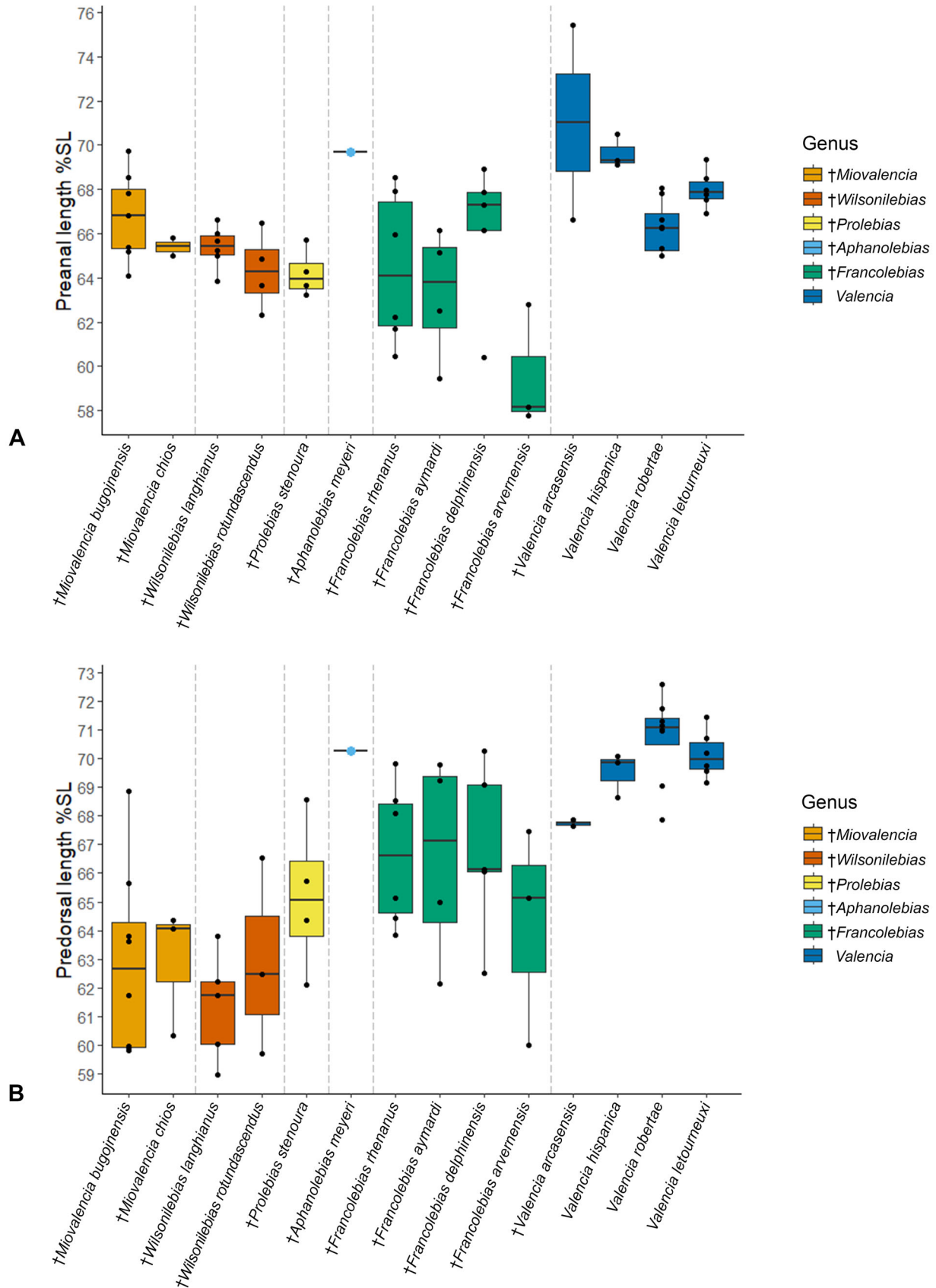


**Figure 16.** **A**, preanal length and **B**, predorsal length (in % of standard length) of the three extant species of *Valencia*, †*Valencia arcasensis* and the species of the five extinct genera of the Valenciidae.

### Internal fertilization in fossil Valenciidae

Internal fertilization is known from multiple groups of fish, including Cyprinodontiformes, and is usually accompanied by a set of modifications in the anal and pelvic fin (Blackburn & Hughes, 2024; Helmstetter et al., 2016; Jones et al., 2016; Parenti, 2005). Accordingly, Costa (2012a) suggested that the anal-fin modifications seen in †*Francolebias* (large anal-fin pterygiophores and robust haemal spines above anal fin) could be an adaptation for internal fertilization. †*Wilsonilebias* gen. nov. shows the same anal-fin modifications as reported for †*Francolebias*. Thus it can be suggested that †*Wilsonilebias* gen. nov. had the same specific mode of reproduction like †*Francolebias*. The presence of two genera within the Valenciidae that possess modifications in the anal fin, and four genera without such modifications (*Valencia*, †*Aphanolebias*, †*Miovalencia* gen. nov., †*Prolebias*, see Table 7) indicates that diverse fertilization modes were present in Valenciidae in prior times. Moreover, Valenciidae would represent the fifth family among the Cyprinodontiformes that has independently developed internal fertilization.

### Remarks on the taxonomic value of the lapillus

Among the three pairs of otoliths, the saccular otolith (sagitta) is long known for its significant taxonomic value as it allows the distinction of species and genera (e.g. Lin & Chien, 2022; Nolf, 2013; Schwarzhans, 1978). The utricular otolith (lapillus), on the other hand, has been considered for the taxonomy of non-Otophysi only by few researchers (e.g. Assis, 2005; Schulz-Mirbach & Plath, 2012). Also in the context of fossils, the lapillus has received little attention due to its small size and infrequent occurrence *in situ* in a skeleton (Assis, 2005). Furthermore, the lapillus appears to be more constrained than the sagitta because it is related to the sense of posture, which may explain why it presents relatively few morphological characters that can be used for taxonomical purposes (Assis, 2005; Schulz-Mirbach et al., 2010; Schulz-Mirbach & Plath, 2012).

Assis (2005) proposed that the lapillus is most useful for diagnosis below the family level, with the most important characters being the outline, and the gibbus maculae and the linea basalis in the ventral face (Fig. 13C). This has been confirmed in a study of fossil Gobiidae from the Middle Miocene of Eastern Europe, in which lapilli preserved *in situ* in skeletal material were found to be diagnostic at genus level (Reichenbacher & Bannikov, 2022). Additionally, research conducted on some Poeciliidae has shown that differences in the lapillus shape between species is

usually noticeable (Schulz-Mirbach et al., 2010; Schulz-Mirbach & Plath, 2012).

The unique *in situ* preservation of lapilli in multiple individuals of *Miovalencia* gen. nov. and †*Wilsonilebias* gen. nov. has provided us with the opportunity to expand our knowledge on this otolith and its discriminative power. We were able to confirm that the lapillus can be useful for both genus and species discrimination since we found clear differences in the lapillus outline between *Valencia*, †*Miovalencia* gen. nov. and †*Wilsonilebias* gen. nov., and some additional differences in the ventral face and the *linea basalis* between species (Fig. 13). Although rare, the presence of lapilli has been reported in other killifish fossil faunas (Caballero-Viñas et al., 2023; Sferco et al., 2022). Our results may encourage further comparative morphological analyses of the lapillus in additional genera and families of Cyprinodontiformes, as such knowledge could significantly aid in fossil classification.

### Palaeoenvironment and palaeoecology of the Bugojno Basin

The Middle Miocene (Langhian, 14.8 to 13.8 Ma) palaeolake deposits at Gračanica in the Bugojno Basin (Dinaride Lake System) yielded a diverse killifish fauna consisting of two new genera and four species. The lacustrine fauna alongside the killifish is composed of a low-diverse mollusc fauna – perhaps because littoral gastropods disappeared during the rise of the lake level (Mandic et al., 2020), an ostracod assemblage, mainly represented by unidentified Candonidae (Hajek-Tadesse, 2020), two genera of march flies (Bibionidae, Diptera) (Wedmann & Skartveit, 2020), as well as salamanders and frogs (Vasilyan, 2020). Pollen surveys of the section revealed high abundance of *Cedrus*, signalling a light cooling period with high humidity, but also presence of subtropical forests (Jiménez-Moreno & Mandic, 2020). Taking all fossil evidence together, a deep, relatively productive lake in an overall humid subtropical climate can be assumed (Hajek-Tadesse, 2020; Jiménez-Moreno & Mandic, 2020; Wedmann & Skartveit, 2020).

Together with the killifish, two partial skeletons of a barb (aff. *Barbus*) have been described from the Bugojno Basin by Vasilyan (2020). The author noted that several otoliths of killifish (Vasilyan, 2020; fig. 2k-m) and vertebrae of a small-sized fish (possibly also a killifish) were preserved together with the bone remains of the barb and suggested that the barb preyed on killifishes. The sagittae shown in Vasilyan (2020, fig. 2l) possibly belong to †*Miovalencia bugojnensis* gen. et sp. nov., while that shown in Vasilyan (2020, fig. 2k) can be referred to †*Wilsonilebias langhianus* gen. et sp. nov. Following the assumption of Vasilyan (2020), the

species of both new genera were possible prey fish of the barb.

Amongst other factors, predation is known to affect body shape, in particular the caudal peduncle and fin positions, which are related to swimming capability (Fletcher *et al.*, 2014; Langerhans & Makowicz, 2009; Maxwell & Wilson, 2013; Moody & Lozano-Vilano, 2018). Regarding dorsal- and anal-fin positions, the dorsal fin is more prone to vary because the anal fin is constrained by the anus position (Mabee *et al.*, 2002). Predatory pressure may explain the more anterior position of the dorsal fin seen in our new taxa relative to other valenciids (Fig. 16). The latter is coupled with a relatively longer caudal peduncle, which could have improved swimming performance and helped the killifish to avoid predation.

Additionally, the two genera could have diversified by exploiting different water column depths. According to previous works, species in deeper areas show a more rounded sagitta shape (Assis *et al.* 2020; Volpedo & Echeverría, 2003), as seen here in †*W. rotundascendus* gen. et sp. nov. Accordingly, †*W. rotundascendus* gen. et sp. nov. possibly inhabited deeper areas, while the other remained in shallower zones.

### Palaeobiogeography of Valenciidae

Killifishes appear to have been very successful in Europe during the Oligocene and Miocene. They had a wide distribution in the Western and Central Paratethys, as well as in the Upper Rhine Graben, Mainz Basin, and further basins in Spain and France (e.g. Bradić-Milinović *et al.*, 2021; Gaudant *et al.*, 2015; Gaudant & Rovira-Sendrós, 1998; Reichenbacher & Prieto, 2006; Reichenbacher & Kowalke, 2009; Vasilyan *et al.*, 2009; von Salis, 1967). The new Valenciidae described here expand their previously known geographical distribution and improve our understanding of their historical biogeography (Fig. 17). They also document the first record of Cyprinodontiformes from the Dinaride Lake System, from where only very poorly preserved fish remains have previously been mentioned (Neubauer *et al.*, 2016).

The extant species of *Valencia* are the sole representatives of Valenciidae today. They are currently restricted to coastal and inland water systems of the Spanish Mediterranean coast, Greece and Albania (Barbieri *et al.*, 2000; Freyhof *et al.*, 2014; Shumka *et al.*, 2020). In contrast, extinct genera of Valenciidae were present in multiple freshwater environments across Europe, and their biogeographical history appears to be

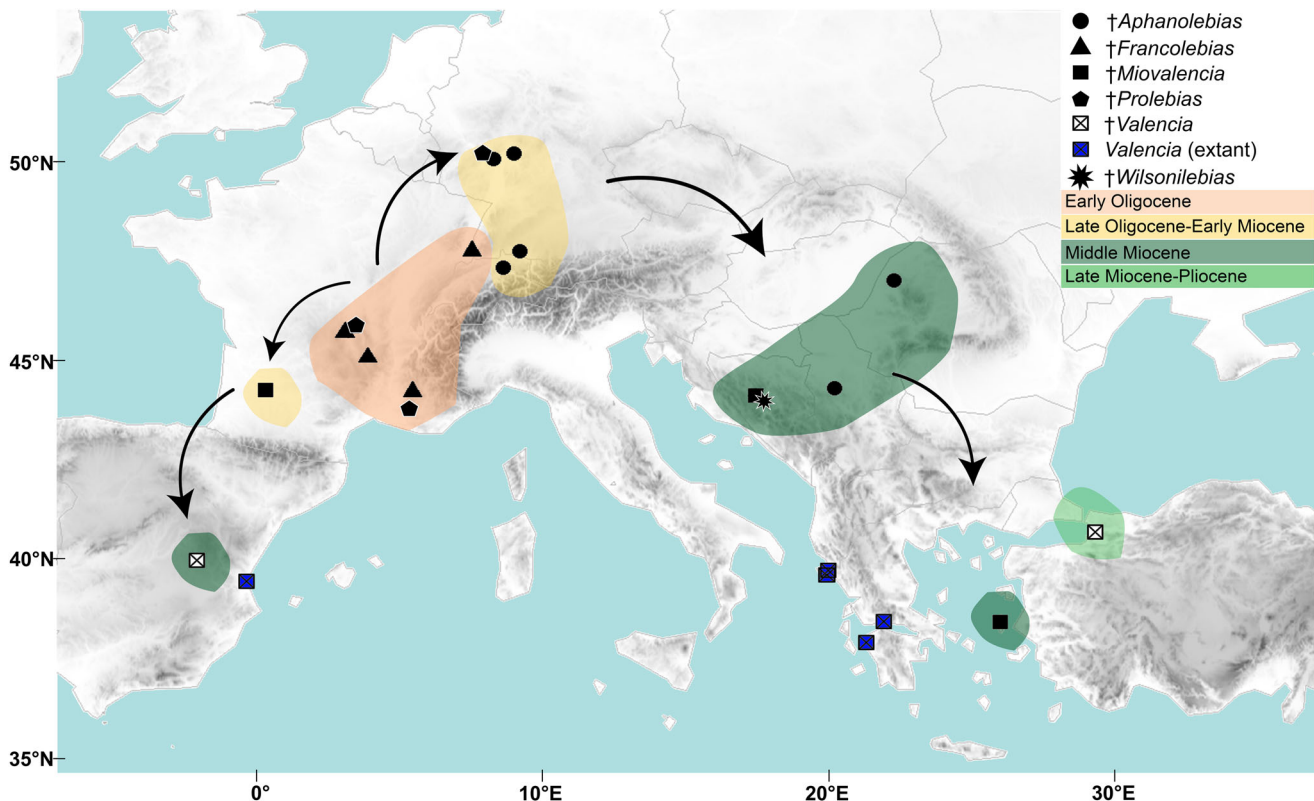


**Figure 17.** Biogeographical map of the extant and fossil species of the Valenciidae showing geographical distribution and temporality of each genus. Source of map: © EuroGeographics.

linked to the geological history of the European continent, as it has been suggested for other freshwater organisms (Neubauer et al., 2015). Their first occurrence is represented by †*Francolebias* and †*Prolebias* from several lower Oligocene basins in France (Limagne Basin, Apt Basin, Potassium salt Basin of Alsace) and southern Germany (southern Upper Rhinegraben, Kleinkems) (Gaudant, 1981a, 1981b, 1988, 1989, 2012, 2016; Reichenbacher & Philippe, 1997). By the end of the early Oligocene and beginning of the late Oligocene, †*Prolebias* moved towards the east, as documented by the presence of †*P. symmetricus* in the northern Upper Rhein Graben and Mainz Basin (Reichenbacher, 2000; Weiler, 1963; this work).

During the Early Miocene, †*Francolebias* and †*Prolebias* became most probably extinct, and Valenciidae is mostly represented by the genus †*Aphanolebias*, which has been registered in Lower Miocene sediments from the northern Upper Rhine Graben (Hanau and Mainz Basins) and the South German Molasse Basin (Reichenbacher, 1988, 1993, 2000; Reichenbacher & Gaudant, 2003; Reichenbacher, Böhme, et al., 2004; Reichenbacher, Gaudant, et al., 2004). However, †*Miovalencia angulosa* from the Lower Miocene of the Aquitaine Basin, France (Steurbaut, 1978) indicates that Valenciidae not only moved to the east, but also to the west (Fig. 17).

During the Middle Miocene, †*Aphanolebias* and †*Miovalencia* gen. nov. moved further east, entering multiple lake systems, such as the Dinaride Lake System (this work), the Serbian Lake System (Bradić-Milinović et al., 2021), and the Pannonian Basin (Reichenbacher et al., 2019). There is no other record of †*Wilsonilebias* gen. nov. However, since its closest relative is †*Francolebias* (only known from France and southern Germany), it is probable that its ancestor also migrated from West to East. Additionally, in the same period, the first appearance of the genus *Valencia* has been recorded from Spain (Gaudant et al., 2015). This indicates that Valenciidae also moved further to the west. Thus, the recent distribution of *Valencia* and Valenciidae, respectively, could have resulted from their Early and Middle Miocene migrations. This suggests that the ancestor of *Valencia hispanica* split from *V. letourneuxi* and *V. robertae* as early as in the Early Miocene (Fig. 17). Notably, this idea is consistent with the hypothesis proposed by Perdices et al. (1996), who, based on molecular work, stated that *Valencia* species must have split since 18 Mya, thus in the Early Miocene.

The fossil record of Valenciidae from the Late Miocene is poorly known, whereas fossils of Aphaniidae are well known from the same time interval (e.g. Carnevale & Schwarzhans, 2022; Reichenbacher & Kowalke, 2009). A single fossil species of *Valencia* has

been described from the Miocene-Pliocene of Turkey (Rückert-Ülkümen, 2006). It could be that changes in climatic conditions and disappearance of suitable lacustrine environments resulted in the decline of the group. This further enhances that the present-day species from Spain and Greece/Albania remained disconnected from each other since the Early Miocene.

## Concluding remarks and outlook

A diverse assemblage of killifish was described from Middle Miocene sediments in the Bugojno Basin within the Dinaride Lake System. The remarkable abundance of well-preserved skeletons with otoliths preserved *in situ* from the Bugojno palaeolake gives the opportunity to enhance our understanding of killifish palaeodiversity, intraspecific variability and biogeographical distribution. Two new genera and four species were found to live in sympatry in the slightly alkaline palaeolake of the Bugojno Basin. The new genera, †*Miovalencia* gen. nov. and †*Wilsonilebias* gen. nov., share the synapomorphies that are known for the family Valenciidae, and each exhibits a distinctive combination of osteological and otolith characteristics that makes it unique. †*Wilsonilebias* gen. nov. is the second genus among the Valenciidae that possesses a modified anal-fin skeleton, similar to the Oligocene valenciid †*Francolebias*. Each of the new genera is represented with two species, of which †*M. chios* is a previously described otolith-based species from the Chios Island, Greece, which is now for the first time represented by skeletal finds. The abundant skeletons with preservation of otoliths *in situ* allowed us to test the usefulness of both the sagitta and lapillus for species and genus recognition, yielding exciting new results on the taxonomical value of the lapillus.

Our findings not only expand our knowledge of the diversity of the family Valenciidae, but also expand their known distribution into the Dinaride Lake System. Considering their fossil record and the biogeography of their extant members, a trend of dispersal from central Europe towards the south-west (Iberian Peninsula) as well as towards the south-east (south-east Europe) is evident. Notably, their historical biogeographical pattern and present biogeography suggest that the recent distribution of the family has its roots in the Early Miocene.

In recent years, significant progress in understanding the diversification, phylogenetic relationship and evolution of Cyprinodontiformes has been made through both molecular methods (Costa et al., 2017; Esmaeili et al., 2020; Freyhof & Yögürtoğlu, 2020; Piller et al., 2022) and ontogenetic studies (Teimori, Motamedi, et al., 2021; Thieme et al., 2021, 2022). However, the last revision of

the European killifish fossil record was done by Costa (2012a, b) and the phylogeny of Cyprinodontiformes has changed radically since then. This has left many fossil species without proper family and genus classification (i.e. †*Eurolebias meridionalis*, ‘*Prolebias*’ *catalaunicus*, ‘*P.*’ *euskadiensis*, ‘*P.*’ *hungaricus*). An updated revision of killifish fossil faunas and morphological characters will allow for a more accurate diagnosis of fossil material and their inclusion into phylogenies, which is crucial for understanding phenotypic diversity through time and space (Lee & Palci, 2015). Not only that, but the inclusion of diverse structures like otoliths, which is sometimes the only element found, provides an exciting prospect for research into the evolutionary history, variability and paleobiogeography of Cyprinodontiformes.

## Acknowledgements

We sincerely thank Hazim Hrvatović (Federal Geological Survey of Bosnia and Herzegovina), Oleg Mandić and Ursula Göhlich (both Natural History Museum Vienna, Austria), Dževad Forčaković (Coal mine Gračanica Gornji Vakuf – Uskoplje), Charlene Gaillard and Renaud Roch (both Fribourg, Switzerland) for their great support in organizing the excavations. We are grateful to Emma Bernard (NHMUK London, UK) for access to the specimens of †*Prolebias stenoura* in the NHMUK fossil fish collection. We also thank Ulrich Schliewen (SNSB-ZSM Munich, Germany) for providing extant specimens of *Valencia* and X-ray facilities, the preparator team from the Bayerische Staatssammlung für Paläontologie und Geologie, Munich, Germany, for technical assistance in the conservation of the samples, Helmut Tischlinger (Stammham, Germany) for providing UV-photos, and Tomáš Přikryl (Czech academy of sciences, Prague, Czech Republic) for donating further material from Bugojno Basin. Finally, we thank the two reviewers for their constructive comments. The study has been partially funded by the German Science Foundation (project number RE 1113/6) and the Swiss National Science Foundation (project Nr. 200021\_197323).

## Disclosure statement

No potential conflict of interest was reported by the author(s).

## Supplemental material

Supplemental material for this article can be accessed online here: <https://doi.org/10.1080/14772019.2024.2412539>.

## Data availability statement

All relevant data are provided within the manuscript and the Supplemental material. The Supplemental material Figures S1–S9 can be found online at <https://figshare.com/s/a368de67e52e743dc6e6>, the Supplemental material Table S1 sheets 1–6 (excel file) and the nexus file for the phylogenetic analysis are available online at <https://figshare.com/s/7d12575f0f2f91c960a5>.

## References

- Agassiz, L. (1839). *Recherches sur les poissons fossiles* (Vol. 5). Société Géologique de Londres.
- Aguilera, G., Terán, G. E., Mirande, J. M., Alonso, F., Rometsch, S., Meyer, A., & Torres-Dowdall, J. (2019). Molecular and morphological convergence to sulfide-tolerant fishes in a new species of *Jenynsia* (Cyprinodontiformes: Anablepidae), the first extremophile member of the family. *PLoS ONE*, *14*(7), e0218810. <https://doi.org/10.1371/journal.pone.0218810>
- Altner, M., & Reichenbacher, B. (2015). †Kenyaichthyidae fam. nov. and †*Kenyaichthys* gen. nov. – first record of a fossil Aplocheiloid Killifish (Teleostei, Cyprinodontiformes). *PLoS ONE*, *10*(4), e0123056. <https://doi.org/10.1371/journal.pone.0123056>
- Arnoult, J. (1963). Un Oryziiné (Pisces, Cyprinodontidae) nouveau de l'est de Madagascar. *Bulletin du Muséum National d'Histoire Naturelle Série 2*, *35*(3), 235–237.
- Arratia, G. (2008). Actinopterygian postcranial skeleton with special reference to the diversity of fin ray elements, and the problem of identifying homologies. In G. Arratia, H.-P. Schultze, & M. V. H. Wilson (Eds.), *Mesozoic Fishes – Systematics, Homology and Nomenclature* (Vol. 4, pp. 49–101). Verlag Dr. Friedrich Pfeil.
- Arratia, G., & Cione, A. (1996). The record of fossil fishes of southern South America. *Münchener Geowissenschaftliche Abhandlungen Reihe A Geologie und Paläontologie*, *30*, 9–72.
- Arratia, G., Vila, I., Lam, N., Guerrero, C. J., & Quezada-Romegialli, C. (2017). Morphological and taxonomic descriptions of a new genus and species of killifishes (Teleostei: Cyprinodontiformes) from the high Andes of northern Chile. *PLoS ONE*, *12*(8), e0181989. <https://doi.org/10.1371/journal.pone.0181989>
- Assis, C. A. (2003). The lagenar otoliths of teleosts: their morphology and its application in species identification, phylogeny and systematics. *Journal of Fish Biology*, *62*(6), 1268–1295. <https://doi.org/10.1046/j.1095-8649.2003.00106.x>
- Assis, C. A. (2005). The utricular otoliths, lapilli, of teleosts: their morphology and relevance for species identification and systematics studies. *Scientia Marina*, *69*, 259–273. <https://doi.org/10.3989/scimar.2005.69n2259>
- Assis, I. O., da Silva, V. E. L., Souto-Vieira, D., Lozano, A. P., Volpedo, A. V., & Fabrè, N. N. (2020). Ecomorphological patterns in otoliths of tropical fishes: assessing trophic groups and depth strata preference by shape. *Environmental Biology of Fishes*, *103*(4), 349–361. <https://doi.org/10.1007/s10641-020-00961-0>

- Aurich, H.** (1935). Mitteilung der Wallacea-Expedition Woltreck. Mitteilung XIII. Fische I. *Zoologischer Anzeiger*, 112, 97–107.
- Barbieri, R., Daoulas, C. H., Psarras, T. H., Stoumboudi, M. T., & Economou, A. N.** (2000). The biology and ecology of *Valencia letourneuxi* Sauvage 1880 (Valenciidae) – prospects for conservation. *Mediterranean Marine Science*, 1(2), 75–90. <https://doi.org/10.12681/mms.291>
- Berg, L. S.** (1940). *Classification of fishes, both recent and fossil* (Reproduced in Russian and English in 1947. ed.). Edwards Bros.
- Betancur-R., R., Broughton, R. E., Wiley, E. O., Carpenter, K., Lopez, J. A., Li, C., Holcroft, N. I., Arcila, D., Sanciangco, M., Cureton II, J. C., Zhang, F., Buser, T., Campbell, M. A., Ballesteros, J. A., Roa-Varon, A., Willis, S., Borden, W. C., Rowley, T., Reneau, P. C., ... Ortí, G.** (2013). The tree of life and a new classification of bony fishes. *PLoS Currents Tree of Life*, April 18 2013(5), 1–45. <https://doi.org/10.1371/currents.tol.53ba26640df0ccaee75bb165c8c26288>
- Betancur-R., R., Wiley, E. O., Arratia, G., Acero, A., Bailly, N., Miya, M., Lecointre, G., & Ortí, G.** (2017). Phylogenetic classification of bony fishes. *BMC Evolutionary Biology*, 17(1), 162. <https://doi.org/10.1186/s12862-017-0958-3>
- Blackburn, D. G., & Hughes, D. F.** (2024). Phylogenetic analysis of viviparity, matrotrophy, and other reproductive patterns in chondrichthyan fishes. *Biological Reviews of the Cambridge Philosophical Society*, 99(4), 1314–1356. <https://doi.org/10.1111/brv.13070>
- Bleeker, P.** (1860). Ordo Cyprini. Karpers. *Verhandelingen der Natuurkundige Vereeniging in Nederlandsch Indië*, 7, 1–492.
- Bogan, S., Contreras, V. H., Agnolin, F., Tomassini, R. L., & Peralta, S.** (2018). New genus and species of Anablepidae (Teleostei, Cyprinodontiformes) from the Late Miocene of Argentina. *Journal of South American Earth Sciences*, 88, 374–384. <https://doi.org/10.1016/j.jsames.2018.09.009>
- Bradić-Milinović, K., Rundić, L., & Schwarzhans, W.** (2021). Middle Miocene otoliths of freshwater fishes from the Vracevic Lake (Serbian Lake System). *Geološki Anali Balkanskoga Poluostrva*, 82(2), 1–24. <https://doi.org/10.2298/GABP210616006B>
- Bragança, P. H. N., Amorim, P. F., & Costa, W. J. E. M.** (2018). Pantanodontidae (Teleostei, Cyprinodontiformes), the sister group to all other cyprinodontoid killifishes as inferred by molecular data. *Zoosystematics and evolution: Mitteilungen aus dem Museum für Naturkunde in Berlin*, 94(1), 137–145. <https://doi.org/10.3897/zse.94.22173>
- Bragança, P. H. N., & Costa, W. J. E. M.** (2019). Multigene fossil-calibrated analysis of the African lampeyes (Cyprinodontoides: Procatopodidae) reveals an early Oligocene origin and Neogene diversification driven by palaeogeographic and palaeoclimatic events. *Organisms Diversity & Evolution*, 19, 303–320. <https://doi.org/10.1007/s13127-019-00396-1>
- Bragança, P. H. N., van Zeeventer, R. M., Bills, R., Tweddle, D., & Chakona, A.** (2020). Diversity of the southern Africa *Lacustricola* Myers, 1924 and redescription of *Lacustricola johnstoni* (Günther, 1894) and *Lacustricola myaposa* (Boulenger, 1908) (Cyprinodontiformes, Procatopodidae). *Zookeys*, 923, 91–113. <https://doi.org/10.3897/zookeys.923.48420>
- Caballero-Viñas, C., Alvarado-Ortega, J., & Magno Cantalice Severiano, K.** (2023). A Pliocene goodeid fish of the Paleolake Amajac, Sanctorum, Hidalgo, Mexico. *Palaentologia Electronica*, 26(6), a30. <https://doi.org/10.26879/1259>
- California Academy of Sciences (2024). *Ichthyology Primary Types Imagebase*. California Academy of Sciences. Retrieved 10 July 2023 from <https://researcharchive.calacademy.org/research/ichthyology/types/index.asp>
- Carnevale, G., & Schwarzhans, W.** (2022). Marine life in the Mediterranean during the Messinian salinity crisis: a paleoichthyological perspective. *Rivista Italiana di Paleontologia e Stratigrafia*, 128(2), 283–324. <https://doi.org/10.54103/2039-4942/15964>
- Charmpila, E. A., Teimori, A., Freyhof, J., Weissenbacher, A., & Reichenbacher, B.** (2020). New osteological and morphological data of four species of *Aphaniops* (Teleostei; Aphaniidae). *Journal of Applied Ichthyology*, 36(5), 724–736. <https://doi.org/10.1111/jai.14074>
- Costa, W. J. E. M.** (1997). Phylogeny and classification of the Cyprinodontidae revisited (Teleostei: Cyprinodontiformes): are Andean and Anatolian killifishes sister taxa. *Journal of Comparative Biology*, 2(1), 1–17.
- Costa, W. J. E. M.** (1998). Phylogeny and classification of the Cyprinodontiformes (Euteleostei: Atherinomorpha): a reappraisal. In L. R. Malabarba, R. E. Reis, R. P. Var, Z. M. Lucena, & C. A. S. Lucena (Eds.), *Phylogeny and classification of Neotropical fishes* (Vol. Part 6 – Atherinomorpha, pp. 537–560). EDIPUCRS.
- Costa, W. J. E. M.** (2011). Redescription and phylogenetic position of the fossil killifish *Carrionellus diumortuus* White from the Lower Miocene of Ecuador (Teleostei: Cyprinodontiformes). *Cybium*, 35(3), 181–187.
- Costa, W. J. E. M.** (2012a). Oligocene killifishes (Teleostei: Cyprinodontiformes) from southern France: relationships, taxonomic position, and evidence of internal fertilization. *Vertebrate Zoology*, 62(3), 371–386. <https://doi.org/10.3897/vz.62.e31397>
- Costa, W. J. E. M.** (2012b). The caudal skeleton of extant and fossil cyprinodontiform fishes (Teleostei: Atherinomorpha): comparative morphology and delimitation of phylogenetic characters. *Vertebrate Zoology*, 62(2), 161–180. <https://doi.org/10.3897/vz.62.e31383>
- Costa, W. J. E. M.** (2013). Historical biogeography of aplocheiloid killifishes (Teleostei: Cyprinodontiformes). *Vertebrate Zoology Senckenberg*, 63(2), 139–154. <https://doi.org/10.3897/vz.63.e31419>
- Costa, W. J. E. M., Amorim, P. F., & Mattos, J. L. O.** (2017). Molecular phylogeny and timing of diversification in South American Cynolebiini seasonal killifishes. *Molecular Phylogenetics and Evolution*, 116, 61–68. <https://doi.org/10.1016/j.ympev.2017.07.020>
- Cuvier, G. L., & Valenciennes, A.** (1846). Des Poecilies, des Cyprinodons, des Fundules, des Hydragyres et Grundules. In P. Bertrand (Ed.), *Histoire naturelle des poissons* (Vol. 18, pp. 105–136).
- Darlim, G., Lee, M. S. Y., Walter, J., & Rabi, M.** (2022). The impact of molecular data on the phylogenetic position of the putative oldest crown crocodylian and the age of the clade. *Biology Letters*, 18(2), 20210603. <https://doi.org/10.1098/rsbl.2021.0603>

- de Leeuw, A., Mandic, O., Krijgsman, W., Kuiper, K., & Hrvatovic, H. (2012). Paleomagnetic and geochronologic constraints on the geodynamic evolution of the Central Dinarides. *Tectonophysics*, 530–531(2), 286–298. <https://doi.org/10.1016/j.tecto.2012.01.004>
- Esmaeili, H. R., Teimori, A., Zarei, F., & Sayyadzadeh, G. (2020). DNA barcoding and species delimitation of the Old World tooth-carps, family Aphaniidae Hoedeman, 1949 (Teleostei: Cyprinodontiformes). *PLoS ONE*, 15(4), e0231717. <https://doi.org/10.1371/journal.pone.0231717>
- Fletcher, T., Altringham, J., Peakall, J., Wignall, P., & Dorrell, R. (2014). Hydrodynamics of fossil fishes. *Proceedings of the Royal Society B: Biological Sciences*, 281(1788), 20140703. <https://doi.org/10.1098/rspb.2014.0703>
- Fowler, H. W. (1916). Cold-blooded vertebrates from Costa Rica and the canal zone. *Proceedings of the Academy of Natural Sciences of Philadelphia*, 68, 389–414.
- Freyhof, J., Kärst, H., & Geiger, M. (2014). *Valencia robertae*, a new killifish from southern Greece (Cyprinodontiformes: Valenciidae). *Ichthyological Exploration of Freshwaters*, 24(4), 289–298.
- Freyhof, J., Weissenbacher, A., & Geiger, M. (2017). *Aphanius kruppi*, a new killifish from Oman with comments on the *A. dispar* species group (Cyprinodontiformes: Aphaniidae). *Zootaxa*, 4338(3), 557–573. <https://doi.org/10.11646/zootaxa.4338.3.10>
- Freyhof, J., & Yöğürtçuoğlu, B. (2020). A proposal for a new generic structure of the killifish family Aphaniidae, with the description of *Aphaniops teimorii* (Teleostei: Cyprinodontiformes). *Zootaxa*, 4810(3), zootaxa.4810.4813.4812. <https://doi.org/10.11646/zootaxa.4810.3.2>
- Fricke, R., Eschmeyer, W. N., & Fong, J. D. (2024). *Species by family/subfamily*. Retrieved 12 March 2024 from <http://researcharchive.calacademy.org/research/ichthyology/catalog/SpeciesByFamily.asp>
- Garman, S. (1895). The Cyprinodonts. *Memoires of the Museum of Comparative Zoology at Harvard College*, 19, 179.
- Gaudant, J. (1978). Sur une nouvelle espèce de Poissons Téléostéens Cyprinodontiformes de l'Oligocène des environs de Manosque (Alpes-de-Haute-Provence). *Géologie Méditerranéenne*, 5(2), 281–289. <https://doi.org/10.3406/geolm.1978.1050>
- Gaudant, J. (1981a). Nouvelles recherches sur l'Ichthyofaune des zones salifères moyenne et supérieure (Oligocène inférieur) du bassin potassique alsacien. *Sciences Géologiques Bulletin (Strasbourg)*, 34(4), 209–218. <https://doi.org/10.3406/sgeol.1981.1601>
- Gaudant, J. (1981b). Un nouveau Cyprinodontidae (poisson téléostéen) de l'Oligocène inférieur de Kleinkems (Pays de Bade, Allemagne): *Prolebias rhenanus* nov. sp. *Sciences Géologiques Bulletin (Strasbourg)*, 34(1), 3–12. <https://doi.org/10.3406/sgeol.1981.1585>
- Gaudant, J. (1982). *Prolebias catalaunicus* nov. sp.: une nouvelle espèce de poissons cyprinodontidae de l'Oligocène de Jarreal (Province de Tarragona, Catalogne). *Estudios geológicos*, 38, 95–102.
- Gaudant, J. (1988). Les cyprinodontiformes (Poissons téléostéens) oligocènes de Ronzon, Le Puy-en-Velay (Haute-Loire): Anatomie et signification paléocéologique. *Geobios*, 21(6), 773–785. [https://doi.org/10.1016/s0016-6995\(88\)80093-7](https://doi.org/10.1016/s0016-6995(88)80093-7)
- Gaudant, J. (1989). Découverte d'une nouvelle espèce de poissons cyprinodontiformes (*Prolebias delphinensis* nov. sp.) dans l'Oligocène du bassin de Montbrun-les-Bains (Drôme). *Géologie Méditerranéenne*, 16(4), 355–367. <https://doi.org/10.3406/geolm.1989.1431>
- Gaudant, J. (2002). The Miocene non-marine fish-fauna of Central Europe: a review. *Bulletin T. CXXV de l'Académie serbe des sciences et des arts-2002 Classe des sciences mathématiques et naturelles Sciences Naturelles*, 41, 65–74.
- Gaudant, J. (2012). Révision de *Prolebias stenoura* Sauvage, 1874 du Stampien (= Rupélien) de Limagne (centre de la France), espèce type du genre *Prolebias* (poisson téléostéen, Cyprinodontiformes). *Geodiversitas*, 34(2), 409–423. <https://doi.org/10.5252/g2012n2a9>
- Gaudant, J. (2013). Occurrence of poeciliid fishes (Teleostei, Cyprinodontiformes) in the European Oligo-Miocene: the genus *Paralebias* nov. gen. *Neues Jahrbuch für Geologie und Paläontologie Abhandlungen*, 267(2), 215–222. <https://doi.org/10.1127/0077-7749/2013/0305>
- Gaudant, J. (2016). *Francolebias arvernensis* n. sp., une nouvelle espèce de poissons cyprinodontiformes oligocènes de Chadrat (Saint-Saturnin, Puy-de-Dôme, France), avec une brève notice sur un Umbridae fossile du même gisement. *Geodiversitas*, 38(3), 435–449. <https://doi.org/10.5252/g2016n3a4>
- Gaudant, J., Barrón, E., Anadón, P., Reichenbacher, B., & Peñalver, E. (2015). Palaeoenvironmental analysis of the Miocene Arcas del Villar gypsum sequence (Spain), based on palynomorphs and cyprinodontiform fishes. *Neues Jahrbuch für Geologie und Paläontologie Abhandlungen*, 277(1), 105–124. <https://doi.org/10.1127/njgpa/2015/0503>
- Gaudant, J., & Rovira-Sendrós, J. (1998). Découverte de la plus ancienne espèce connue du genre *Aphanius* Nardo (Poissons téléostéens) dans le Miocène inférieur évaporitique de la Catalogne. *Batalleria*, 8, 55–60.
- Ghedotti, M. J. (2000). Phylogenetic analysis and taxonomy of the poecilioid fishes (Teleostei: Cyprinodontiformes). *Zoological Journal of the Linnean Society*, 130(1), 1–53. <https://doi.org/10.1111/j.1096-3642.2000.tb02194.x>
- Ghedotti, M. J., & Davis, M. P. (2013). Phylogeny, classification, and evolution of salinity tolerance of the North American topminnows and killifishes, family Fundulidae (Teleostei: Cyprinodontiformes). *Fieldiana Life and Earth Sciences*, 7, 1–65. <https://doi.org/10.3158/2158-5520-12.7.1>
- Gill, T. (1865). Synopsis of fishes in the Gulf of St. Lawrence and Bay of Fundy. *Canadian Naturalist*, 2(4), 244–266.
- Göhlich, U. B., & Mandic, O. (2020). Introduction to the special issue “The drowning swamp of Gračanica (Bosnia-Herzegovina)—a diversity hotspot from the middle Miocene in the Bugojno Basin”. *Palaeobiodiversity and Palaeoenvironments*, 100(2), 281–293. <https://doi.org/10.1007/s12549-020-00437-0>
- Goloboff, P. A. (1993). Estimating character weights during tree search. *Cladistics*, 9(1), 83–91. <https://doi.org/10.1111/j.1096-0031.1993.tb00209.x>
- Goloboff, P. A., Farris, J. S., & Nixon, K. C. (2008). TNT, a free program for phylogenetic analysis. *Cladistics*, 24(5), 774–786. <https://doi.org/10.1111/j.1096-0031.2008.00217.x>
- Goloboff, P. A., Torres, A., & Arias, J. S. (2018). Weighted parsimony outperforms other methods of phylogenetic inference under models appropriate for morphology.

- Cladistics*, 34(4), 407–437. <https://doi.org/10.1111/cla.12205>
- Günther, A.** (1894). Second report on the reptiles, batrachians and fishes transmitted by Mr. H.H. Johnston C.B. from British Central Africa. *Proceedings of the Zoological Society of London*, 1894, 616–628.
- Gut, C., Vukić, J., Šanda, R., Moritz, T., & Reichenbacher, B.** (2020). Identification of past and present gobies: distinguishing *Gobius* and *Pomatoschistus* (Teleostei: Gobioidae) species using characters of otoliths, meristics and body morphometry. *Contributions to Zoology*, 89(3), 282–323. <https://doi.org/10.1163/18759866-bja10002>
- Hajek-Tadesse, V.** (2020). Ostracods and the middle Miocene evolution of the Bugojno Basin (Bosnia and Herzegovina). *Palaeobiodiversity and Palaeoenvironments*, 100(2), 561–576. <https://doi.org/10.1007/s12549-019-00403-5>
- Halliday, T. J., Upchurch, P., & Goswami, A.** (2017). Resolving the relationships of Paleocene placental mammals. *Biological Reviews of the Cambridge Philosophical Society*, 92(1), 521–550. <https://doi.org/10.1111/brv.12242>
- Hamilton, F.** (1822). XI. Genus.—Esox. In *An account of the fishes found in the river Ganges and its branches* (pp. 211–212, pl. III, fig. 269). George Ramsay and Co., Edinburgh.
- Helmstetter, A. J., Papadopoulos, A. S., Igea, J., Van Dooren, T. J., Leroi, A. M., & Savolainen, V.** (2016). Viviparity stimulates diversification in an order of fish. *Nature Communications*, 7, 11271. <https://doi.org/10.1038/ncomms11271>
- Herbert Mainero, A., Al-Jufaili, S. M., Jawad, L., & Reichenbacher, B.** (2023). Sex dimorphism and evidence of sexually selected traits: A case study on the killifish *Aphaniops stoliczkanus* (Day, 1872). *Acta Zoologica*, 104(3), 473–487. <https://doi.org/10.1111/azo.12436>
- Hernandez, L. P., Adriaens, D., Martin, C. H., Wainwright, P. C., Masschaele, B., & Dierick, M.** (2018). Building trophic specializations that result in substantial niche partitioning within a young adaptive radiation. *Journal of Anatomy*, 232(2), 173–185. <https://doi.org/10.1111/joa.12742>
- Hernangómez, D.** (2023). *giscoR: Download Map Data from GISCO API - Eurostat*. In (Version 0.3.3.) <https://ropengov.github.io/giscoR/>
- Hoedemann, J. J.** (1949). Cyprinodontidae & Cyprinodontini. In *Encyclopaedie voor de Aquariumhouder* (Looseleaf ed., Vol. 10, pp. 211). De Regenboog.
- Hollister, J., Shah, T., Nowosad, J., Robitaille, A., Beck, M., & Johnson, M.** (2023). *elevatr: Access elevation data from various APIs*, R package version 0.4.2. <https://doi.org/10.5281/zenodo.5809645>
- Hughes, L. C., Orti, G., Huang, Y., Sun, Y., Baldwin, C. C., Thompson, A. W., Arcila, D., Betancur, R. R., Li, C., Becker, L., Bellora, N., Zhao, X., Li, X., Wang, M., Fang, C., Xie, B., Zhou, Z., Huang, H., Chen, S., ... Shi, Q.** (2018). Comprehensive phylogeny of ray-finned fishes (Actinopterygii) based on transcriptomic and genomic data. *Proceedings of the National Academy of Sciences of the United States of America*, 115(24), 6249–6254. <https://doi.org/10.1073/pnas.1719358115>
- Jiménez-Moreno, G., de Leeuw, A., Mandić, O., Harzhauser, M., Pavelić, D., Krijgsman, W., & Vranjković, A.** (2009). Integrated stratigraphy of the Early Miocene lacustrine deposits of Pag Island (SW Croatia): Palaeovegetation and environmental changes in the Dinaride Lake System. *Palaeogeography, Palaeoclimatology, Palaeoecology*, 280(1–2), 193–206. <https://doi.org/10.1016/j.palaeo.2009.05.018>
- Jiménez-Moreno, G., & Mandić, O.** (2020). Middle Miocene climatic oscillations controlled by orbital-scale changes triggered environmental and vegetation variability in the Dinarides Lake System (Bugojno Basin, Bosnia and Herzegovina). *Palaeobiodiversity and Palaeoenvironments*, 100(2), 493–506. <https://doi.org/10.1007/s12549-020-00416-5>
- Jones, J. C., Fruciano, C., Keller, A., Schartl, M., & Meyer, A.** (2016). Evolution of the elaborate male intromittent organ of *Xiphophorus* fishes. *Ecology and Evolution*, 6(20), 7207–7220. <https://doi.org/10.1002/ece3.2396>
- Kassambara, A.** (2023). *rstatix: Pipe-Friendly Framework for Basic Statistical Tests*, R package version 0.7.2. <https://rpkgs.datanovia.com/rstatix/>
- Krstić, N., Savić, L., & Jovanović, G.** (2012). The Neogene lakes on the Balkan land. *Annales Géologiques de la Péninsule Balkanique*, 73, 37–60. <https://doi.org/10.2298/gabp1273037k>
- Langerhans, R. B., & Makowicz, A. M.** (2009). Shared and unique features of morphological differentiation between predator regimes in *Gambusia caymanensis*. *Journal of Evolutionary Biology*, 22(11), 2231–2242. <https://doi.org/10.1111/j.1420-9101.2009.01839.x>
- Lee, S. Y. M., & Palci, A.** (2015). Morphological phylogenetics in the genomic age. *Current Biology*, 25(19), R922–R929. <https://doi.org/10.1016/j.cub.2015.07.009>
- Lin, C.-H., & Chien, C.-W.** (2021). Late Miocene otoliths from northern Taiwan: insights into the rarely known Neogene coastal fish community of the subtropical northwest Pacific. *Historical Biology*, 34(2), 361–382. <https://doi.org/10.1080/08912963.2021.1916012>
- López-Solano, A., Nester, T. L., Perea, S., & Doadrio, I.** (2023). Complete mitochondrial genome of the Spanish toothcarp, *Aphaniops iberus* (Valenciennes, 1846) (Actinopterygii, Aphaniidae) and its phylogenetic position within the Cyprinodontiformes order. *Molecular Biology Reports*, 50(4), 2953–2962. <https://doi.org/10.1007/s11033-022-08236-w>
- Mabee, P. M., Crotwell, P. L., Bird, N. C., & Burke, A. C.** (2002). Evolution of median fin modules in the axial skeleton of fishes. *Journal of Experimental Zoology*, 294(2), 77–90. <https://doi.org/10.1002/jez.10076>
- Malz, H.** (1978). Vergleichend-morphologische Untersuchungen an aquitanen Fisch-Otolithen aus dem Untergrund von Frankfurt am Main. *Senckenbergiana Lethaea*, 59, 441–481.
- Mandić, O., de Leeuw, A., Vuković, B., Krijgsman, W., Harzhauser, M., & Kuiper, K. F.** (2011). Palaeoenvironmental evolution of Lake Gacko (Southern Bosnia and Herzegovina): Impact of the Middle Miocene Climatic Optimum on the Dinaride Lake System. *Palaeogeography Palaeoclimatology Palaeoecology*, 299(3–4), 475–492. <https://doi.org/10.1016/j.palaeo.2010.11.024>
- Mandić, O., Harzhauser, M., & Neubauer, T. A.** (2020). Taxonomy, palaeoecology and stratigraphy of the middle Miocene mollusk fauna from the Gračanica coal pit near Bugojno in Bosnia and Herzegovina. *Palaeobiodiversity*

- and Palaeoenvironments*, 100(2), 519–549. <https://doi.org/10.1007/s12549-020-00423-6>
- Marković, Z., Milivojević, M., De, B., Wessels, W., Van, D., Renovica, S., Šišić, E., & Modrić, K. (2018).** Paleontological research on fossil small mammals from the open-pit coal mines of Bosnia and Herzegovina: Overview of results. *Bulletin of the Natural History Museum*(11), 7–17. <https://doi.org/10.5937/bnhmb1811007M>
- Maxwell, E. E., & Wilson, L. A. (2013).** Regionalization of the axial skeleton in the 'ambush predator' guild – are there developmental rules underlying body shape evolution in ray-finned fishes? *BMC Evolutionary Biology*, 13, 265. <https://doi.org/10.1186/1471-2148-13-265>
- Meyer, A., & Lydeard, C. (1993).** The evolution of copulatory organs, internal fertilization, placentae and viviparity in killifishes (Cyprinodontiformes) inferred from a DNA phylogeny of the tyrosine kinase gene *X-src*. *Proceedings of the Royal Society of London Series B: Biological Sciences*, 254(1340), 153–162. <https://doi.org/10.1098/rspb.1993.0140>
- Meyer, D., Brownstein, C. D., Jenkins, K. M., & Gauthier, J. A. (2023).** A Morrison stem gekkotan reveals gecko evolution and Jurassic biogeography. *Proceedings of the Royal Society of London Series B: Biological Sciences*, 290(2011), 20232284. <https://doi.org/10.1098/rspb.2023.2284>
- Mongiardino Koch, N., Garwood, R. J., & Parry, L. A. (2021).** Fossils improve phylogenetic analyses of morphological characters. *Proceedings of the Royal Society. Biological sciences*, 288(1950), 20210044. <https://doi.org/10.1098/rspb.2021.0044>
- Moody, E. K., & Lozano-Vilano, M. L. (2018).** Predation drives morphological convergence in the *Gambusia panuco* species group among lotic and lentic habitats. *Journal of Evolutionary Biology*, 31(4), 491–501. <https://doi.org/10.1111/jeb.13226>
- Morcillo, F., Ornelas-Garcia, C. P., Alcaraz, L., Matamoros, W. A., & Doadrio, I. (2016).** Phylogenetic relationships and evolutionary history of the Mesoamerican endemic freshwater fish family Profundulidae (Cyprinodontiformes: Actinopterygii). *Molecular Phylogenetics and Evolution*, 94(Pt A), 242–251. <https://doi.org/10.1016/j.ympev.2015.09.002>
- Myers, G. S. (1928).** Two new genera of fishes. *Copeia*, 166(Jan.—Mar., 1928), 7–8.
- Myers, G. S. (1955).** Notes on the classification and names of cyprinodont fishes. *The Tropical Fish Magazine*, 4(4), 7.
- Nardo, J. D. (1827).** Prodrromus Observationum et Disquisitionum Ichthyologiae Adriaticae. *Isis von Oken*, 20(6).
- Neubauer, T. A., Harzhauser, M., Georgopoulou, E., Kroh, A., & Mandic, O. (2015).** Tectonics, climate, and the rise and demise of continental aquatic species richness hotspots. *Proceedings of the National Academy of Sciences of the United States of America*, 112(37), 11478–11483. <https://doi.org/10.1073/pnas.1503992112>
- Neubauer, T. A., Mandic, O., & Harzhauser, M. (2016).** The early middle Miocene lacustrine gastropod fauna of Džepi, Bosnia and Herzegovina (Dinaride Lake System): high endemism in a small space. *Bulletin of Geosciences*, 91(2), 271–296. <https://doi.org/10.3140/bull.geosci.1584>
- Neubauer, T. A., Mandic, O., Harzhauser, M., & Hrvatović, H. (2013).** A new Miocene lacustrine mollusc fauna of the Dinaride Lake System and its palaeobiogeographic, palaeoecologic and taxonomic implications. *Palaeontology*, 56(1), 129–156. <https://doi.org/10.1111/j.1475-4983.2012.01171.x>
- Nolf, D. (2013).** *The diversity of fish otoliths, past and present*. Royal Belgian Institute of Natural Sciences.
- Parenti, L. R. (1981).** A phylogenetic and biogeographic analysis of cyprinodontiform fishes (Teleostei, Atherinomorpha). *Bulletin of the American Museum of Natural History*, 168(4), 335–557. <http://hdl.handle.net/2246/438>
- Parenti, L. R. (2005).** The phylogeny of Atherinomorphs: evolution of a novel fish reproductive system. In M. Uribe & H. J. Grier (Eds.), *Viviparous Fishes: Proceedings of the I and II International Symposia on Livebearing Fishes* (pp. 13–30). New Life Publications. <http://hdl.handle.net/10088/10942>
- Paterson, R. S., Rybczynski, N., Kohno, N., & Maddin, H. C. (2020).** A total evidence phylogenetic analysis of pinniped phylogeny and the possibility of parallel evolution within a monophyletic framework. *Frontiers in Ecology and Evolution*, 7(457), 1–16. <https://doi.org/10.3389/fevo.2019.00457>
- Perdices, A., Machordom, A., & Doadrio, I. (1996).** Allozymic variation and relationships of the endangered cyprinodontid genus *Valencia* and its implications for conservation. *Journal of Fish Biology*, 49(6), 1112–1127. <https://doi.org/10.1111/j.1095-8649.1996.tb01782.x>
- Piller, K. R., Parker, E., Lemmon, A. R., & Lemmon, E. M. (2022).** Investigating the utility of Anchored Hybrid Enrichment data to investigate the relationships among the Killifishes (Actinopterygii: Cyprinodontiformes), a globally distributed group of fishes. *Molecular Phylogenetics and Evolution*, 173, 107482. <https://doi.org/10.1016/j.ympev.2022.107482>
- Pisera, A., Siver, P. A., & Mandic, O. (2019).** Miocene siliceous microfossils from the open cast coal mine Gračanica (Bugojno paleolake, Bosnia and Herzegovina) and their significance: a preliminary report. *Palaeobiodiversity and Palaeoenvironments*, 100(2), 507–517. <https://doi.org/10.1007/s12549-019-00378-3>
- Pohl, M., Milvertz, F., Meyer, A., & Vences, M. (2015).** Multigene phylogeny of cyprinodontiform fishes suggests continental radiations and a rogue taxon position of *Pantanodon*. *Vertebrate Zoology*, 65(1), 37–44. [https://www.senckenberg.de/wp-content/uploads/2019/08/05\\_vertebrate\\_zoology\\_65-1\\_pohl\\_et\\_al\\_37-44.pdf](https://www.senckenberg.de/wp-content/uploads/2019/08/05_vertebrate_zoology_65-1_pohl_et_al_37-44.pdf)
- R Core Team (2023). *R: A language and environment for statistical computing*. In R Foundation for Statistical Computing. <https://www.R-project.org/>
- Reichenbacher, B. (1988).** Die Fischfauna der Kirchberger Schichten (Unter-Miozän) an der Typuslokalität Illerkirchberg bei Ulm. *Stuttgarter Beitrage zur Naturkunde Serie B (Geologie und Palaeontologie)*, 139, 1–53.
- Reichenbacher, B. (1993).** Mikrofaunen, Paläogeographie und Biostratigraphie der miozänen Brack- und Süßwassermolasse in der westlichen Paratethys unter besonderer Berücksichtigung der Fisch-Otolithen. *Senckenbergiana Lethaea*, 73(2), 277–374.
- Reichenbacher, B. (2000).** Das brackisch-lakustrine Oligozän und Unter-Miozän im Mainzer Becken und Hanauer Becken: Fischfaunen, Paläoökologie, Biostratigraphie, Paläogeographie. *Courier Forschungsinstitut Senckenberg*, 222, 1–143.

- Reichenbacher, B., & Bannikov, A. F. (2022).** Diversity of gobioid fishes in the late middle Miocene of northern Moldova, Eastern Paratethys – part I: an extinct clade of *Lesueurigobius* look-alikes. *PalZ*, 96, 67–112. <https://doi.org/10.1007/s12542-021-00573-8>
- Reichenbacher, B., Böhme, M., Heissig, K., Prieto, J., & Kossler, A. (2004).** New approach to assess biostratigraphy, palaeoecology and past climate in the South German Molasse Basin during the Early Miocene (Ottangian, Karpatian). *Courier Forschungsinstitut Senckenberg*, 249, 71–89.
- Reichenbacher, B., Filipescu, S., & Miclea, A. (2019).** A unique middle Miocene (Sarmatian) fish fauna from coastal deposits in the eastern Pannonian Basin (Romania). *Palaeobiodiversity and Palaeoenvironments*, 99(2), 177–194. <https://doi.org/10.1007/s12549-018-0334-3>
- Reichenbacher, B., & Gaudant, J. (2003).** On *Prolebias meyeri* (Agassiz) (Teleostei, Cyprinodontiformes) from the Oligo-Miocene of the Upper Rhinegraben area, with the establishment of a new genus and a new species. *Eclogae Geologicae Helvetiae*, 96(3), 509–520.
- Reichenbacher, B., Gaudant, J., & Sienknecht, U. (2004).** The new fossil killifish genus *Aphanolebias* Reichenbacher & Gaudant 2003 (Teleostei, Cyprinodontiformes) and its fossil record. *Mitteilungen aus dem Hamburgischen Zoologischen Museum und Institut*, 101, 47–54.
- Reichenbacher, B., & Kowalke, T. (2009).** Neogene and present-day zoogeography of killifishes (*Aphanius* and *Aphanolebias*) in the Mediterranean and Paratethys areas. *Palaeogeography, Palaeoclimatology, Palaeoecology*, 281(1–2), 43–56. <https://doi.org/10.1016/j.palaeo.2009.07.008>
- Reichenbacher, B., & Philippe, M. (1997).** Les otolithes de Téléostéens oligocènes du bassin d'Apt (Vaucluse, France). *Neues Jahrbuch für Geologie und Paläontologie – Abhandlungen*, 203(3), 391–423. <https://doi.org/10.1127/njgpa/203/1997/391>
- Reichenbacher, B., & Prieto, J. (2006).** Lacustrine fish faunas (Teleostei) from the Karpatian of the northern Alpine Molasse Basin, with a description of two new species of *Prolebias* Sauvage. *Palaeontographica Abteilung A Palaeozoologie-Stratigraphie*, 278(1–6), 87–95. <https://doi.org/10.1127/pala/278/2006/87>
- Reichenbacher, B., Sienknecht, U., Kuchenhoff, H., & Fenske, N. (2007).** Combined otolith morphology and morphometry for assessing taxonomy and diversity in fossil and extant killifish (*Aphanius*, *Prolebias*). *Journal of Morphology*, 268(10), 898–915. <https://doi.org/10.1002/jmor.10561>
- Reichenbacher, B., & Weidmann, M. (1992).** Fisch-Otolithen aus der oligo-/miozänen Molasse der West-Schweiz und der Haute-Savoie (Frankreich). *Stuttgarter Beiträge zur Naturkunde Serie B (Geologie und Paläontologie)*, 184, 1–83.
- Riesch, R., Duwe, V., Herrmann, N., Padur, L., Ramm, A., Scharnweber, K., Schulte, M., Schulz-Mirbach, T., Ziege, M., & Plath, M. (2009).** Variation along the shy-bold continuum in extremophile fishes (*Poecilia mexicana*, *Poecilia sulphuraria*). *Behavioral Ecology and Sociobiology*, 63(10), 1515–1526. <https://doi.org/10.1007/s00265-009-0780-z>
- Rodgers, R., Roach, J. L., Reid, N. M., Whitehead, A., & Duvernell, D. D. (2018).** Phylogenomic analysis of Fundulidae (Teleostei: Cyprinodontiformes) using RNA-sequencing data. *Molecular Phylogenetics and Evolution*, 121, 150–157. <https://doi.org/10.1016/j.ympev.2017.12.030>
- Rosen, D. E. (1965).** *Oryzias madagascariensis* Arnoult redescribed and assigned to the East African fish genus *Pantanodon* (Atheriniformes, Cyprinodontoidei). *American Museum Novitates*, 2240, 1–10.
- Rückert-Ülkümen, N. (2006).** Otolithen aus dem Mio-Pliozän von Yalova bei Istanbul, Türkei. *Neues Jahrbuch für Geologie und Paläontologie Monatshefte*, 10, 577–594. <https://doi.org/10.1127/njgpm/2006/2006/577>
- Sauvage, H. E. (1869).** Notes sur les poissons du calcaire de Ronzon, près Le Puy-en-Velay. *Bulletin de la Société Géologique de France*, 26(2), 1069–1075.
- Sauvage, H. E. (1874).** Notice sur les Poissons tertiaires de l'Auvergne. *Bulletin de la Société d'Histoire Naturelle de Toulouse*, 8, 171–198.
- Sauvage, H. E. (1880).** Note sur quelques poissons recueillis par M. Letourneux en Épire, à Corfou et dans le lac Maréotis. *Bulletin de la Société Philomathique de Paris*, 7(4), 211–215.
- Schneider, C. A., Rasband, W. S., & Eliceiri, K. W. (2012).** NIH Image to ImageJ: 25 years of image analysis. *Nat Methods*, 9(7), 671–675. <https://doi.org/10.1038/nmeth.2089>
- Schulz-Mirbach, T., Ladich, F., Riesch, R., & Plath, M. (2010).** Otolith morphology and hearing abilities in cave- and surface-dwelling ecotypes of the Atlantic molly, *Poecilia mexicana* (Teleostei: Poeciliidae). *Hearing Research*, 267(1–2), 137–148. <https://doi.org/10.1016/j.heares.2010.04.001>
- Schulz-Mirbach, T., & Plath, M. (2012).** All good things come in threes – species delimitation through shape analysis of saccular, lagenar and utricular otoliths. *Marine and Freshwater Research*, 63(10). <https://doi.org/10.1071/MF12132>
- Schwarzahns, W. (1978).** Otolith-morphology and its usage for higher systematical units, with special reference to the Myctophiformes s.l. *Mededelingen van de Werkgroep voor Tertiaire en Kwartaire Geologie*, 15(4), 167–185.
- Sferco, E., Aguilera, G., Góngora, J. M., & Mirande, J. M. (2022).** The eldest grandmother, late Miocene †*Jenynsia herbsti* sp. nov. (Teleostei, Cyprinodontiformes), and the early diversification of the Anablepidae. *Journal of Vertebrate Paleontology*, 41(6). <https://doi.org/10.1080/02724634.2022.2039168>
- Sferco, E., Herbst, R., Aguilera, G., & Mirande, J. M. (2018).** The rise of internal fertilization in the Anablepidae (Teleostei, Cyprinodontiformes): two new genera and species from the Miocene of Tucumán, Argentina. *Papers in Palaeontology*, 4(2), 177–195. <https://doi.org/10.1002/spp2.1102>
- Shumka, S., Kalogianni, E., Šanda, R., Vukić, J., Shumka, L., & Zimmerman, B. (2020).** Ecological particularities of the critically endangered killifish *Valencia letourneuxi* and its spring-fed habitats: a long-lost endemic species of south Albania. *Knowledge & Management of Aquatic Ecosystems*, 421 (45), 1–10. <https://doi.org/10.1051/kmae/2020036>
- Smith, G. R. (1981).** Late Cenozoic Freshwater Fishes of North America. *Annual Review of Ecology and Systematics*, 12(1), 163–193. <https://doi.org/10.1146/annurev.es.12.110181.001115>

- Smithsonian National Museum of Natural History (2024). *Search the Division of Fishes Collections*. Retrieved 19 July 2023 from <https://collections.nmnh.si.edu/search/fishes/?ark=ark:/65665/3e51a7363a1024735b2e0d8d8e4da03b2>
- Springer, M. S., Teeling, E. C., Madsen, O., Stanhope, M. J., & de Jong, W. W. (2001).** Integrated fossil and molecular data reconstruct bat echolocation. *Proceedings of the National Academy of Sciences of the United States of America*, 98(11), 6241–6246. <https://doi.org/10.1073/pnas.111551998>
- Steurbaut, E. (1978).** Otolithes de teleosteens de quelques formations continentales d'age Aquitanien du midi de la France. *Bulletin de la Societe Belge de Geologie*, 87(3), 179–188.
- Teimori, A., Iranmanesh, N., Hesni, M. A., & Motamedi, M. (2021).** Within-and among-population differentiation of *Aphaniops hormuzensis* from ecologically diverse environments (Cyprinodontiformes; Aphaniidae). *Acta Zoologica*, 102(4), 420–436. <https://doi.org/10.1111/azo.12350>
- Teimori, A., Motamedi, M., & Zeinali, F. (2021).** Intrapopulation variation of otolith associated with ontogeny and morphological dimorphism in Hormuz tooth-carp *Aphaniops hormuzensis* (Teleostei: Aphaniidae). *Acta Zoologica*, 102(3), 250–264. <https://doi.org/10.1111/azo.12332>
- Teimori, A., Schulz-Mirbach, T., Esmacili, H. R., & Reichenbacher, B. (2012).** Geographical differentiation of *Aphaniops dispar* (Teleostei: Cyprinodontidae) from Southern Iran. *Journal of Zoological Systematics and Evolutionary Research*, 50(4), 289–304. <https://doi.org/10.1111/j.1439-0469.2012.00667.x>
- Thieme, P., Schnell, N. K., Parkinson, K., & Moritz, T. (2022).** Morphological characters in light of new molecular phylogenies: the caudal-fin skeleton of Ovalentaria. *Royal Society Open Science*, 9(1), 211605. <https://doi.org/10.1098/rsos.211605>
- Thieme, P., Warth, P., & Moritz, T. (2021).** Development of the caudal-fin skeleton reveals multiple convergent fusions within Atherinomorpha. *Frontiers in Zoology*, 18(1), 20. (Front Zool) <https://doi.org/10.1186/s12983-021-00408-x>
- van der Made, J. (2020).** The Suoidea from the Middle Miocene of Gračanica (Bugojno Basin, Bosnia and Herzegovina)—evolution, taxonomy, and biostratigraphy. *Palaeobiodiversity and Palaeoenvironments*, 100(2), 321–349. <https://doi.org/10.1007/s12549-020-00420-9>
- Vasilyan, D. (2020).** Fish, amphibian and reptilian assemblage from the middle Miocene locality Gračanica—Bugojno palaeolake, Bosnia and Herzegovina. *Palaeobiodiversity and Palaeoenvironments*, 100(2), 437–455. <https://doi.org/10.1007/s12549-019-00381-8>
- Vasilyan, D., Reichenbacher, B., & Carnevale, G. (2009).** A new fossil *Aphaniops* species from the Upper Miocene of Armenia (Eastern Paratethys). *Palaeontologische Zeitschrift*, 83(4), 511–519. <https://doi.org/10.1007/s12542-009-0034-4>
- Volpedo, A., & Echeverría, D. D. (2003).** Ecomorphological patterns of the sagitta in fish on the continental shelf off Argentina. *Fisheries Research*, 60(2–3), 551–560. [https://doi.org/10.1016/s0165-7836\(02\)00170-4](https://doi.org/10.1016/s0165-7836(02)00170-4)
- von Salis, K. (1967).** Geologische und sedimentologische Untersuchungen in Molasse und Quartär südöstlich Wolhusen. *Mitteilungen der Naturforschenden Gesellschaft Luzern*, 21, 1–107. <https://doi.org/10.5169/seals-523384>
- Weber, M. (1907).** Süßwasserfische von Neu-Guinea. Ein Beitrag zur Frage nach dem früheren Zusammenhang von Neu-Guinea und Australien. In A. Wichmann (Ed.), *Résultats de l'expédition scientifique Néerlandaise à la Nouvelle-Guinée en 1903* (Vol. 5 (Zool.), pp. 201–267). Librairie et Imprimerie E. J. Brill, Leiden.
- Wedmann, S., & Skartveit, J. (2020).** First record of March flies (Insecta: Diptera: Bibionidae) from the Miocene Gračanica mine (Bugojno, Bosnia-Herzegovina). *Palaeobiodiversity and Palaeoenvironments*, 100(2), 585–591. <https://doi.org/10.1007/s12549-018-00369-w>
- Weiler, W. (1963).** Die Fischfauna des Tertiärs im oberrheinischen Graben, des mainzer Beckens, des unteren Maintals und der Wetterau, unter besonderer Berücksichtigung des Untermiozäns. *Abhandlungen der Senckenbergischen Naturforschenden Gesellschaft*, 504, 1–75.
- Wildekamp, R. H. (1993).** The genera *Adamas*, *Adinia*, *Aphaniops*, *Aphyoplatys* and *Aphyosemion*. In B. R. Watters (Ed.), *A World of Killies: Atlas of the Oviparous Cyprinodontiform fishes of the world* (Vol. 1, pp. 67). The American Killifish Association.
- Zar, J. H. (2010).** *Biostatistical Analysis* (D. Lynch, Ed. 5th ed.). Pearson Prentice Hall Inc.

**Associate Editor: Erin Maxwell**